Institut für Veterinärbiochemie und Molekularbiologie
der Vetsuisse-Fakultät Universität Zürich

Direktor: Prof. Dr. Michael O. Hottiger

Role of TIP5 in Metastatic Prostate Cancer and Osteosarcoma Cells

Inaugural-Dissertation

zur Erlangung der Doktorwürde der
Vetsuisse-Fakultät Universität Zürich

vorgelegt von

Cristina Yasoma Gerig

Tierärztin
von Basel BS und Wassen UR

genehmigt auf Antrag von

PD Dr. Raffaella Santoro, Hauptreferentin
Prof. Dr. med. vet. Hanspeter Nägeli, Korreferent

2014

Institut für Veterinärbiochemie und Molekularbiologie
der Vetsuisse-Fakultät Universität Zürich

Direktor: Prof. Dr. Michael O. Hottiger

Role of TIP5 in Metastatic Prostate Cancer and Osteosarcoma Cells

Inaugural-Dissertation

zur Erlangung der Doktorwürde der
Vetsuisse-Fakultät Universität Zürich

vorgelegt von

Cristina Yasoma Gerig

Tierärztin
von Basel BS und Wassen UR

genehmigt auf Antrag von

PD Dr. Raffaella Santoro, Hauptreferentin
Prof. Dr. med. vet. Hanspeter Nägeli, Korreferent

2014

Table of Contents

1 Zusammenfassung

Die neoplastische Entartung erfolgt durch ein Zusammenspiel von genetischen und epigenetischen Veränderungen (wie CpG Hypermethylierungen von Promotern und Histon-Modifizierungen). Zusammengenommen führen diese Veränderungen zu genomischer Instabilität, zur Ausschaltung von Tumorsuppressorgenen und zur Aktivierung von Proto-Onkogenen.
Hier zeigen wir, dass TIP5 (ein Protein mit Bromodomäne, das normalerweise zur epigenetischen Inaktivierung von rRNA Genen benötigt wird) in metastatischem Prostatakrebs (PKr) überexprimiert wird und Gene reguliert, die in metastatischen Prostatatumoren häufig supprimiert sind. Expressionslevel von TIP5 sind frühe prognostische Marker zur Unterscheidung von aggressivem und weniger aggressivem PKr. Anomale Geninaktivierung im PKr durch TIP5 entsteht unter Zutun von EZH2 (Bestandteil des Polycomb Repressive Complex 2). Diese H3K27-Methyltransferase wurde bereits als überexprimiert in PKr beschrieben, was mit schlechten Prognosen einher ging. Wir definieren ein Set von Genen, die von TIP5 und EZH2 supprimiert werden und in metatastischem PKr inaktiv sind (RTEM). Die Inaktivierung dieser Gene ist nicht auf PKr beschränkt, sondern kann auch in den Osteosarkomzellen U2OS nachgewiesen werden. Dies deutet darauf hin, dass epigenetische Veränderungen der RTEM Gene typisch für einen neoplastischen Phänotyp sind. Wir zeigen zudem, dass TIP5 durch ähnliche Mechanismen zu den RTEM Promotern gelangen könnte wie in gesunden Zellen zu den rRNA Genen.

Schlüsselwörter: TIP5, EZH2, Prostatakrebs, Osteosarkom, Epigenetik

2 Summary

Neoplastic transformation is driven by an alliance of genetic alterations and epigenetic abnormalities such as CpG hypermethylation of promoters and histone modifications. Collectively, these alterations promote genomic instability and lead to silencing of tumor-suppressor genes and activation of proto-oncogenes.

Here we show that TIP5, a bromo domain-containing protein normally required for epigenetic silencing of ribosomal RNA genes, is overexpressed in metastatic prostate cancer (PCa) tissue and regulates genes frequently repressed in prostate metastatic tumors. Expression levels of TIP5 serve as an early prognostic marker to distinguish indolent from aggressive PCa. Aberrant gene silencing in PCa cells mediated by TIP5 acts in cooperation with EZH2, a component of Polycomb repressive complex 2 and H3K27 methyltransferase, previously reported to be overexpressed in metastatic PCa and linked to poor prognosis. This study defines a set of genes repressed by TIP5 and EZH2 and silenced in metastatic PCa (RTEM). Repression of these genes is not only limited to PCa cells but also found in osteosarcoma U2OS cells, indicating that epigenetic alterations at RTEM genes are common to cancer phenotype. We also show that recruitment of TIP5 to RTEM promoters in cancer might share similar mechanisms to that one found for ribosomal RNA genes in healthy cells.

Keywords: TIP5, EZH2, prostate cancer, osteosarcoma, epigenetic

3 Introduction

Adapted and modified from my master thesis "Role of TIP5 in Metastatic Prostate Cancer Cells".

3.1 Chromatin structure

Eukaryotic cells contain a nucleus in which the genomic DNA is organized in a complex structure called chromatin. The minimal and fundamental structural unit of chromatin is the nucleosome, comprised of ~147 base pairs of DNA wrapped around a histone octamer core in a left-handed superhelix [1, 2]. The histone octamer is a protein complex composed of one histone H3-H4 tetramer that is flanked by two histone H2A-H2B dimers [2]. Except for their N-terminal tails, the core histones are predominantly globular. A linker DNA of variable length is located between two nucleosomes and bound by the linker histone H1 or in avian erythrocytes H5 [3].
The nucleosomal array, a 'beads-on-a-string' fiber with a diameter of 11 nm, represents the next level of chromatin organization [2]. The binding of the linker histone organizes the nucleosome arrays into a more condensed 30 nm chromatin fiber that is also called "solenoid" [4]. Additional factors such as non-histone and nuclear scaffold proteins facilitate establishment of large chromatin loop domains that can be compacted further to generate interphase and mitotic chromosomes [5]. These different levels of chromatin structure are depicted and commented in Figure 1. Packing of eukaryotic genomes into high-order chromatin structures is critical for controlling processes derived from DNA like replication, transcription, recombination and repair.

Chromatin is primarily organized in two different structural states: heterochromatin and euchromatin. The term heterochromatin was characterized in 1928 by Heitz who visualized chromosomal regions in moss that were deeply stained at prophase and remained compact throughout the mitotic cell cycle. ([6] reviewed in [7, 8]). Fractions of the chromosome that were condensed at metaphase but diffuse and decondensed during interphase were referred to as euchromatin. Further studies revealed that heterochromatin is mainly located around centromeres and close to telomeres, is gene-poor, contains regular nucleosomal arrays of hypoacetylated histones and its transcription factor binding is limited (reviewed in [9]). On the other hand, euchromatin is gene-rich, contains irregular nucleosomal arrays, is associated with acetylated histones and is easily accessible to transcription factors. Also in term of replication euchromatin and heterochromatin are different: euchromatic DNA regions replicate in the early S-phase [10] while heterochromatin is replicated in late S-phase of the cell cycle (reviewed in [11]).

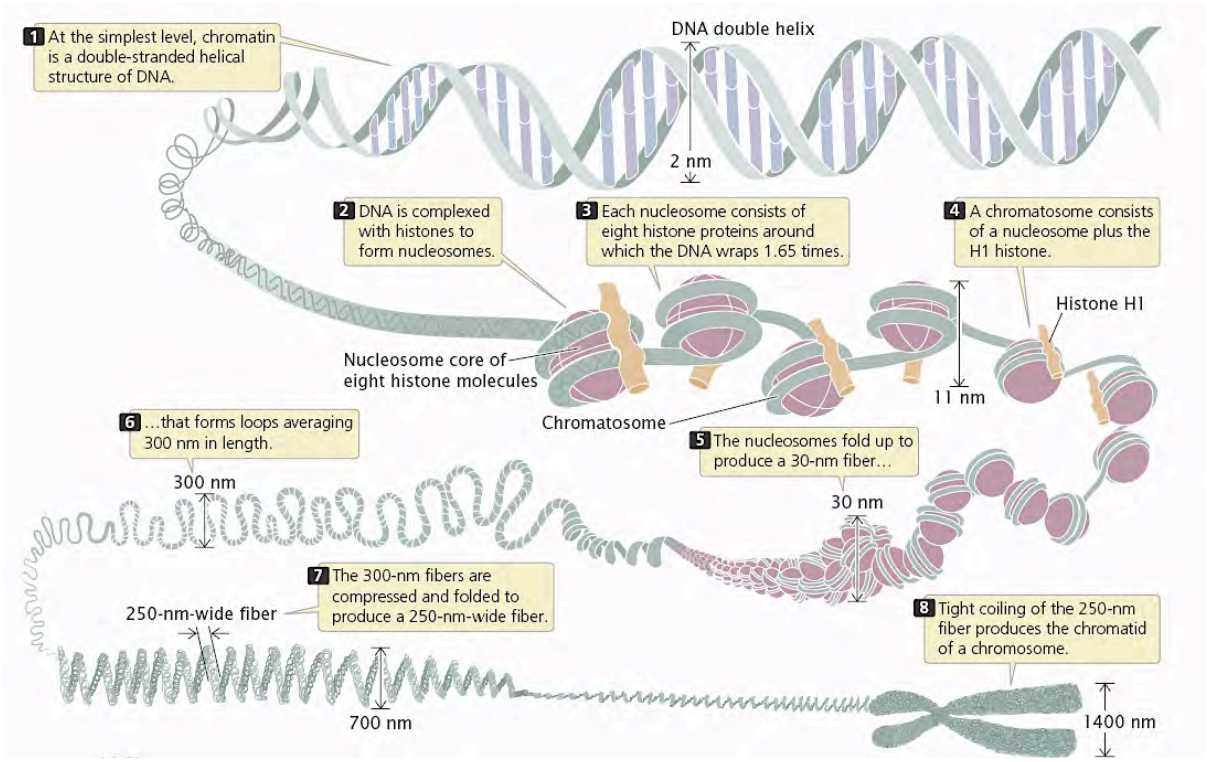

Figure 1 | Different levels of chromatin structure
Picture taken from Pierce, Benjamin. *Genetics: A Conceptual Approach*, 2nd ed. (New York: W. H. Freeman and Company), 2005

3.2 Epigenetic regulation

Cells of multicellular organisms contain essentially identical components of DNA though they are structurally and functionally heterogeneous. They differentiate to form distinct tissues and organs through differences in gene expression, based on environmental cues, cell-to-cell signals and other, probably random, factors. This variable transcriptional potential is a defining aspect of a cell's identity and is mainly founded at the level of epigenetic signature and chromatin structure.

Epigenetics is defined as changes in gene expression pattern heritable during cell division that are not caused by alterations of the DNA sequence, unlike mutations that are defined as a change of the nucleotide sequence. DNA methylation, histone modifications and non-coding RNAs are the predominant epigenetic mechanisms. Epigenetic mechanisms play an important role in gene regulation during development; one popular example is the transcriptional inactivation of one X-chromosome in female mammals.

Research indicates long-term and wide-ranging effects of epigenetic on health. Diet and environmental exposures may potentially alter the level and scope of epigenetic regulation, thus interesting developments in the epigenomic research might explain correlations between lifestyle and risk of disease. Aberrant epigenetic patterns have been linked to a number of diseases including obesity, diabetes and cancer. Cancer was the first disease described to have altered epigenetic marks in the year 1983 (reviewed in [12]). Epigenetic modifications of DNA in cancer and precancerous

lesions give up hope of novel biomarkers for early cancer diagnosis, accurate prognosis, and efficient therapy. Furthermore, reversal of epigenetic changes is a potential target of novel therapeutic strategies and medication design. In the future, it is expectable that innovative diagnostic tests, drug regimens and even lifestyle modifications will be based on epigenetic mechanisms which will be incorporated into the practice of medicine.

3.2.1 DNA methylation

DNA methylation is one of the best-studied epigenetic mechanisms and a highly conserved epigenetic modification of DNA. Methylated cytosine has been found in the genome of organisms ranging from prokaryotes to mammals and is typically associated with gene silencing.
In eukaryotic species, 5-Methylcytosine is found frequently within CpG dinucleotides. CpCs are distributed non-randomly in the genome and concentrated in genomic regions called CpG islands that are usually unmethylated. CpG methylation of promoters and enhancers is a mark of silent, inactive genes and associated with negative regulation of transcription. The transfer of a methyl group from S-adenosyl-methionine (SAM) to cytosine of CpG dinucleotides is catalyzed by DNA methyltransferases (DNMTs) (reviewed in [13]). Genome-wide cytosine methylation patterns are established during embryogenesis and are stably propagated throughout cell division by combined actions of DNMTs. DNA methylation is the only epigenetic mark which is not removed by the replication fork and serves consequently as a strong memory mark for inheritance of heterochromatin.

DNMT1, DNMT3A and DNMT3B are the three enzymatically active DNMTs in mammalians and are divided into maintenance and *de novo* methyltransferases. DNMT1 is the primary maintenance methyltransferase and has a preference for hemimethylated CpG sites like those generated by DNA replication [14]. Its main function is to copy the methylation patterns during replication. DNMT3A and DNMT3B are essential for *de novo* methylation and responsible for the establishment of distinct methylation patterns during embryogenesis. Inactivation of the genes encoding these two methyltransferases blocks *de novo* methylation in ES cells and mouse embryos. Both methyltransferases are required for normal mammalian development but do not influence the maintenance of imprinted methylation patterns [15].

DNA methylation affects gene expression directly or indirectly. Several DNA binding proteins, for example transcription factors, can only interact with unmethylated DNA [16], whereas CpG methylation abolishes the interaction with their target sequences what leads to a lower transcription level. On the other hand, specific proteins, called MBD (methyl-CpG-binding domain) proteins, recognize CpG methylation and attract multiprotein complexes, which can change chromatin structure from open to close state.

DNA methylation is essential for normal mammalian development [17] and involved in several fundamental processes, such as genomic imprinting, X chromosome inactivation and suppression of retrotransposon elements [18]. Although methylation patterns are largely maintained through

somatic cell divisions, changes in methylation patterns occur during mammalian development and cell differentiation. In addition to these changes, the DNA methylation pattern can alter in some adult somatic cells during aging and in pathologies such as cancer, causing aberrant repression of tumor suppressor genes through DNA hypermethylation of the CpG islands in promoters (reviewed in [19] and [20]).

3.2.2 Histone modifications

The core histones contain a globular C-terminal domain and highly dynamic N-terminal tail extending from the nucleosome. The N-terminal tail is enabled to experience different posttranslational modifications such as acetylation, methylation, phosphorylation, ubiquitylation, sumoylation, ADP-ribosylation, deiminiation, proline isomerization, citrullination, butyrylation, propionylation and glycosylation (reviewed in [21] and [22]). All histone tails within the nucleosome can be multiple posttranslational modified and thereby induce a distinct chromatin signature and epigenetic profile. Most of the histone modifications are reversible and represent a fundamental regulatory mechanism for chromatin function [23]. They regulate key cellular processes such as transcription, replication and repair [21].

Histone acetylation is a histone mark associated with transcriptional active state. The acetylation of lysines is highly dynamic and controlled by the opposing action of two families of enzymes. The histone acetyltransferases (HATs) catalyze the transfer of an acetyl group from acetyl-CoA to lysine residues [24] what neutralizes lysine's positive charge and weakens the interaction between histones and DNA and thus increases the accessibility of DNA to the transcription machinery. HATs opponents are the histone deacetylases (HDACs) that remove acetyl groups from histone lysines and restore the positive charge of the lysine what possibly stabilizes the local chromatin architecture (reviewed in [25]). HDACs contribute to transcriptional repression through chromatin compaction and are frequently associated with other transcriptional repressor proteins.

Histone methylation takes place on N-terminal tails of histones H3 and H4 and mainly occurs on the side chains of lysines and arginines. Lysine methylation can occur as mono-, di- or tri-methylation while arginines may be mono-, symmetrically or asymmetrically di-methylated. Histone methyltransferases (HMTs) catalyze the transfer of a methyl group from SAM to lysine or arginine amino acids what has different effects to chromatin structure and transcription. Histone methylation does not alter the charge of the histones (reviewed in [25]). The two main silencing mechanisms in mammalian cells are tri-methylation of histone H3 lysine 9 (H3K9me3) and H3K27me3, where H3K9me3 mediates chromatin recruitment of heterochromatin protein 1 (HP1), heterochromatin condensation and gene silencing [26, 27]. H4K20 methylation is another chromatin repressing mark, however, lysine methylation is also associated with transcriptionally active genes. For instance methylation of H3K4, H3K36 and H3K79 are active histone marks. Recently, several histone demethylases were discovered.

Histone phosphorylation takes place on serines, threonine and tyrosines, predominantly on N-terminal histone tails. The phosphorylation of histones is highly dynamic and controlled by the opposing action of two families of enzymes. Histone kinases transfer a phosphate group from ATP to the target amino acid what adds negative charge to the histone. The changes in charge influence the chromatin structure and suggest that histone phosphorylation has a similar function than acetylation in nucleosome dynamics (reviewed in [25]). The histone phosphatases are the opponents of the kinases and remove the phosphate group from the amino acid.

All four core histones, as well as linker histone H1, are known to be mono–ADP ribosylated and poly–ADP ribosylated on glutamate and arginine residues [28]. The modification is reversible and performed by the poly(ADP-ribose) polymerase (PARP) family of enzymes. ADP ribosylation achieves a negative charge to the histone what is according with a more relaxed structure of poly-ADP ribosylated chromatin [29]. This modification is removed by the poly-ADP-ribose-glycohydrolase family of enzymes.

Histone modifications are occurring in a variety of different combinations, each of those affect chromatin structure and gene transcription in their own way. Silent heterochromatin is a functional interaction of many epigenetic mechanisms including DNA methylation and a specific pattern of histone modifications such as low levels of acetylation and high levels of certain methylated lysine residues.

3.3 Epigenetics of cancer cells

Cancer develops through formation of distinct abilities such as sustaining proliferative signaling, evading growth suppressors, resisting cell death, enabling replicative immortality, inducing angiogenesis and activating invasion and metastasis. These so called hallmarks of cancer originate from aberrant gene function and altered patterns of gene expression. It is now clear that not only genetic alterations like mutation, copy number alteration, insertion, deletion, and recombination but also acquired epigenetic abnormalities contribute to cause this dysregulation [30]. Aberrant epigenetic mechanisms are manifest in both global changes in chromatin packaging and in localized gene promoter changes that influence the transcription of genes important to cancer progress [31, 32]. This implicates a central role of epigenetic processes in cancer causation, progression and treatment.
In mammalian cells, a dynamic regulation of DNA CpG methylation, nucleosome remodeling and a set of acetylation, methylation and other modifications at histone amino acid residues is needed for proper DNA packaging to ensure the balance between transcriptional activation and repression. Although CpG methylation controls gene activity, it is insufficient to repress transcription by itself and the local chromatin structure also contributes in determining whether genes are transcribed or repressed. Increasing evidences indicate that there is a tight interdependence between DNA methylation and chromatin modifications for DNA packaging [33]. Consistent with this, DNMTs have been shown to interact with histone modifier enzymes (HDACs and HMTs), pointing to interdependence between silent epigenetic marks [34].

3.3.1 DNA methylation and cancer

Cancer cells undergo dramatic changes in the level and distribution of global DNA methylation pattern. Loss of DNA methylation and genomic instability is implicated in a variety of human cancers [35]; on the other hand, site-specific hypermethylation of CpG islands is a common mechanism used by tumor cells to silence tumor suppressor genes [31, 32]. Several genome-wide studies reported that a large number of promoter regions become *de novo* methylated in cancer [36, 37] and that most of these events occur at genes that are involved in growth selection (reviewed in [38]). Further, many studies confirmed that this *de novo* methylation is targeted and is predominantly specific for CpG islands marked with Polycomb repressor (reviewed in [38]) and some DNA methylation changes seem to be essential for cancer cell survival, indicating an acquired addiction to epigenetic alterations [39].

There is no question that abnormal methylation is important in tumorigenesis. Indeed, there are already therapies directed towards aberrant hypermethylation. Hypomethylating agents such as 5-aza-2′deoxycytidine (Decitabine) and 5-azacytidine (Vidaza) are approved for the treatment of myelodysplastic syndromes [40] and clinical studies are also performed for solid tumors such as refractory advanced non-small cell lung cancer treated with combination of azacitidine and entinostat, inhibitors of DNA methylation and histone deacetylation [41].

3.3.2 Histone modifications and cancer

In cancer, global alterations in histone acetylation appear including a global loss of acetylated H4K16 [42] which results in gene repression. This loss of acetylation is mediated by HDACs whose overexpression is found in various types of cancer [43, 44]. To maintain histone acetylation levels HDACs collaborate with HATs which may be altered in cancer as well (reviewed in [45]).

Further epigenetic alterations occurring in cancer are changes in histone methylation patterns. For example, chromosomal translocations of the trithorax homolog myeloid-lymphoid leukaemia (MLL), the H3K4 HMT, play a key role in leukemic progression by changing the pattern of the active histone mark H3K4 methylation, leading to ectopic expression of various homeotic (Hox) genes [46]. However, histone methylation marks leading to gene repression show irregular patterns in cancer as well. Besides DNA hypermethylation, cancer associated silenced gene promoters have diminished active marks like H3K9 acetylation and H3K4 methylation but enriched H3K9 and H3K27 methylation, known to be associated with transcriptional repression [47].

Indeed, there is already precedence for efficacious clinical application of therapies directed toward epigenetic mechanisms. Hypomethylating agents are approved for the treatment of myelodysplastic syndromes, and the histone deacetylase inhibitors vorinostat and romidepsin are approved for the treatment of cutaneous T-cell lymphoma [40].

3.3.3 Polycomb group (PcG) proteins and cancer

PcG proteins are epigenetic regulators that act via chromatin organization and play key roles in multiple aspects of cell physiology and identity, including regulation of all developmental genes, cell differentiation, stem and somatic cell reprogramming and response to environmental stimuli (reviewed in [48]). They form several multiprotein complexes where Polycomb Repressive Complex 1 and 2 (PRC1 and PRC2) are the main complexes in mammals.
The core of PRC1 includes one subunit of the PCGF, CBX, PHC, SCML and RING1 paralogous groups ([49, 50] reviewed in [51]). PRC1 catalyzes the lysine 119 monoubiquitylation of H2A after binding of its chromodomain to H3K27me3 or independent of PRC2 (reviewed in [51]).
PRC2 is composed of four core components: the histone methyltransferase enhancer of zeste homologue 1 (EZH1) or 2 (EZH2), EED, SUZ12 and RbAp46/48. EZH2 catalyzes di- and trimethylation of the lysine 27 residue of histone H3 (H3K27me2/3), this activity requires that EZH2 is in complex with the other PRC2 components [52-55]. Trimethylation of H3K27 is a distinct histone modification involved in the regulation of Hox gene expression and in the early steps of X-chromosome inactivation in females [56]. This histone modification is associated with repressed chromatin states and genome-wide approaches revealed that H3K27me3 is widely distributed among genes encoding developmental regulators [19, 57-60].

Deregulation of PcG proteins has been observed in several types of cancer. BMI-1, belonging to PCGF group of PRC1, is overexpressed in squamous cell carcinomas, in neuroblastomas, in bladder tumors and in human medulloblastoma cell lines and primary tumors ([61], reviewed in [62]). Additionally, several studies describe its deregulation in leukemia (reviewed in [62]). Overexpression of EZH2 (part of PRC2) is found in various solid tumors including prostate, breast, bladder, colon, skin and lung cancer and is frequently positively correlated with aggressive disease and poor prognosis [63-66]. Various somatic mutations at Y641 in EZH2 were found in 7% of follicular lymphomas and in around 20% of diffuse large cell B-cell lymphomas of germinal center origin [67] and showed altered catalytic activity of PRC2 increasing H3K27me *in vitro* [68].
Recent results showed that genes repressed by PcG proteins in embryonic stem cells are marked by DNA hypermethylation in cancer, suggesting that PcG marks may be the main template for DNA methylation in cancer [58, 69, 70]. A biochemical study shows that EZH2 can interact with DNMTs and is responsible for *de novo* DNA methylation of CpG island genes in the osteosarcoma cell line U2OS [71]. This indicates a direct control of DNA methylation by EZH2, whereas this conflicts with a lack of DNA hypomethylation after knockdown of EZH2 in cancer cells [72]. However, the interaction between DNA methylation and the PcG proteins remains unclear.
These studies imply that deregulation of PcG proteins and the appropriate histone methylation pattern are intimately associated with tumor initiation and development.

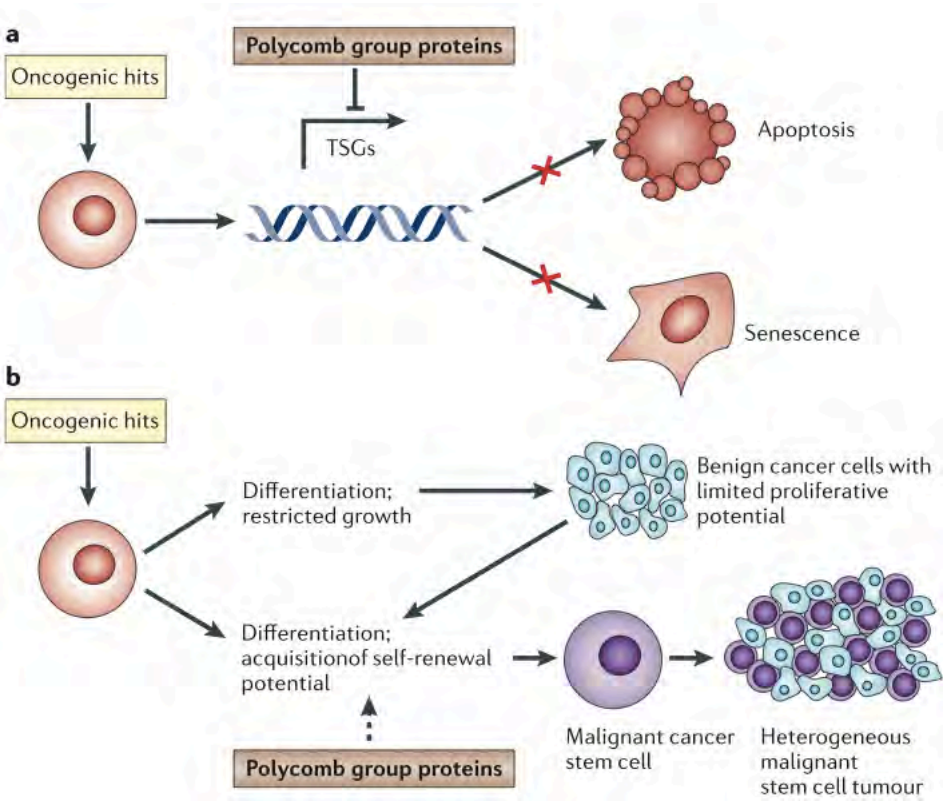

Sparmann and Lohuizen *Nature Reviews Cancer* **6**, 846–856 (November 2006) | doi:10.1038/nrc1991

nature REVIEWS CANCER

Figure 2 | Polycomb group proteins and cancer

A | Polycomb group (PcG) proteins like EZH2 transcriptionally repress tumour-suppressor genes, which normally prevent uncontrolled proliferation by cellular precautions such as apoptosis or senescence. **B |** The involvement of PcG proteins in the maintenance and acquisition of pluripotency might also contribute to cancer cell progression through the opportunity of gaining stem cell fate and unlimited proliferation.

3.4 Ribosomal RNA (rRNA) genes

Ribosomal RNA (rRNA) genes are located in the well-defined nuclear compartment called nucleolus. In human, 400 rRNA gene copies are located in a non-uniform manner between the short arm and the satellite body of the five acrocentric chromosomes 13, 14, 15, 21 and 26, in a telomere-to-centromer orientation [73]. Mammalian rDNA transcription units are large, comprising approximately 43 kb nts in human and 45 kb nts in mice [74-76]. rDNA clusters are characterized by multiple alternating modules of a precursor rRNA sequence (pre-rRNA, approximately 13 kb) separated by long intergenic spacer sequences (IGS, approximately 30 kb). IGS contains elements important for the regulation of rDNA transcription, such as rDNA promoter, spacer promoter, repetitive enhancer elements and transcription termination sequences. Transcription of rRNA genes is performed by RNA polymerase I (Pol I) and a designated set of transcription factors as for instance upstream binding factor (UBF). It generates the 45S pre-rRNA precursor that is subsequently cleaved and processed into 28S, 18S and 5.8S rRNAs. These rRNAs are then packaged with ribosomal proteins to form the large and small subunits of ribosomes.

Ribosomes are macromolecular protein-RNA complexes required for translation of messenger RNA (mRNA) into proteins. Physiologically, ribosome production is associated with accurate cell growth and proliferation and regulated strictly throughout the cell cycle. In cancer cells, this regulation can be impaired, resulting in uncoupled protein synthesis from cell growth and proliferation and in the aberrant regulation of translation (reviewed in [77]).

In proliferating cells, ribosomal gene transcription accounts for 35-60% of all cellular transcription and 80% of total RNA content [78]. Previous studies showed that not all the rRNA genes are competent for transcription [79, 80]. Distinct and specific epigenetic marks characterize active and silent rRNA genes (Figure 3). The promoter of active rRNA genes is free of CpG methylation and associated with histones that are acetylated. The opposite pattern is predominant among silent genes [81]. In addition, silent genes are associated with histones modified with repressive marks (H3K9me2, H4K20me3 and H3K27me3). To note is that the levels of active and silent rRNA gene chromatin is similar both in growing and resting cells as well as during interphase and metaphase, although their run-on activities differ significantly [79]. This result suggested that chromatin of active and silent rRNA genes is stably propagated throughout the cell cycle and maintained independently of transcriptional activity. This is also consistent with data showing that in mouse cells the epigenetic and chromatin state of a given CpG methylated silent rRNA gene is propagated to the daughter cells [82]. Moreover, studies in a HeLa cell line showed that Pol I, UBF and SL1 are always associated with the same nucleolar organizing regions (NORs), the chromosomal regions containing rRNA genes [83].

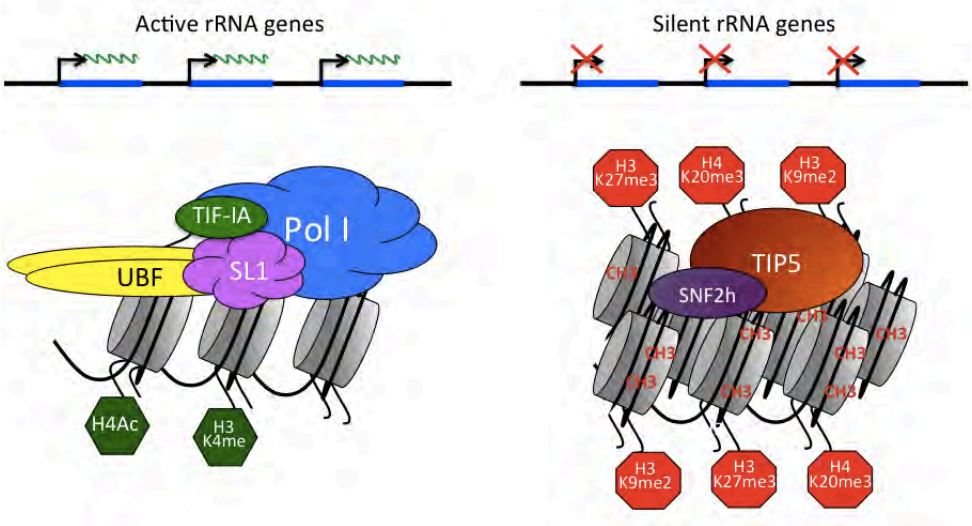

Figure 3 | Active and silent rRNA genes

Active rRNA genes (left panel) are associated with active histone marks and bound by UBF (upstream binding factor) and SL1 (selectivity factor 1) to recruit Pol I (RNA polymerase I) and multiple Pol I-associated factors such as TIF-IA (transcription initiation factor IA). Silent rRNA genes (right panel) are DNA methylated, associated with silent histone marks and bound by NoRC consistent of TIP5 and SNF2H.

3.4.1 Nucleolar remodeling complex (NoRC)

The identification of the nucleolar remodeling complex NoRC was a gain of insights into the mechanisms that establish and propagate silent rDNA chromatin [81, 84, 85]. NoRC is composed of two subunits, the ATPase SNF2H and the 205 kDa protein TIP5 (TTF1 interacting protein 5) and is the key determinant that maintains individual rDNA repeats in a heterochromatic and silent state [81, 82, 86]. The recruitment of NoRC to rDNA promoter is mediated by the interaction of TIP5 and TTF1, which is a transcription termination factor for Pol I and bound to the upstream terminator T_0 proximal of the rDNA promoter. Once bound to the promoter, NoRC represses rRNA transcription through recruitment of histone-modifying (HDAC, H3K9 and H3K27 HMTs, Poly(ADP-ribose) polymerase 1 (PARP1)) and DNA methylating enzymes (DNMT1 and 3b) [81, 84, 87]. The association of NoRC with rRNA genes takes place immediately after rDNA replication and its silencing activity is modulated by the association with a non-coding RNA originating from the intergenic rRNA region [82, 87, 88]. Taken together, NoRC coordinates epigenetic events that lead to transcriptional silencing and heterochromatin formation at the rDNA locus, linking "histone code", "DNA methylation code" and "RNA world".

3.4.2 Ribosomal RNA genes and cancer

The relationship between the nucleolus and cancer has been subject of studies for many years. Upregulation of ribosome production might contribute to neoplastic transformation by affecting the balance of protein translation, thus altering the synthesis of proteins that play an important role in the genesis of cancer [89]. The association in human carcinomas of nucleolar hypertrophy with bad prognosis is noteworthy. Abnormalities in the nucleolar morphology of cancer cells attracted the attention of tumor pathologists as early as the late 19th century. From that moment on, a series of studies have been performed to clarify whether these nucleolar changes were a consequence of the cancerous state or if, instead, they might represent a cause of neoplastic transformation. As cell proliferation appears to be closely coordinated with nucleolar function, nucleolar structural-functional changes in tumors were considered as a mere consequence of both the proliferative activity of cancer cells and alterations of the mechanisms controlling cancer cell proliferation. In the last years some data have been produced that also suggest an active role of ribosome biogenesis in tumorigenesis. For example, human non-tumor lesions characterized by an upregulation of nucleolar function were found to be associated with an increased risk of neoplastic transformation. Evidence shows that people with inherited diseases characterized by the production of abnormal ribosomes have a very high incidence of cancer.

Hypomethylation of the rRNA genes has been observed in several tumors like lung cancer, Wilms tumor and hepatocellular carcinomas [90-93]. Moreover, rDNA CpG methylation levels were found to be higher in ovarian cancer patients with long progression survival as compared with that in patients with short survival, an indication that rDNA silencing levels may influence cell growth properties essential for active tumor proliferation and tumor aggressiveness [91, 94]. Decreased CpG methylation of rRNA genes was found in many African–American women who suffer

disproportionately worse outcomes from endometrial cancer (even after controlling for socioeconomic factors and tumor stage/grade) [91]. These women possess notably lower rDNA methylation than non-African–American women. Consequently, it was proposed that rDNA methylation changes contribute in numerous ways to endometrial cancer and profiles of such alterations will likely be valuable for prognosis and therapeutic decision-making. To note, more aggressive type II endometrial cancer tumors possess significantly reduced levels of DNA methylation, as compared with the less aggressive type I endometrial cancers, possibly contributing to the type II endometrial cancer characteristic of genomic instability [95].
Taken together, all these studies suggested that controlling the CpG methylation state of rRNA genes might contribute to the aggressiveness of tumors.

3.4.3 TIP5 and cancer

Recent studies of our laboratory demonstrated that NIH3T3 cells depleted of TIP5 do not only display impairment of rRNA gene silencing but they undergo genomic instability. Knockdown of TIP5 promotes higher rRNA synthesis and formation of enlarged nucleoli, a typical result of elevated nucleolar activities [87]. Consistent with this, depletion of TIP5 and consequent impairment of rDNA silencing promoted ribosome synthesis and enhanced the productivity of recombinant proteins in NIH3T3, CHO and HEK293T cells [96]. Importantly, these cells did not only proliferate at higher rates but they also grew beyond confluence and displayed a transformed phenotype. Surprisingly, upregulation of rRNA transcription in TIP5-depleted cells does not depend on the de-repression of silent genes. Whereas the amount of CpG methylated silent genes decreases in these cells, the number of active genes is not affected. Therefore, it seems that TIP5 and (or) presence of heterochromatic silent repeats indirectly affect(s) the transcription rate of active genes, probably by enriching the nucleolar compartment of the chromatin repressor complexes. However, it cannot be excluded that upregulation of rDNA transcription is a consequence of genome instability that caused the acquisition of aberrant mechanisms of rDNA transcriptional regulation, thus representing an advantage for the elevated protein synthesis necessary for high proliferative rates.
Recently, a screen was performed to identify genes required for Ras-mediated epigenetic silencing of the pre-apoptotic Fas gene in K-ras-transformed NIH3T3 cells [97]. These results demonstrated the existence of a group of Ras epigenetic silencing effectors (RESEs) responsible for Ras-mediated epigenetic silencing of Fas. These RESEs included transcriptional regulators, DNA binding proteins, proteins involved in histone and DNA modifications (DOT1L, SMYD1, HDAC9 and DNMT1), several PcG proteins (BMI-1, EED and EZH2) and TIP5. The results described in Gazin *et al.* (2007) showed that depletion of TIP5 in K-ras-transformed NIH3T3 cells impairs DNA methylation of the Fas, Sfrp1 and Plagl1 genes. Moreover, the levels of TIP5 and the other RESEs proteins were upregulated in K-ras-transformed cells. Importantly, knockdown of TIP5 markedly inhibited anchorage-independent growth and tumor growth of the transformed cells. These results indicated that TIP5 together with PcG proteins is involved in the "elaborate" pathway for Ras-mediated epigenetic silencing.
Interestingly, putative TIP5 deregulation has been implicated in a paediatric case of pre-B acute lymphoblastic leukemia (ALL) in which a cryptic rearrangement between chromosome 12p13 and

12q13 generated a fusion of E-twenty six translocation variant (ETV) with an intronic sequence of TIP5 [98]. The authors do acknowledge, however, that the leukaemogenic impact of putative TIP5 deregulation remains undetermined at present. An additional study proposed TIP5 as an eventual biomarker for early diagnosis of osteosarcoma since the expression levels of TIP5 were higher in three osteosarcoma cell lines (U2OS, MG-63, Saos-2) than in the osteoblastic cell line hFOB1.19 [99]. TIP5 was found abundantly expressed in ovarian cancer cell lines including OVCAR3, A2780, ES2, and MPSC1, whereas its expression levels were relatively low in the OSE4 cell line that was derived from normal ovarian surface epithelium [100]. A recent study underlines the role of miR-let7c, miR-100, and miR-218 that are less expressed in metastatic prostate carcinoma. The authors proposed a role of these miRNA in the process of metastasization of prostate carcinoma and in controlling the expression of RAS, MYC, Laminin 5-β3, THAP2, SMARCA5, and TIP5 [101]. Taken together, these studies suggest that deregulation of TIP5 may have an impact on tumor development.

3.5 Aim of the thesis

The aim of this work is to determine whether:

- TIP5 plays a role in the epigenetic gene silencing process in metastatic prostate cancer cells
- This process is mediated by the association of TIP5 with EZH2
- TIP5 plays a similar role in osteosarcoma cells
- TTF1 recruits TIP5 to other gene promoters as described for rRNA genes

To test these working hypotheses, the following experimental strategies were performed:

- Examination of the microarray results of PC3 cells depleted of TIP5 and EZH2 by siRNA technology
- Analysis of gene expression profiles of prostate cancer tumors that are benign, clinically localized or metastatic and refractory to hormones
- Establishment of TIP5 and EZH2 siRNA knockdown in osteosarcoma cell line U2OS to analyze epigenetics and transcription of genes found repressed by TIP5 and EZH2 in metastatic prostate cancer cells PC3 and repressed in prostate metastatic tissues
- Identification of genes that are bound by TIP5, EZH2 and TTF1 in U2OS cells
- Investigate the association of TIP5 with EZH2 in PC3 cells

4 Material and methods

Adapted and modified from my master thesis "Role of TIP5 in Metastatic Prostate Cancer Cells".

4.1 Material

4.1.1 Cell lines

Name	Origin
HEK293T	Human Embryonic Kidney
PC3	Human Prostate Carcinoma (Bone Metastasis)
U2OS	Human Osteosarcoma

4.1.2 Media

Name	Company
DMEM	PAA
Ham's F-12	PAA
RPMI 1640	PAA
Opti-MEM	Gibco® Invitrogen

4.1.3 Buffers and solutions

Name	Composition
1x PBS buffer	140 mM NaCl 2.7 mM KCl 8.1 mM Na_2HPO_4 1.5 mM KH_2PO_4 pH 7.4
PBS-T buffer	1x PBS-buffer 0,1% Tween-20
2x BES	50 mM BES 280 mM NaCl 1.5 mM Na_2HPO_4 pH 6.96 or 7.0
1x TAE buffer	40 mM Tris-acetate 1 mM EDTA
Chromatin Extraction buffer	200 mM NaCl 10 mM HEPES 10 mM $MgCl_2$ 0.5% Triton X-100
Hypotonic buffer	0.5% NP-40 85 mM KCl 5 mM HEPES (pH 7.4)

Nuclear extraction (NE) buffer	50 mM Tris-HCl (pH 7.5) 150 mM KCl 5. mM $MgCl_2$ 0.2 mM EDTA 20% Glycerol Add prior to use: 1x Proteinase Inhibitor cocktail 0.5 mM DTT 0.1% NP-40
Washing buffer	20 mM Tris-HCl (pH 7.5) 100 mM KCl 5 mM $MgCl_2$ 0.2 mM EDTA 10% Glycerol 0.1% Tween-20 Add prior to use: 1x Proteinase Inhibitor cocktail
10x Running buffer	1% SDS 250 mM Tris 1.92 M Glycine
Laemmli buffer	2% SDS 10% Glycerol 100 mM DTT 60 mM Tris-HCl, pH 6.8 0.001% Bromphenol blue
Blocking solution	1x PBS-T 5% milk
10x Transfer buffer	250 mM Tris 1.92 M Glycine
1x Transfer buffer	10x Transfer buffer 20% Methanol 0.01% SDS
Buffer A	100 mM Tris-HCl, pH 8 10 mM DTT
Buffer B	10 mM EDTA 10 mM HEPES 10 mM EGTA 0.25% Triton X-100
Buffer C	10 mM EDTA 10 mM HEPES 0.5 mM EGTA 200 mM NaCl
Buffer D	1% SDS 50 mM Tris-HCl, pH 8 10 mM EDTA

ChIP buffer	16.7 mM Tris-HCl, pH 8 16.7 mM NaCl 1.2 mM EDTA 0.01% SDS 1.1% Triton X-100
Elution buffer	1% SDS 100 mM $NaHCO_3$
Wash buffer 1	0.1% SDS 0.167 mM NaCl 16.7 mM Tris-HCl, pH 8 1% Triton X-100
Wash buffer 2	0.1% SDS 16.7 mM Tris-HCl, pH 8 0.5 mM NaCl 1% Triton X-100
LiCl wash buffer	0.25 mM LiCl 0.5% Na-deoxycholate 0.5% NP40 1 mM EDTA 10 mM Tris-HCl, pH 8
TE buffer	10 mM Tris-HCl, pH 8 5 mM EDTA

4.1.4 Chemicals, enzymes, reagents and kits

Name	Company	Further Information
Acrylamide	SERVA	40% Acrylamide/Bis solution
Agarose	Promega Corporation	
Agarose beads	MILLIPORE	Protein A or G agarose/Salmon Sperm DNA, 50% slurry
Ammonium persulfate	SIGMA-ALDRICH	
Anti-FLAG M2 beads	SIGMA-ALDRICH	ANTI-FLAG M2 Affinity Gel A2220
BES	SIGMA-ALDRICH	Bis(2-hydroxyethyl)-2-aminoethanesulfonic acid
Bradford reagent	BIO-RAD laboratories GmBH	BIO-RAD Protein Assay
Chloroform	SIGMA-ALDRICH	
Coomassie blue	Fluka	Coomassie Brilliant Bue R 250
DMSO	SIGMA-ALDRICH	Dimethyl sulfoxide
DNase I	Thermo Scientific	
dNTPs	Fermentas	dATP, dCTP, dGTP and dTTP; 100mM
DTT	SIGMA-ALDRICH	DL-Dithiothreitol
EDTA	SIGMA-ALDRICH	Ethylenediaminetetraacetic acid
EGTA	SIGMA-ALDRICH	Ethylene glycol-bis(2-aminoethylether)-tetraacetic acid
Ethanol	MERCK	Absolute for analysis
FBS	Gibco® Invitrogen	Fetal bovine serum

Formaldehyde	SIGMA-ALDRICH	Formaldehyde solution, 36.5%
Glycin	Roche	
Glycine	BIOSOLVE	
Glycogen	Roche	
HCl	MERCK MILLIPORE	32% for analysis
HEPES	BIOSOLVE	4-(2-hydroxyethyl)-1-piperazineethanesulfonic acid
Isopropanol	MERCK	
KCl	SIGMA-ALDRICH	
Lipofectamine® RNAiMAX	Invitrogen	
Lithiumchlorid	AppliChem GmbH	
Magnetic beads	Invitrogen	Dynabeads® Protein A or G
Methanol	MERCK	
$MgCl_2$	Applied Biosystems, Roche	TaqMan®, 25mM
Milk	Migros	Rapilait, milk powder
MultiScribe™ Reverse Transcriptase	Applied Biosystems, Roche	TaqMan®, MuLV, 50 U/µl
NaCl	SIGMA-ALDRICH	
NP-40	Fluka	Nonidet P 40 Substitute
NucleoSpin RNA II Kit	Machery-Nagel	
Penicillin/Streptomycin	Gibco® Invitrogen	10'000 U/ml Penicillin, 10'000 µg/ml Streptomycin
Phenol chloroform	SIGMA-ALDRICH	Phenol:Chloroform:Isoamyl aclohol
Polybrene	SIGMA-ALDRICH	20 mg/ml
Ponceau S	SIGMA-ALDRICH	
Primer random $p(dN)_6$	Roche	2 µg/µl
Protease Inhibitor cocktail	Roche	Complete, EDTA-free
Proteinase K	Fermentas	21.2 mg/ml
PVDF membrane	MILLIPORE	Immobilon®-FL
RNase A	Fermentas	DNase and protease-free, 10 mg/ml
Rnase Inhibitor	Applied Biosystems, Roche	TaqMan®, 20 U/µl
RT Buffer 10x	Applied Biosystems, Roche	TaqMan®
SDS	SIGMA-ALDRICH	Sodium dodecyl sulfate
SYBR GREEN master mix	BIOLINE	2x SensiMix™ SYBR Kit
TEMED	SIGMA-ALDRICH	Tetramethylethylenediamine
Tris	BIOSOLVE	Tris(hydroxymethyl)aminomethane
Triton® X-100	SIGMA-ALDRICH	
TRIzol Reagent	Invitrogen	
Trypsin-EDTA	Gibco® Invitrogen	10x, 5% Trypsin
Tween® 20	SIGMA	
X-tremeGene HP DNA Transfection Reagent	Roche	
β-mercaptoethanol	SIGMA-ALDRICH	2-Mercatpo-ethanol

4.1.5 Equipment

Name	Company	Further Information
Cell Counter	INNOVATIS	Casy®
Fluorescence microscope	Leica Microsystems	Leica DMI6000 B
NanoDrop®	NanoDrop technologies, Thermo Scientific	ND-1000, Spectrophotometer
Odyssey scanner	LI-COR Biosciences	Two channel infrared detection
PCR machine	Applied Biosystems	GeneAmp® PCR System 2700
Protein separating device	BIO-RAD	Mini-PROTEAN Tetra Cell
Protein wet transfer device	BIO-RAD	Mini Trans-Blot Cell
qPCR machine	Corbett Research	Rotor-Gene RG-3000 A
Sonifier	Diagenode	BIORUPTOR®
Spectrophotometer	Thermo Spectronic	GENESYS 10uv

4.1.6 Antibodies

Antibodies	IgG	Origin	Application
Anti-TIP5 Zürich	Rabbit	Raffaella Santoro	ChIP, Western Blot
Anti-EZH2	Mouse	BD Transduction Laboratories	ChIP
Anti-EZH2	Mouse	Cell Signaling Technology	Western Blot
Anti-HA	Mouse	Santa Cruz Biotechnology	Western Blot
Anti-HA	Rabbit	Santa Cruz Biotechnology	Western Blot
Anti-PARP1	Rabbit	Santa Cruz Biotechnology	Western Blot
Anti-PARP1	Mouse	Santa Cruz Biotechnology	Western Blot
Anti-SNF2H	Rabbit	Santa Crus Biotechnology	Western Blot
Anti-TTF1	Rabbit	Raffaella Santoro	ChIP
Anti-UBF	Mouse	Santa Cruz Biotechnology	Western Blot
Anti-Rabbit	Goat	Li-Cor	Western Blot
Anti-Mouse	Goat	Li-Cor	Western Blot

4.1.7 Oligonucleotides

Name	siRNA Target Sequence	Qiagen Productname
siRNA-CTRL	not available	AllStars Negative Control siRNA
siRNA-TIP5	5′-CACTGAGAAGGCTAAGACTAA-3′	Hs_BAZ2A_4
siRNA-EZH2	not available	Hs_EZH2_7

Primer	Nucleotide Sequence	Description
ORS57	5′-TACTTGTGGAGCCGCTGAC-3′	Forward oligo hybridizing to the cDNA of human EZH2 mRNA.
ORS58	5′-CTGCCACGTCAGATGGTG-3′	Reverse oligo hybridizing to the cDNA of human EZH2 mRNA.
ORS111	5′-TGGACGATGTGCTCTATGCC-3′	Forward oligo hybridizing to the cDNA of human DAB2IP mRNA.

ORS112	5′-GGATGGTGATGGTTTGGTAG-3′	Reverse oligo hybridizing to the cDNA of human DAB2IP mRNA.
ORS168	5′-TTCCTCTTTGCATGGAATTTG-3′	Forward oligo hybridizing to the cDNA of human ADRB2 mRNA.
ORS169	5′-AGAGGAGTGGGGGAAGAGTC-3′	Reverse oligo hybridizing to the cDNA of human ADRB2 mRNA.
ORS170	5′-TGCACCACCAACTGCTTAGC-3′	Forward oligo hybridizing to the cDNA of human GAPDH mRNA.
ORS171	5′-GGCATGGACTGTGGTCATGAG-3′	Reverse oligo hybridizing to the cDNA of human GAPDH mRNA.
ORS181	5′-CGAGCCCCTAGCACCCGACA-3′	Forward oligo hybridizing to the human ADRB2 gene at positions -171 to -152.
ORS182	5′-GGTCCGGCGCATGGCTTCTA-3′	Reverse oligo hybridizing to the human ADRB2 gene at positions +45 to +64.
ORS184	5′-CAACCGTCCCGGCGTCTTCC-3′	Forward oligo hybridizing to the human DAB2IP gene at positions -225 to -204.
ORS185	5′-CCCCTTTCCAGCCCTCGCCT-3′	Reverse oligo hybridizing to the human DAB2IP gene at positions -96 to -77.
ORS214	5′-TCGGCCTGAGACACCGGAGG-3'	Forward oligo hybridizing to the cDNA of human MKX mRNA.
ORS215	5′-CGTCATCTGCGAGCCGAGGG-3′	Reverse oligo hybridizing to the cDNA of human MKX mRNA.
ORS216	5′-TTGACGCAGAGCGCAGCCAA-3′	Forward oligo hybridizing to the cDNA of human HOMER2 mRNA.
ORS217	5′-TGCAGTGCTGTGGTCAGCCG-3′	Reverse oligo hybridizing to the cDNA of human HOMER2 mRNA.
ORS218	5`-CCGACAAGCCCAGCGACAGG-3′	Forward oligo hybridizing to the cDNA of human AOX1 mRNA.
ORS219	5`-GTGGCTGGACCAACGCCTCC-3′	Reverse oligo hybridizing to the cDNA of human AOX1 mRNA.
ORS220	5`-GCTTGTGGCCCTGAGGCTGG-3′	Forward oligo hybridizing to the cDNA of human LAMB3 mRNA.
ORS221	5`-TGGGCATTGAAGCCCCGCAG-3′	Reverse oligo hybridizing to the cDNA of human LAMB3 mRNA.
ORS222	5`-AGCAGCCCCAGCGGATCTGA-3′	Forward oligo hybridizing to the cDNA of human ZNF185 mRNA.
ORS223	5`-GTCCTGCCAGGCCTCTCCGA-3′	Reverse oligo hybridizing to the cDNA of human ZNF185 mRNA.
ORS226	5`-GCCTCAACACCCGTGGGAGC-3′	Forward oligo hybridizing to the cDNA of human FBN1 mRNA.
ORS227	5`-GCACTCGTCCTGGTTGGGGC-3′	Reverse oligo hybridizing to the cDNA of human FBN1 mRNA.

ORS228	5`-CCCATCACCACGGGAGGGGT-3′	Forward oligo hybridizing to the cDNA of human FHL2 mRNA.
ORS229	5`-CTGTGAGGAAGCCACGCCCC-3′	Reverse oligo hybridizing to the cDNA of human FHL2 mRNA.
ORS230	5`-CCTACGGCAACCTGCCCTGC-3′	Forward oligo hybridizing to the cDNA of human HOXA7 mRNA.
ORS231	5`-GCGCCTTTGGCGAGGTCACT-3′	Reverse oligo hybridizing to the cDNA of human HOXA7 mRNA.
ORS232	5`-ACCTCCGACCCCATTGGCGA-3′	Forward oligo hybridizing to the cDNA of human KLF6 mRNA.
ORS233	5`-AAGTCCCGCTGCGCACCTTC-3′	Reverse oligo hybridizing to the cDNA of human KLF6 mRNA.
ORS244	5`-AGGGCTAGTGTGCTCTAGGGGT-3`	Forward oligo hybridizing to the human LAMB3 gene.
ORS245	5`-TGGGGTGATCCCCAGAAAGGACC-3`	Reverse oligo hybridizing to the human LAMB3 gene.
ORS244 Z	5′-CAACGCTTGCCACCCCCGAT-3′	Forward oligo hybridizing to the human ZNF185 gene.
ORS245 Z	5′-TTGGTGCGGCCTCCAAGAGC-3′	Reverse oligo hybridizing to the human ZNF185 gene.
ORS250	5`-AGGTTGCTGAAAAGCCAGGAGTCA-3`	Forward oligo hybridizing to the human FHL2 gene.
ORS251	5`-AAGAGAGATTCGTTGCAATGGTGGC-3′	Reverse oligo hybridizing to the human FHL2 gene.
ORS252	5`-CCTGTGAGGACTGCTGAGATTG-3`	Forward oligo hybridizing to the human HOXA7 gene
ORS253	5`-CCCCCAGATTTACACCAAACC-3`	Reverse oligo hybridizing to the human HOXA7 gene.
ORS254	5`-CCACAAAAAGTGTGTCGGCTTCGAG-3`	Forward oligo hybridizing to the human HOXB8 gene
ORS255	5`-TTCGCCGGCTCCTAGTCACCC-3`	Reverse oligo hybridizing to the human HOXB8 gene.
ORS260	5′-GAACCAGCGCGGACACCACA-3′	Forward oligo hybridizing to the human AOX1 gene.
ORS261	5′-GCTCACCTTGCGGCCGTTCA-3′	Reverse oligo hybridizing to the human AOX1 gene.
ORS262	5`-GCGCTCCGGGGAGACTTTCG-3`	Forward oligo hybridizing to the human KLF6 gene.
ORS263	5`-GGGAGCACGTCCATGTCGGG-3`	Reverse oligo hybridizing to the human KLF6 gene.
ORS317	5′-TACTAGCGGTTTTACGGGCG-3′	Forward oligo hybridizing to the human GAPDH gene.
ORS318	5′-TCGAACAGGAGGAGCAGAGAGCG-3′	Reverse oligo hybridizing to the human GAPDH gene.
ORS339	5′-GCACATGGAGCCAATATGCG-3′	Forward oligo hybridizing to the cDNA of human MYT1 mRNA.

ORS340	5′-GAGGGAGGTAAACGGTGTGG-3′	Reverse oligo hybridizing to the cDNA of human MYT1 mRNA.
ORS347	5′-CCACTCCAAGCTCCTAAGGG-3′	Forward oligo hybridizing to the cDNA of human KCNA1 mRNA.
ORS348	5′-CTCTCCAGTTCCCTTCGCTC-3′	Reverse oligo hybridizing to the cDNA of human KCNA1 mRNA.
ORS349	5′-GATGACTGCGGGAGACAACC-3′	Forward oligo hybridizing to the cDNA of human CNR1 mRNA.
ORS350	5′-AGTTCTCCCCACACTGGATG-3′	Reverse oligo hybridizing to the cDNA of human CNR1 mRNA.
ORS361	5′-CAGGAAGACACCTCTCACAC-3′	Forward oligo hybridizing to the cDNA of human MYT1 mRNA.
ORS362	5′-ACAGTGTCCAGGGGCTTTGC-3′	Reverse oligo hybridizing to the cDNA of human MYT1 mRNA.
ORS363	5′-ATCTGGCACCACACCTTCTACA-3′	Forward oligo hybridizing to the cDNA of human β-ACTIN mRNA.
ORS364	5′-TCACCGGAGTCCATCACGAT-3′	Reverse oligo hybridizing to the cDNA of human β-ACTIN mRNA.
Hottiger 711 F	5′-CCTCACCCTCCAACAAAGAT-3′	Forward oligo hybridizing to the human IL6 gene.
Hottiger 712 R	5′-GCCTCAGACATCTCCAGTCC-3′	Reverse oligo hybridizing to the human IL6 gene.
hrDNA -150	5′-CGATGGTGGCGTTTTTGG-3′	Forward oligo hybridizing to the human rRNA promoter at positions -150 to -132.
hrDNA +9/+21	5′-GACAGGTCGCCAGAGGACAGC-3′	Reverse oligo hybridizing to the human rRNA gene at positions +9 to +21.
hrDNA +502/19	5′-CGTCCTTCTCGCTCCGCC-3′	Forward oligo hybridizing to the human rDNA at positions +502 to +519 used for 45S pre-rRNA amplification.
hrDNA +705/687	5′-GTGGTTGTCGACTTGCGGG-3′	Reverse oligo hybridizing to the human rDNA at positions +687 to +705 used for 45S pre-rRNA amplification.
mhTIP5 625–644 F	5′-AAGATGTGTGGCTACAATGG-3′	Forward oligo hybridizing to the mouse and human TIP5 gene at positions +625 to +644 used for cDNA amplification.
mhTIP5 842–860 R	5′-TCTGCACCCATCAGCTCCG-3′	Reverse oligo hybridizing to the mouse and human TIP5 gene at positions +842 to +860 used for cDNA amplification.
mh28S F +8124	5′-GCGACCTCAGATCAGACGTGG-3′	Forward oligo hybridizing to the mouse and human 28S rRNA.

mh28S R +8246	5′-CTGTTCACTCGCCGTTACTGAG-3′	Reverse oligo hybridizing to the mouse and human 28S rRNA.
H4 F	5′-CGACGACCCATTCGAACGTCT-3′	Forward oligo hybridizing to the human rDNA coding region at positions +3990 to +4010.
H4 R	5′-CTCTCCGGAATCGAACCCTGA-3′	Reverse oligo hybridizing to the human rDNA coding region at positions +4072 to +4092.
MYT1 F	5′-AGGCACCTTCTGTTGGCCGA-3′	Forward oligo hybridizing to the human MYT1 gene at positions -550 to -530.
MYT1 R	5′-AGGCAGCTGCCTCCCGTACA-3′	Reverse oligo hybridizing to the human MYT1 gene at positions -220 to -201.
KCNA1 F	5′-TGACGGTGATGTCTGGGGAG-3′	Forward oligo hybridizing to the human KCNA1 gene at positions +1107 to +1126.
KCNA1 R	5′-GGTTGCGGTCGAAGAAGTAC-3′	Reverse oligo hybridizing to the human KCNA1 gene at positions +1342 to +1361.
CNR1 F	5′-GCAGAGCTCTCCGTAGTCAG-3′	Forward oligo hybridizing to the human CNR1 gene.
CNR1 R	5′-AACAGGCTGGGGCCATACAG-3′	Reverse oligo hybridizing to the human CNR1 gene.

4.2 Cell culture methods

4.2.1 Cell culture

HEK293T and U2OS cells were cultured in DMEM containing stable glutamine. PC3 cells were cultured in RPMI and Ham's F-12 (1:1). Both media were supplemented with 10% fetal calf serum and 1% Penicillin/Streptomycin. Cells were grown at 37 °C with 5% CO_2 in humid environment.
To trypsinize cells, plates containing adherent cells were washed with 1x PBS (HEK293T: once; U2OS and PC3: three times) and then 1x Trypsin-EDTA was added. After removing Trypsin, HEK293T cells were collected with 3 ml DMEM from the plate and transferred into a falcon tube containing 7 ml medium. U2OS and PC3 cells were collected in trypsin, transferred into a falcon tube containing 5 ml Ham's F-12 and RPMI, centrifuged (1'000 rpm, 3 min) and cell pellet was dissolved in fresh medium. Cells were then seeded directly or first counted with Casey Counter.

4.2.2 Freezing and thawing of cultured cells

To make cell aliquots, cells were trypsinized as previously described and centrifuged (1'000 rpm, 3 min). Cells were resuspendend in 500 µl medium per aliquot. 500 µl cell suspension were pipetted into a 1 ml cryotube and 500 µl mix consisting of 200 µl medium, 200 µl FBS and 100 µl DMSO were

slowly added to the cells. The tube was inverted instantly, put into a box that was wrapped with paper towel to guarantee a slow freezing process and stored at -80 °C for 15-72 h before transferring it into liquid nitrogen.
Cell aliquots were taken into culture by thawing them at 37 °C for 5-10 min. Cells were collected into a falcon tube and the cryotube was rinsed with 2 ml medium to collect all cells. After centrifugation (1'000 rpm, 5 min), cells were resuspended in fresh medium and seeded on a plate.

4.2.3 Transient transfection

4.2.3.1 Calcium phosphate transfection

24 h prior transfection, cells were seeded. DNA mix was prepared as follows:

Size of plate	Cell number	DNA	2.5 M $CaCl_2$	H_2O
24-well plate	50'000	525 ng	732.5 nl	Fill up to 14.65 µl
10 cm Ø plate	10^6	20 µg	50 µl	Fill up to 500 µl
15 cm Ø plate	2.5 x 10^6	40 µg	100 µl	Fill up to 1 ml

While vortexing the DNA mix, one volume of 2x BES solution was added dropwise. The mix was incubated for 10 s at room temperature and vortexed for another 10 s before distributing it equally on adherent cells.
After 12 h, medium was changed and two or three days past transfection cells were harvested for analysis.

4.2.3.2 X-tremeGENE HP transfection

The X-tremeGene HP DNA Transfection Reagent was used to transfect PC3 cells for CoIP.
5 x 10^6 cells were seeded on a 15 cm diameter plate and 24 h later cells were transfected. Transfection mix consisted of 20 µg DNA, 20 µl transfection reagent and 1960 µl Opti-MEM medium and was incubated 15 min at room temperature prior to the transfection.
After 12h, mediudm was changed and three days past transfection cells were harvested for analysis.

4.2.3.3 Lipofectamine® RNAiMAX transfection

For each 6-well plate, 500 µl Opti-MEM were mixed with 4 µl siRNA in a 1,5 ml tube. After short vortexing, 4 µl Lipofectamine RNaiMAX were added and again vortexed. The mix was incubated for 20 min at room temperature.
PC3 cells were splitted, counted and diluted with medium to a concentration of 0.2 x 10^6 per ml. For each 6-well plate, 1 ml of cell suspension and the transfection mix were added and gently mixed by pipetting. U2OS cells were seeded in the same amount of medium with the same concentration as PC3 cells but 24 h before the transfection mix was added.

For ChIP 10 cm plates were transfected: 10^6 cells were seeded in 6 ml medium and the mix consisted of 24 µl siRNA, 24 µl Lipofectamine RNaiMAX and 3 ml Opti-MEM.
Approximately 16 hours post transfection, medium containing transfection agents was removed and replaced by 2.5 ml standard medium. Three days past transfection, cells were collected for analysis.

4.2.4 Retrovirus production

Viruses were produced in HEK293T cells. 3 x 10^6 cells were seeded on a 10 cm diameter plate and 24 h later, cells were transfected with 6 µg pcDN-LBH, 6 µg LTR-G and 12 µg of the required plasmid. After 12 h, medium was replaced with standard medium. 24 h and 48 h later, medium containing virus particles was collected. Virus aliquots were centrifuged (3'000 rpm, 5 min), 9 ml of supernatant were taken carefully without contacting cell pellet, collected into a new falcon tube and stored at -80 °C. Tubes were labeled as day1 and day2.

4.2.5 Retroviral transduction

To transduce PC3 cells, 10^6 cells were seeded on a 10 cm diameter plate. 24 h later, virus aliquots from day1 and day2 were mixed together and 36 µg polybrene (PB) were added to 9 ml virus mix. 9 ml medium were removed from PC3 cells and virus-PB mix was added to the cells. 12 h later, the whole medium was replaced and three days after the infection cells were harvested for analysis or splitted.

4.3 RNA analysis

4.3.1 RNA extraction with TRIzol Reagent

To isolate RNA, cells were lysed with 500 µl TRIzol Reagent and incubated for 5 min at room temperature. After centrifugation (10'000 rpm, 10 min, 4 °C), supernatant was transferred into a new 1.5 ml safe lock reaction tube, 100 µl chloroform were added and after vigorous mixing, incubated for 15 min at room temperature and centrifuged (12'000 rpm, 15 min, 4 °C). The aqueous phase containing RNA was transferred into a 1.5 ml safe lock reaction tube containing 250 µl isopropanol. 1 µl glycogen was added to samples containing low RNA amounts. Samples were vortexed, RNA was pelleted by centrifugation (13'000 rpm, 10 min, 4 °C) and washed with 250 µl 75% EtOH (13'000 rpm, 5 min, 4 °C). Prior to centrifugation, samples containing low amounts of RNA were incubated for 10 min at -80 °C. Supernatant was discarded and RNA was air-dried. Pellets were dissolved in 40 µl H_2O and incubated for 5 min in the heatblock at 60 °C. RNA concentration was measured with NanoDrop and RNA was stored at -80 °C.

4.3.2 RNA extraction with NucleoSpin RNA II Kit

To isolate RNA, cells were washed with cold PBS and centrifuged (3'000 rpm, 5 min, 4 °C). All the following steps were performed at room temperature. Cell pellets were resuspended in 350 µl RA1 buffer containing 3,5 µl β-mercaptoethanol and vortexed vigorously. The lysate was loaded into the violet column and centrifuged (11'000 g, 1 min). The column was discarded and 350 µl 75% EtOH were added to the flow through and mixed by pipetting. The mixture was transferred into the blue column and centrifuged (11'000 g, 30 s). Flow through was discarded and 350 µl MDB buffer were added to the blue column in order to dry the membran. After centrifugation (11'000 g, 1 min), the flow through was discarded and 95 µl DNAse mix (10 µl rDNAse and 90 µl 10x reaction buffer) were pipetted on the column membrane and incubated for 15 min at room temperature. 200 µl RA2 buffer were added, column was centrifuged (11'000 g, 30 s) and flow through discarded. 600 µl RA3 buffer were added, column was centrifuged (11'000 g, 30 s) and flow through discarded. Next, 250 µl RA3 buffer were added and centrifuged (11'000 g, 2 min) to dry membrane. To elute RNA, the column was placed into a new safe lock reaction tube, 60 µl H_2O were added on the column and centrifuged (11'000 g, 1 min). RNA concentration was measured with NanoDrop and samples were stored at -80 °C.

4.3.3 Reverse transcription

Reverse transcription reactions were performed in a total volume of 20 µl and contained 5.5 mM $MgCl_2$, 1x RT buffer, 0.5 mM dNTPs, 0.5 µg dN6 random primers, 25 U MuLV Reverse Transcriptase, 5 U RNase Inhibitor, 500-1'000 ng RNA and H_2O. Reactions were incubated for 10 min at room temperature to allow hybridization of primers with RNA and then for 61 min at 42 °C followed by 5 min at 90 °C. Synthesized cDNA was stored at -20 °C. Samples were diluted 1:5 prior to qPCR measurements.

4.4 Quantitative PCR (qPCR)

Quantitative PCR reactions were performed in 10 µl volume and contained 2 µl DNA or cDNA sample, 1x SYBR GREEN master mix, 2 pmoles forward primer, 2 pmoles reverse primer. To amplify CG rich regions (e.g. human rDNA sequences), reactions were performed in the presence of 3.25 M DMSO and 4 pmoles of each primer. Standard reaction conditions were as follows: 10 min at 95 °C; 40-45 cycles of 20 s at 95 °C, 30 s at 55 °C or 60 °C and 30 s at 72 °C; melting from 55 °C or 60 °C to 99 °C with steps of +1 °C, the first raise took 45 s and the following ones 10 s each.
Quantifications were performed either using standard curve or Ct values. Standard curves represent serial dilutions of genomic DNA (100 ng to 0.1 ng) or cDNA (dilution 2:1, 1:1, 1:2 to 1:4). Quantifications by Ct were performed using the formula $2^{-\Delta Ct}$. ΔCt represents either $Ct_{Sample} - Ct_{Normalization\ sample}$ for cDNA samples or $Ct_{Sample} - Ct_{Input}$ for ChIP samples.

4.5 Protein analysis

4.5.1 Chromatin extraction

Cells were washed twice with 800 µl cold PBS (3'000 rpm, 5 min, 4 °C), resuspended with Chromatin Extraction buffer supplemented with 1x protease inhibitor (PI) and mixed by rotating on a wheel during 30 min at room temperature. Soluble and chromatin-bound proteins were separated by centrifugation (10'000 rpm, 10 min, 4 °C), supernatant was transferred into a new reaction tube and the pellet was resuspended in the same volume of Chromatin Extraction buffer + PI as used before. Protein concentration of soluble proteins was measured by Bradford assay using Chromatin Extraction buffer as blank. Supernatant was sonicated 1x 30s and resuspended pellet was sonicated several times till a low viscosity was reached.

4.5.2 Co-Immunoprecipitation (CoIP)

5 x 10^6 cells were seeded on a 15 cm diameter plate, transfected with HA-Flag- and control-plasmids and grown for 3 – 4 days.
After removing medium, cells were harvested in 1.6 ml cold PBS, transferred into a 2 ml tube, centrifuged (3'000 rpm, 5 min, 4 °C) and washed twice with 800 µl cold PBS (3'000 rpm, 5 min, 4 °C). Pellets were then resuspended in 500 µl hypotonic buffer, centrifuged (8'000 rpm, 10 min, 4 °C) and nuclei were resuspended in 300 µl NE buffer. After sonication (twice for 30 s at 4 °C), 10 µl DNase I were added to the nuclear extracts and incubated for 1 h on ice (interrupted by short mixing every 15 min). Then the samples were sonicated again 2x 30 s, centrifuged (6'000 rpm, 10 min, 4 °C) and supernatants were taken to perform Bradford protein assay.
Anti-FLAG M2 beads were washed three times with 1 ml cold PBS (500 g, 5 min, 4 °C), two times with 1 ml NE buffer (500 g, 5 min, 4 °C) and then resuspended in NE buffer.
For the input, 100 µg protein sample was stored at -20 °C. For the immunoprecipitation 1 mg protein sample was used and and diluted to 1 mg/ml using NE buffer (total volume 1 ml). Beads were equally distributed to samples and incubated at 4 °C overnight by gently rotation using a rotating wheel.
IP samples were washed three times with 950 µl washing buffer. The washing steps consist of centrifugation (500 g, 5 min, 4 °C) and incubation with washing buffer (rotating on a wheel, 5 min, 4 °C). Afterwards beads were resuspended in 40 µl 1x Laemmli buffer, boiled for 5 min at 95 °C, centrifuged and supernatant and the input samples (3x Laemmli buffer added, cooked 5 min at 95 °C) were analyzed by SDS-PAGE followed by western blot.

4.5.3 Bradford protein assay

To measure protein concentration the Bradford assay was performed. 5x Bradford buffer was diluted with H_2O to 1x and 1 µl protein sample or adequate buffer were added.

Absorbance was measured at 595 nm using a spectrophotometer. The following formula was used to calculate the concentration:

$$\frac{\mathrm{OD595} - 0.095}{0.065} = \text{concentration } \mu g/\mu l$$

4.5.4 SDS polyacrylamide gel electrophoresis (SDS-PAGE)

SDS-PAGE was used to separate proteins. Gels were made as follows:

Solution components	6% Separation gel	15% Separation gel	5% Stacking gel
H_2O	5.8 ml	3.55 ml	3.6 ml
40% acrylamide mix	1.5 ml	3.75 ml	0.63 ml
1.5 M Tris (pH 8.8)	2.5 ml	2.5 ml	
1 M Tris (pH 6.8)			0.63 ml
10% SDS	0.1 ml	0.1 ml	0.05 ml
10% ammonium persulfate	0.1 ml	0.1 ml	0.05 ml
TEMED	0.016 ml	0.008 ml	0.01 ml

Polymerized gel was placed in a running unit that was filled with 1x Running buffer. Protein samples were supplemented with Laemmli buffer containing 10% β-mercaptoethanol and boiled at 95 °C for 5 min before loading. Electrophoretic separation was performed at 120 V during 1-2 h.

4.5.4.1 Coomassie staining

Coomassie staining was performed to normalize protein amounts on a 15% histone gel. The gel was incubated 10 min in Coomassie blue solution (0.25% Coomassie blue, 40% methanol, 10% acetic acid) and afterwards destained with fast destainer solution (25% Ethanol, 10% acetic acid).

4.5.5 Western blot

Proteins separated by SDS-PAGE were blotted on a polyvinylidene fluoride (PVDF) membrane by wet transfer (see 4.5.5.1). Efficiency of protein transfer was checked by Ponceau staining (see 4.5.5.2). The membrane was blocked by incubation with blocking solution for 1 h and incubated with the primary antibody diluted in blocking solution with moderate shaking at 4 °C overnight or 3-5 h at room temperature. The membrane was washed twice 20 min with PBS-T and incubated with the secondary antibody for 1-3 h at room temperature by moderate shaking. After 2x 20 min wash steps in PBS-T, signals were detected by scanning two infrared channels with Odyssey.

4.5.5.1 Wet transfer

To perform wet transfer, a "sandwich" was assembled in a running unit filled with 1x transfer buffer as follows: a sponge, three blotting papers, a methanol-activated PVDF membrane, the

polyacrylamide gel, three blotting papers and on top a sponge. A cooling element and a magnetic stirrer were added to the unit, which was installed in the cold room (4 °C), run at 30 V overnight and at 100 V for the last hour.

4.5.5.2 Ponceau staining

To check transfer efficiency, membranes were incubated with Ponceau red (1% Ponceau S, 0.1% Acetic acid) for 2 min and destained with double distilled H_2O.

4.6 Chromatin immunoprecipitation (ChIP)

10^6 or 2.5x 10^6 cells were seeded on a 10 or 15 cm diameter plate and grown for 4 days.
Chromatin was crosslinked by adding 1% formaldehyde to the medium and incubating cells for 10 min at room temperature. To stop crosslinking-reaction, 0.1 M glycine (final concentration) was included and the reaction was incubated for 10 min at room temperature. After removal of the medium, cells were collected, washed twice with 800 µl cold PBS (6'000 rpm, 5 min, 4 °C) and resuspended thoroughly in 600 µl buffer A to purify nuclei. Cells were incubated for 15 min at 4 °C, vortexed and then incubated for 15 min at 30 °C under light agitation. After centrifugation (6'000 rpm, 5 min, 4 °C), supernatant was discarded and nuclei were resuspended in 500 µl buffer B and kept on ice for 5 min. After centrifugation (6'000 rpm, 5 min, 4 °C), nuclei were resuspended in 800 µl buffer C and incubated on ice for 5 min. After centrifugation (6'000 rpm, 5 min, 4 °C), nuclei were resuspended in 300 µl freshly prepared buffer D at room temperature.
Chromatin was fragmented by ultra sonication using a sonifier. Samples were sonicated twice for 15 min with cycles of 30 s on and 30 s off. Fragmented chromatin was centrifuged (7'000 rpm, 7 min) and supernatant transferred into a new reaction tube.
To measure the concentration and check the size of sonicated chromatin, an aliquot of 5 µl chromatin was further analysed, while the rest of chromatin was stored at -80 °C. 5 µl chromatin were incubated with 20 µl Proteinase K mix (20 µg of Proteinase K in 0.39 M Tris-HCl (pH 8), 1.95 M NaCl and 0.1 M EDTA) in the presence of 300 µl elution buffer. The reaction was incubated for 1 h at 42 °C and overnight at 65 °C. After conclusion of the reaction, 350 µl phenol chloroform were added. Mixture was vortexed, centrifuged (7'000 rpm, 10 min), inverted and centrifuged again. The aqueous phase containing RNA and DNA was transferred into a new reaction tube containing 1 µl glycogen, 35 µl 3M NaAcetate (pH5.5) and 700 µl absolute EtOH, vortexed, incubated 10 min at -80 °C and centrifuged (13'000 rpm, 10 min, 4 °C). The pellet was air-dried and dissolved in 20 µl H_2O. The concentration of RNA and DNA was measured with NanoDrop. The size of the fragmented chromatin was analysed by incubating the samples with 0.2 µg RNase A for 20 min at 37 °C and analysing 1 µg of sample by agarose gel electrophoresis (1% agarose, 1x TAE, 120 V, 15 min). Only samples with a DNA size of 200-400 bp were used for ChIP assay.

To perform ChIP experiments, 5 µg of chromatin were used as input and stored at -20 °C. For each ChIP assay, 20 µg of chromatin were incubated with indicated antibodies in a reaction volume of 500 µl containing 1x PI and ChIP buffer and mixed on a rotating wheel overnight at 4 °C. Agarose or magnetic beads were added and incubated on a wheel for 4 h at 4 °C. Bead-bound chromatin samples were washed (5 min incubation on a wheel; 6'000 rpm 1 min or 1 min on magnetic rack) as follows: 2x 800 µl wash buffer 1, 1x 800 µl wash buffer 2, 2x 800 µl LiCl wash buffer, 1x 800 µl TE buffer and 1x 500 µl TE buffer. Elution of chromatin from beads was performed by incubating the samples with 300 µl elution buffer by rotation on a wheel for 20 min. Samples were centrifuged (6'000 rpm, 2 min) and supernatant was transferred into a new reaction tube containing 20 µl Proteinase K mix. Input samples were dissolved in 300 µl elution buffer and 20 µl of Proteinase K mix. Samples and inputs were incubated for 1 h at 42 °C and at 65 °C overnight. Phenol chloroform extraction and EtOH precipitation were performed as previously described. Pellets were air-dried and dissolved in 30 µl H_2O for ChIP samples or 100 µl H_2O for inputs. Target gene regions were analysed by qPCR.

5 Results

5.1 TIP5 levels are upregulated in metastatic prostate cancer

The study of Gazin *et al.* suggests that TIP5 and the histone methyltransferase enhancer of zeste homolog 2 (EZH2) might share a common pathway to epigenetically silence genes that are critical for cancer initiation and tumor development [97]. Previous studies showed that EZH2 is overexpressed in hormone-refractory, metastatic prostate cancer [65] and that strong EZH2 expression is associated with increased tumor cell proliferation in different cancer types as well as with decreased long time survival rate in metastatic prostate cancer [63]. Interestingly, previous results from our laboratory identified EZH2 as TIP5-interacting protein in HEK293T cells.

As already shown in my master thesis, we analyzed gene expression profiles (GDS1439 and GDS2545) published at Gene Expression Omnibus database (GEO) for TIP5 and EZH2 expression levels in different prostate tissues including normal prostate tissue, tissue adjacent to tumor, clinically localized and metastatic tumors (Figure 4). As expected, EZH2 expression levels were higher in metastatic tumor tissue compared to benign and clinically localized samples. Notably, also TIP5 levels increased in the metastatic samples while the expression of the Pol I transcription factor UBF was not affected. These results suggest that TIP5 and EZH2 might share a common pathway to epigenetically silence genes in metastatic cancer.

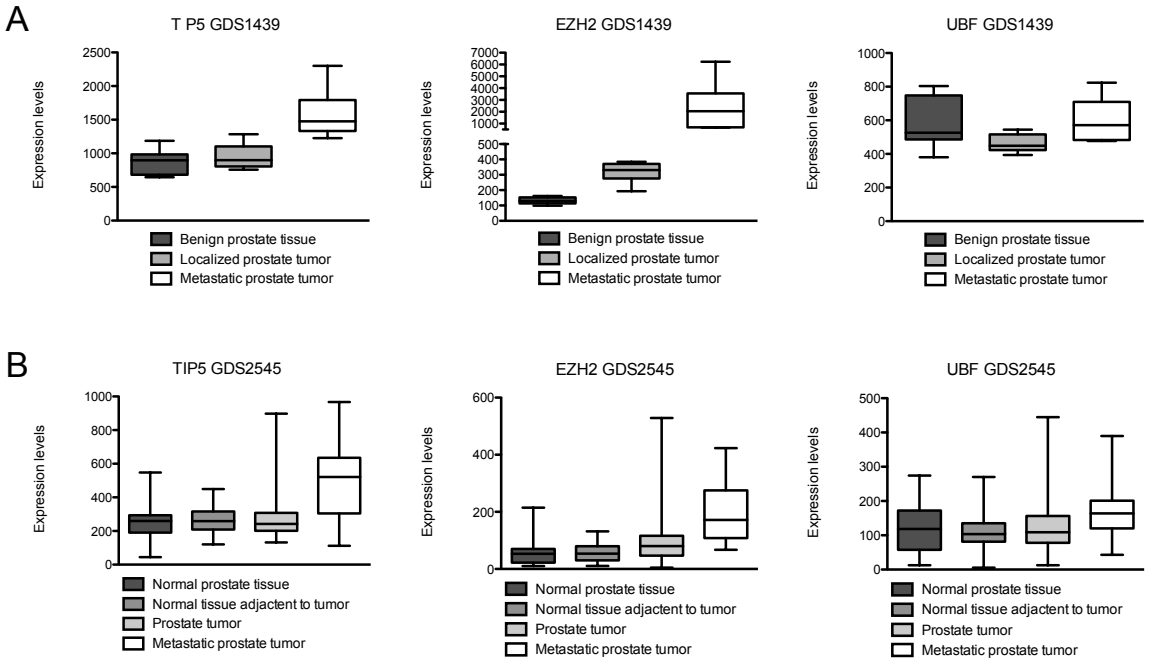

Figure 4 | Increased TIP5 expression levels in metastatic prostate tumors

A | GEO expression profiling (GDS1439) of 6 benign prostate tissue samples (4 samples and 2 pooled samples), 7 clinically localized primary prostate cancer tissue samples (5 samples and 2 pooled samples) and 6 hormone-refractory metastatic prostate cancer tissue samples (4 samples and 2 pooled samples). **B |** GEO expression

profiling (GDS2545) of normal prostate tissues from 18 donors, normal prostate tissue adjacent to the tumor of 63 donors, 65 primary prostate tumor samples and 25 metastatic prostate tumor samples (location of metastatic samples: 5 liver, 1 lung, 1 recurrent in prostate, 1 kidney, 2 adrenal gland, 3 retroperitoneal lymph node, 1 inguinal lymph node, 8 para-tracheal lymph node, 3 para-aortic lymph node). Expression profiles of TIP5, EZH2 and UBF are shown.

5.2 TIP5 and EZH2 regulate genes implicated in developmental processes in metastatic prostate cancer cells (PC3)

Based on the results described above, we carried out a transcriptomic analysis to determine whether TIP5 regulates together with EZH2 gene expression in metastatic prostate cancer cells. We performed a RNA exon microarray analysis to measure and compare transcript levels of metastatic prostate cancer cells PC3 that were depleted either of TIP5 or EZH2 by siRNA. As control we used PC3 cells transfected with siRNA-CTRL (control).
Transcriptomic analysis revealed that TIP5 regulates 1904 genes and EZH2 1787 genes in PC3 cells (fold change > 1.5 or < 0.75 and $P < 0.005$; Figure 5). Remarkably, 626 genes are regulated by both TIP5 and EZH2, indicating that about 30% of genes regulated by TIP5 are also regulated by EZH2 and *vice versa* (Figure 5). We classified genes both regulated by EZH2 and TIP5 into two groups: upregulated and downregulated transcription upon knockdown of TIP5 or EZH2. Of the 626 genes that were regulated by both TIP5 and EZH2, 309 genes (49%) were both upregulated by depletion of TIP5 or EZH2 and 276 (44%) both downregulated, indicating that TIP5 and EZH2 affect transcription levels in a similar manner and might probably operate on the same pathway.
We named the 309 genes whose expression increased upon knockdown of both TIP5 and EZH2 RTEM (repressed by TIP5 and EZH2 in metastasis) genes. The counterpart of 276 downregulated genes we referred to as ATEM (activated by TIP5 and EZH2 in metastasis) genes.

In order to determine which biological functions characterize those genes regulated by TIP5 and/or EZH2 in PC3 cells we performed Gene Ontology (GO) term biological functional analysis with the Database for Annotation, Visualization and Integrated Discovery (DAVID) according to the protocol published in Nature Protocols 4, 2009 [102]. The top seven functional categories of every gene subgroup are shown in Figure 5. Remarkably, upregulated genes in PC3 cells depleted of TIP5 or EZH2 were highly enriched in developmental processes whereas the downregulated genes are related to immunological processes and responses to different stimuli. RTEM and ATEM genes displayed similar functional classifications, indicating that TIP5 and EZH2 operate on the same biological processes in metastatic prostate cancer cells. Of note is the enrichment of genes upregulated by TIP5 or EZH2 in developmental processes. Indeed, EZH2 is well known to be a key regulator of embryonic stem cell self-renewal and accumulating evidences suggested prostate cancer stem cells to be responsible for tumor initiation, progression, therapy resistance, relapse and metastasis [63, 103].
Sandra Frommel, PhD student of Dr. Santoro's laboratory, performed a similar transcriptomic analysis with non-cancer epithelial prostate cells RWPE1. Interestingly, genes regulated by TIP5 and EZH2 in RWPE1 cells were enriched in cell cycle processes but not in developmental processes (data

not shown). These results strongly suggested that the function of TIP5 and EZH2 in neoplastic cells is not the same one as in normal cells.

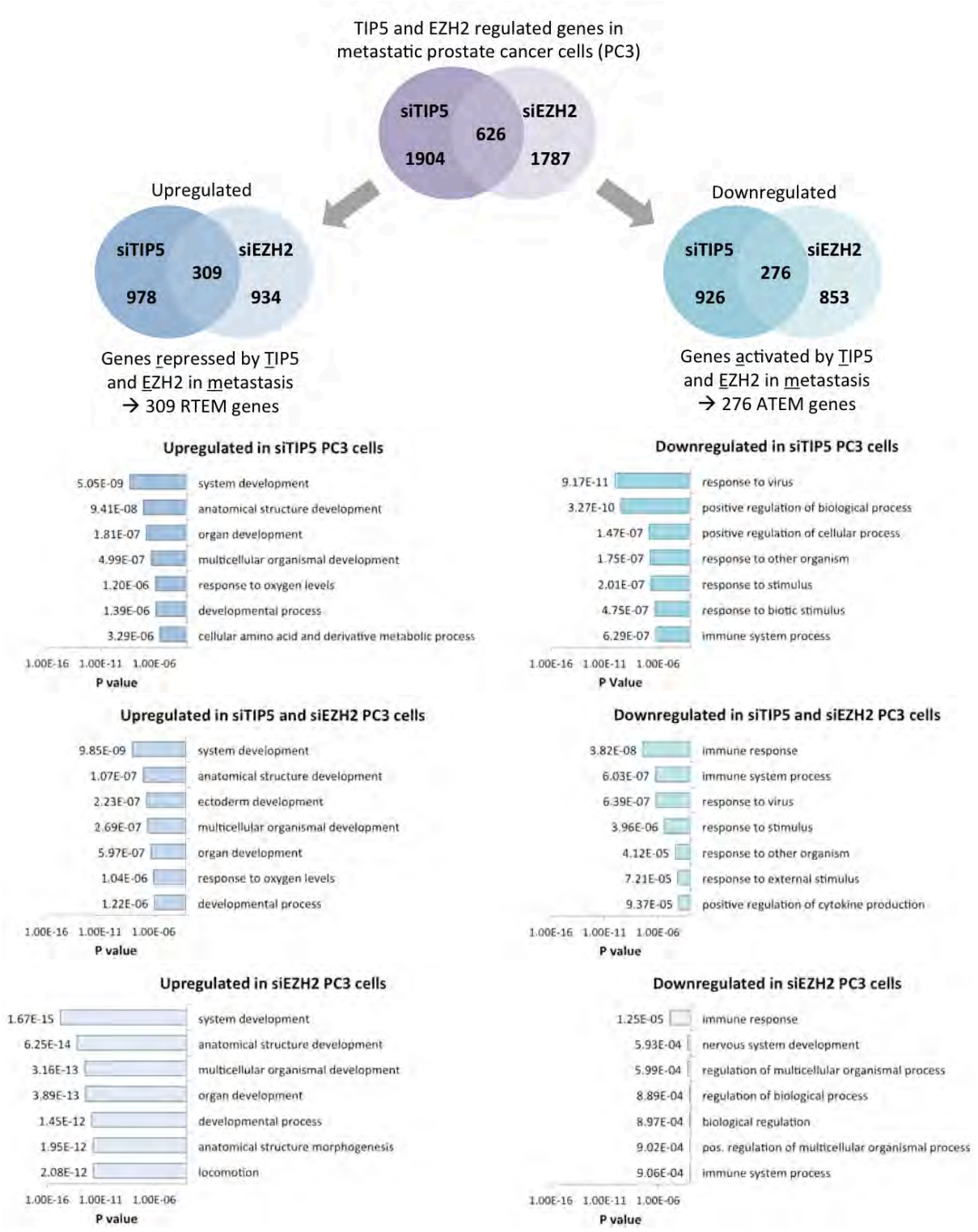

Figure 5 | Analysis of exon microarray data upon siRNA-mediated TIP5 and EZH2 knockdown in PC3 cells
PC3 cells were transfected with siRNA-CTRL, -TIP5 and EZH2 and three days post-transfection RNA was isolated with NucleoSpin RNA II Kit and passed to the Functional Genomics Center of the University of Zurich. The exon microarray was performed with three biological replicates.

In the upper part of the figure, the numbers of genes are shown that have a different expression upon TIP5 or EZH2 knockdown compared to siRNA-CTRL transfected cells. 1904 genes showed an altered expression upon TIP5 knockdown, 1787 upon EZH2 knockdown and 626 genes' expression was changed by TIP5 and EZH2 knockdown. These genes were further divided into two groups: upregulated or downregulated expression. 41 genes of the 626 that were influenced by TIP5 and EZH2 knockdown could not be subdivided, as they do not react in the same way on both knockdowns.
The six lower panels show Gene Ontology (GO) analysis of upregulated and downregulated genes. Analysis was performed with the Database for Annotation, Visualization and Integrated Discovery 6.7 (DAVID 6.7, http://david.abcc.ncifcrf.gov/). P values of the top seven functional categories are shown.

5.3 Genes repressed by TIP5 and EZH2 in metastasis (RTEM genes)

To select genes that are directly regulated by TIP5 and EZH2 in PC3 cells and functionally relevant to cancer, we used the following criteria:

1. **Genes upregulated in PC3 cells upon siRNA-TIP5 and siRNA-EZH2 treatment**
   Since TIP5 and EZH2 are transcriptional repressors, we reasoned to select genes that showed transcriptional upregulation upon knockdown of TIP5 and EZH2 in PC3 cells in our microarray analysis.
2. **Genes transcriptionally repressed in cancer and metastatic prostate cancer**
   We initially analyzed expression profiles (GDS1439 and GDS2545) of RTEM genes and selected genes that were transcriptionally repressed in metastatic prostate tissues (Figure 6 A and B). We also investigated the current literature and selected those RTEM genes that were previously described to be transcriptionally repressed and implicated in cancer progression.

Using these criteria, we selected 10 RTEM genes that will be used for subsequent analyses.
These genes are listed in Table 1.

Table 1 | List of RTEM genes that were selected for further analyses

RTEM gene	Full name	Function
AOX1	Aldehyde oxidase 1	Production of hydrogen peroxide
FBN1	Fibrillin 1	Extracellular matrix glycoprotein
FHL2	Four and a half LIM domains 2	Assembly of extracellular membranes, transcriptional coregulator
HOMER2	Homer homolog 2 (Drosophila)	Regulator of glutamate receptor function, scaffolding protein
HOXA7	Homeobox A7	Transcription factor, involved in morphogenesis and differentiation
HOXB8	Homeobox B8	Transcription factor, involved in developmental regulation
KLF6	Krüppel-like factor 6	Zinc finger protein, transcriptional activator
LAMB3	Laminin, beta 3	Attachment, migration and organization of cells into tissues
MKX	Mohawk homeobox	Transcription factor, regulator of cell adhesion
ZNF185	Zinc finger protein 185 (LIM domain)	Regulation of cellular proliferation/differentiation

Aldehyde oxidase 1 (AOX1) is a variant of aldehyde oxidase (AO), a complex molybdoflavoprotein that belongs to the xanthine oxidase family. An early study showed that AOX1 activity could be measured in normal liver but not in tumor [104]. Another study showed reduced AOX1 expression in hepatocellular carcinomas and that the loss of AOX1 was associated with higher tumor stages, positive nodal status and occurrence of distant metastases [105]. Normal pancreatic acinar cells showed a strong expression of AOX1 but a complete loss of AOX1 in pancreatic ductal adenocarcinoma [106]. Additionally, AOX1 was found hypermethylated in colorectal cancer [107, 108] and in prostate cancer [109, 110] where the hypermethylation was associated with reduced AOX1 gene expression [111].

The gene Fibrillin 1 (FBN1) encodes a member of the fibrillin family. The encoded protein is a large, extracellular matrix glycoprotein that serves as a structural component of 10-12 nm calcium-binding microfibrils. These microfibrils provide force bearing structural support in elastic and non-elastic connective tissue throughout the body [112]. Recently, increased expression of FBN1 was associated with low proliferation in non-small cell lung cancer [113]. FBN1 was identified as cancer-related gene in primary breast cancer [114]. In colorectal adenomas and cancers, FBN1 was frequently hypermethylated and the DNA methylation was associated with reduced or lost gene expression in cell lines [115]. FBN1 was also found hypermethylated in prostate cancer cells (PC3M) compared to immortalized prostate epithelial cells (267B1) associated with a reduced RNA expression [116, 117].

Four and a half LIM domains 2 (FHL2) gene encodes a member of the four-and-a-half-LIM-only protein family. Family members contain two highly conserved, tandemly arranged zinc finger

domains with four highly conserved cysteines binding a zinc atom in each zinc finger. This protein is thought to have a role in the assembly of extracellular membranes [112]. FHL2 was suggested to act as an oncoprotein or a tumor suppressor in a tissue-dependent manner [118]. FHL2 was found overexpressed in several human osteosarcoma cell lines and correlated positively with aggressiveness, indicating a positive role of FHL2 in bone tumor development [119]. Overexpression of FHL2 was also found in breast cancer tissue samples [120], in glioma tissue samples [121], in bone marrow samples of acute erythroid leukemia patients [122], in epithelial ovarian cancer [123], in colon adenomas and carcinomas [124] as well as in cancerous gastric and colon tissue samples [125]. On the other hand, FHL2 showed tumor suppressor function in colon carcinoma cell line HT-29 that exhibits very low basal levels of FHL2 [126] and 7 of 8 breast cancer cell lines expressed FHL2 mRNA much lower than an immortalized normal breast epithelial cell line [127]. Downregulated FHL2 expression was detected in liver cancer patient samples [128], in rhabdomyosarcoma cell lines [129] and in early prostate cancer samples [130]. In LNCaP prostate adenocarcinoma cells androgen exposure led to an increase in FHL expression at mRNA and protein levels [131].

Homer homolog 2 (HOMER2) gene encodes a member of the homer family of dendritic proteins [112]. Members of this family regulate group 1 metabotrophic glutamate receptor function. HOMER2 was found to be hypermethylated in primary colorectal cancers [132]. The expression of HOMER2 was shown to enhance the ability of MYO18B to suppress anchorage-independent growth in human non-small cell lung carcinoma cell line H1299, suggesting that HOMER2 may have a tumor suppressor role [133].

In vertebrates, the genes encoding the class of transcription factors called homeobox genes are found in clusters named A, B, C and D on four separate chromosomes. Expression of these proteins is spatially and temporally regulated during embryonic development. Homeobox A7 (HOXA7) gene is part of the A cluster on chromosome 7 and encodes a DNA-binding transcription factor which may regulate genes expression, morphogenesis and differentiation [112]. HOXA7 was found to be overexpressed in 16 glioma samples compared to primary astrocytes [134] and in esophageal squamous cell carcinoma tissue samples compared to noncancerous mucosa, too [135]. Novak *et al.*, 2006 showed a decrease in the expression of HOXA7 in breast cancer samples when compared to normal breast tissue and confirmed it in cell line models as well. The authors concluded that the silencing of the HOXA gene cluster in breast cancer is associated with the acquisition of the repressive epigenetic mark of DNA hypermethylation and the loss of permissive histone modifications [136]. Further HOXA7 was studied in several other cancers such as leukemia [137-140], ovarian tumors [141-144], lung cancer [145, 146], hepatocellular carcinomas [147] and oral squamous cell carcinomas [148].

Homeobox B8 (HOXB8) gene is a member of the Antp homeobox family and encodes a nuclear protein with a homeobox DNA-binding domain. It is included in a cluster of homeobox B genes located on chromosome 17. The encoded protein functions as a sequence-specific transcription factor

that is involved in development [112]. HOXB8 was reported to be overexpressed in colorectal cancer whereas the level in the tested esophageal and gastric cancers was below detection [149]. In HT-29 cells (human colorectal adenocarcinoma) and in CACO-2 cells (human Caucasian colon adenocarcinoma) HOXB8 was found to be upregulated as well, but in LS174T cells (Dukes type B, colorectal adenocarcinoma) it was downregulated [150]. In colorectal cancer HOXB8 was negatively correlated with chemotherapy [151]. HOXB8 was found to be overexpressed in serous ovarian cancer [152] and its expression was associated with poorer outcome [153]. HoxB8 was the first Hox protein found to be transcriptionally activated in murine acute myeloid leukemia (in WEHI3B mouse myeloid leukemia cells) and its overexpression was shown to prevent differentiation of myeloid progenitors [154]. Moreover, several studies analyzed HoxB8 in terms of inhibited myeloid differentiation [155-158].

Krüppel-like factor 6 (KLF6) gene encodes a member of the Krüppel-like family of transcription factors [112]. Different studies described KLF6 as a novel tumor suppressor gene involved in growth suppression and differentiation stimulation [159-165]. KLF6 was found mutated or downregulated in astrocytic gliomas [166], in colorectal cancer [167, 168], in lung cancer [165, 169, 170], in esophageal cancer [171, 172], in hepatocellular carcinoma [173, 174], in gastric cancer [175], in epithelial ovarian cancer [176] and in prostate cancer [163, 177]. In prostatic carcinoma DU145 and renal carcinoma OS-RC-2 cell lines overexpression of KLF6 was shown to inhibit proliferation and to enhance the amounts of cells with apoptotic signals [178].

The product encoded by Laminin, beta 3 (LAMB3) gene is a laminin that belongs to a family of basement membrane proteins. This protein is a beta subunit laminin, which forms laminin-5 together with an alpha and a gamma subunit [112]. LAMB3 was reported to be upregulated in nasopharyngeal carcinoma [179], in biliary cancer [180] and in esophageal squamous cell carcinoma [181]. On the other hand it was downregulated in lung cancer [182] and in bladder cancer [183] and methylated in small bowel carcinoid tumors [184]. In six prostate cancer cell lines LAMB3 expression was shown to be decreased and the methylation frequency was increased; the hypermethylation was confirmed in prostate cancer tissues [185]. Restoration of LAMB3 beta 3A isoform expression in LNCaP cells led to increased cell spreading and migration *in vitro* and when injected into mice to increased tumor growth [186]. Another study described the LAMB3 expression in different stages of prostate cancer: LAMB3 was maintained in localized and lymph node metastases but was almost completely absent in bone metastases [187].

The protein encoded by Mohawk homeobox (MKX) gene is an IRX family-related homeobox protein that may play a role in cell adhesion[112]. So far, there is no report concerning the role of MKX in cancer. However, we decided to include MKX in our analysis since homeobox genes have been demonstrated to play important roles during cancer differentiation and embryonic development.

Zinc finger protein 185 (ZNF185) gene encodes a LIM-domain zinc finger protein. The LIM domain is composed of two contiguous zinc finger domains, separated by a two-amino acid residue hydrophobic linker and mediates protein-protein interactions [112]. ZNF185 was shown to be overexpressed in leiomyoma samples compared to myometrium [188]. ZNF185 expression was decreased in lung primary tumors and lung cancer cell lines [189], in head and neck squamous cell carcinomas and cell lines [190] and in prostate cancer [191]. Treatment of LAPC4, LNCaP and PC3 prostate cancer cell lines with 5-Aza-CdR showed an ~2-fold increase in mRNA levels of ZNF185 indicating that the gene might be partially silenced by methylation [191]. Overexpression of full-length ZNF185 in LNCaP and DU145 cells was found associated with slower cell growth [192].

As shown in Figure 6, most of the RTEM genes (AOX1, FBN1, FHL2, HOXA7, LAMB3, MKX, ZNF185) showed a lower expression level in prostate cancer tissue than in normal prostate tissue and also a further reduction of the level in metastatic prostate cancer compared to localized prostate tumors. HOMER2 and KLF6 did not show such a transcriptional profile in the analyzed arrays. However, we decided to include these genes in our analysis due to strong evidences reported in literature (see above) describing down-regulation and tumor suppressor features in prostate and other types of cancer.

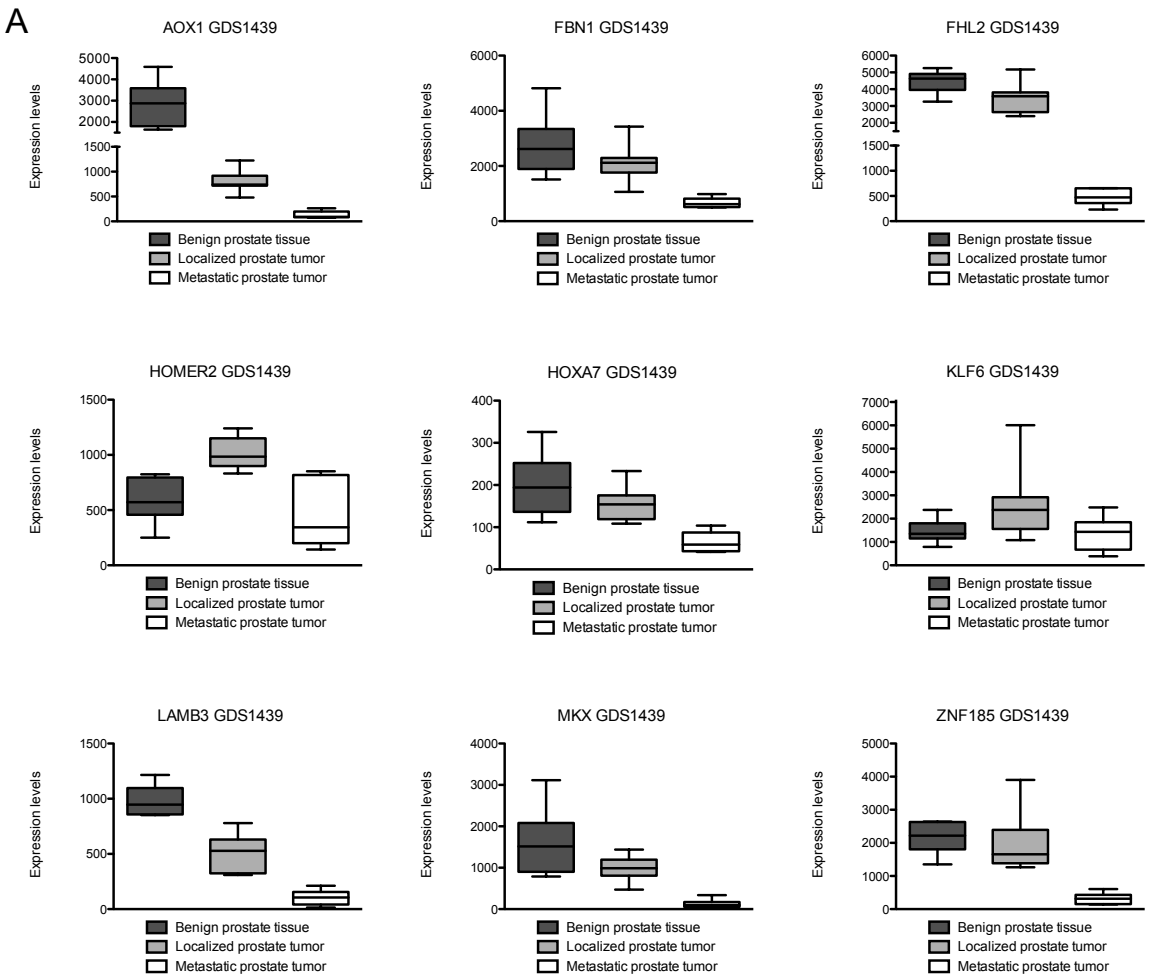

Figure 6 | Decreased RTEM genes expression levels in metastatic prostate tumors

A | GEO expression profiling (GDS1439) of 6 benign prostate tissue samples (4 samples and 2 pooled samples), 7 clinically localized primary prostate cancer tissue samples (5 samples and 2 pooled samples) and 6 hormone-refractory metastatic prostate cancer tissue samples (4 samples and 2 pooled samples). Expression profiles of AOX1, FBN1, FHL2, HOMER2, HOXA7, KLF6, LAMB3, MKX and ZNF185 are shown.

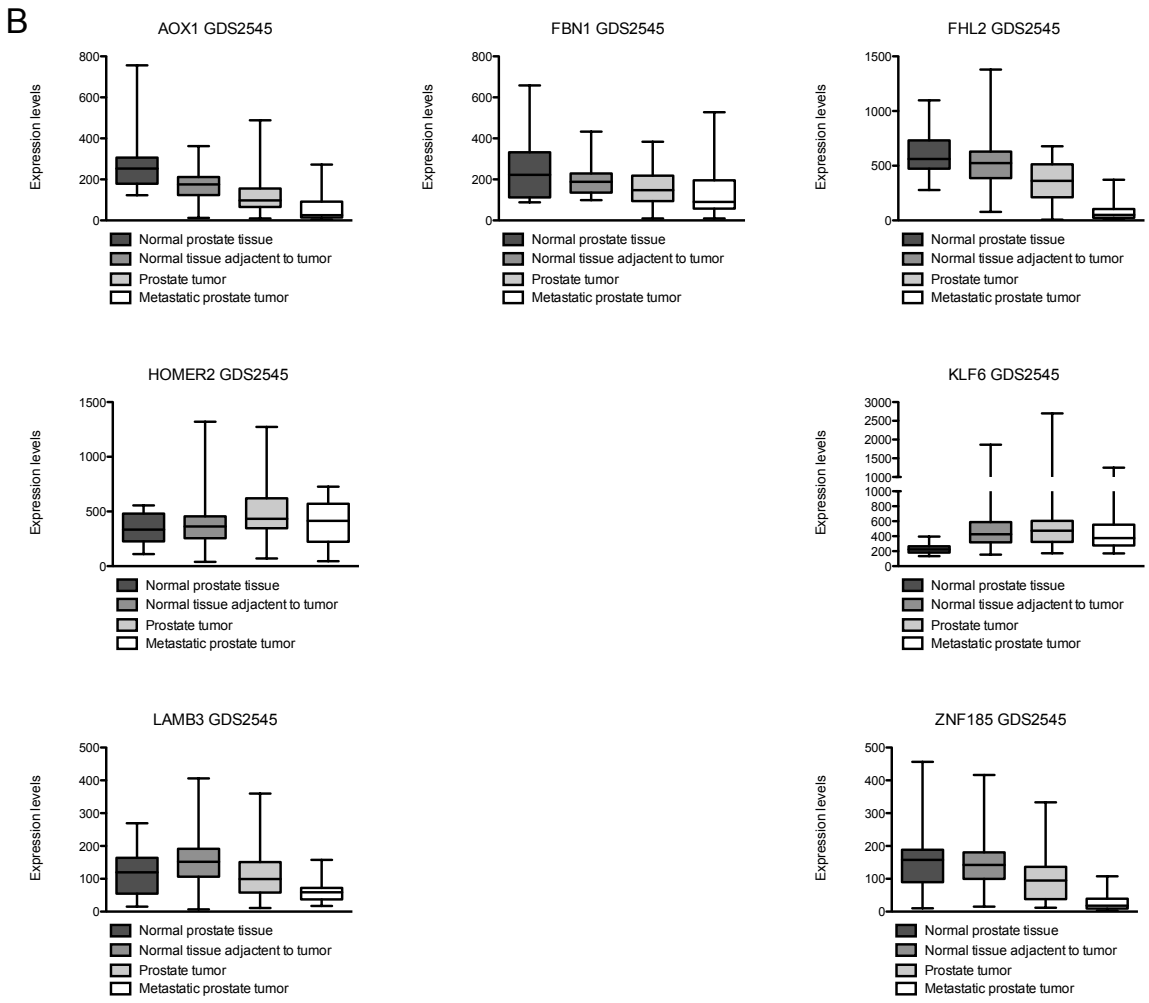

Figure 6 | Decreased RTEM genes expression levels in metastatic prostate tumors
B | GEO expression profiling (GDS2545) of normal prostate tissues from 18 donors, normal prostate tissue adjacent to the tumor of 63 donors, 65 primary prostate tumor samples and 25 metastatic prostate tumor samples (location of metastatic samples: 5 liver, 1 lung, 1 recurrent in prostate, 1 kidney, 2 adrenal gland, 3 retroperitoneal lymph node, 1 inguinal lymph node, 8 para-tracheal lymph node, 3 para-aortic lymph node). Expression profiles of AOX1, FBN1, FHL2, HOMER2, KLF6, LAMB3 and ZNF185 are shown.

5.4 Analysis of RTEM genes' expression levels in prostate and osteosarcoma cancer cell lines

Since RTEM genes are upregulated after knockdown of TIP5 and EZH2, we reasoned that their expression levels must be lower in cancer cells when compared to non-cancer cells. To test this, we measured and compared RTEM transcription levels in 3 different cancer cell lines: human metastatic prostate adenocarcinoma cell line PC3, human androgen-sensitive metastatic prostate carcinoma cell line LNCaP and human osteosarcoma cell line U2OS. The choice of U2OS was motivated by the fact that this cell line is very well described for the EZH2-mediated silencing process (see 5.5) and TIP5 was found upregulated in this cell line [99]. The analysis of human prostate epithelial cell line RWPE1 - that are of non-cancer origin - represents a further control of this analysis. Measurements were

performed by RT-qPCR and transcript levels were normalized to 28S rRNA that serves to equalize the total amounts of RNA between samples. Indeed, classical housekeeping genes could not be used for normalization as their expression levels differ among the analyzed different cell lines.
Compared to non-cancer prostate epithelium RWPE1 cells, TIP5 levels were higher in PC3 and U2OS cells while LNCaP cells did not display elevated TIP5 expression. Whether the expression levels of TIP5 might distinguish the androgen-sensitive signature of prostate cancer will be an issue of future studies. Remarkably, EZH2 was overexpressed in all three analyzed cancer cell lines (Figure 7 A). Interestingly, a recent study showed overexpression of EZH2 in osteosarcoma cell lines and patient samples [193]. The elevated levels of TIP5 and EZH2 measured in U2OS cells might suggest the existence of a crosstalk between TIP5 and EZH2 also in osteosarcoma cancer.

Analysis of RTEM gene expression levels revealed that only FHL2, HOMER2, HOXA7 and LAMB3 are higher expressed in RWPE1 cells than in PC3 cells (Figure 7 B). HOXB8 could not be included in this analysis due to the lack of primers able to efficiently amplify the selected transcript. All RTEM genes were strongly downregulated in LNCaP cells except HOMER2 and FBN1, indicating that expression levels of these two RTEM genes in LNCaP cells do not depend on TIP5 expression levels. For example, HOMER2 showed the highest expression level in LNCaP cells and is strongly downregulated in PC3 cells (Figure 7 B). Consistent with a previous study, KLF6 displayed the highest expression level in PC3 cells, followed by RWPE1 and nearly no expression in LNCaP cells [177], supporting the accuracy of our analysis. These results indicated that the lowest expression level of RTEM genes characterizes androgen-sensitive metastatic prostate cancer cell line LNCaP. Moreover, they indicated that although RTEM gene transcription is upregulated in PC3 cells upon TIP5 or EZH2 knockdown, RTEM expression levels in PC3 cells are not significantly downregulated when compared to non-cancer cells. As RTEM genes are transcriptionally silenced in metastatic prostate tissues (Figure 6), we conclude that the use of PC3 cells is instructive to determine which and how these genes are regulated by TIP5 and EZH2 but not to determine the correlation between transcriptional state and cancer progression.

A previous report showed downregulation of KLF6 in osteosarcoma cell lines (MG63 and Saos2) when compared to normal bone control cells (hFOB1.19). Similarly, in osteosarcoma tissues KLF6 levels were shown to be lower than in normal bone tissue [194]. Compared to RWPE1 cells, U2OS cells displayed equal to higher expression levels of RTEM genes (including KLF6) with the exception of FHL2 and LAMB3 that showed lower levels (Figure 7 B). A limitation of our analysis is that RWPE1 does not represent the correct cell line to be compared with U2OS cells. Thus, the lack of RTEM transcriptional analysis in a benign bone cell line does not allow a functional analysis for these results.

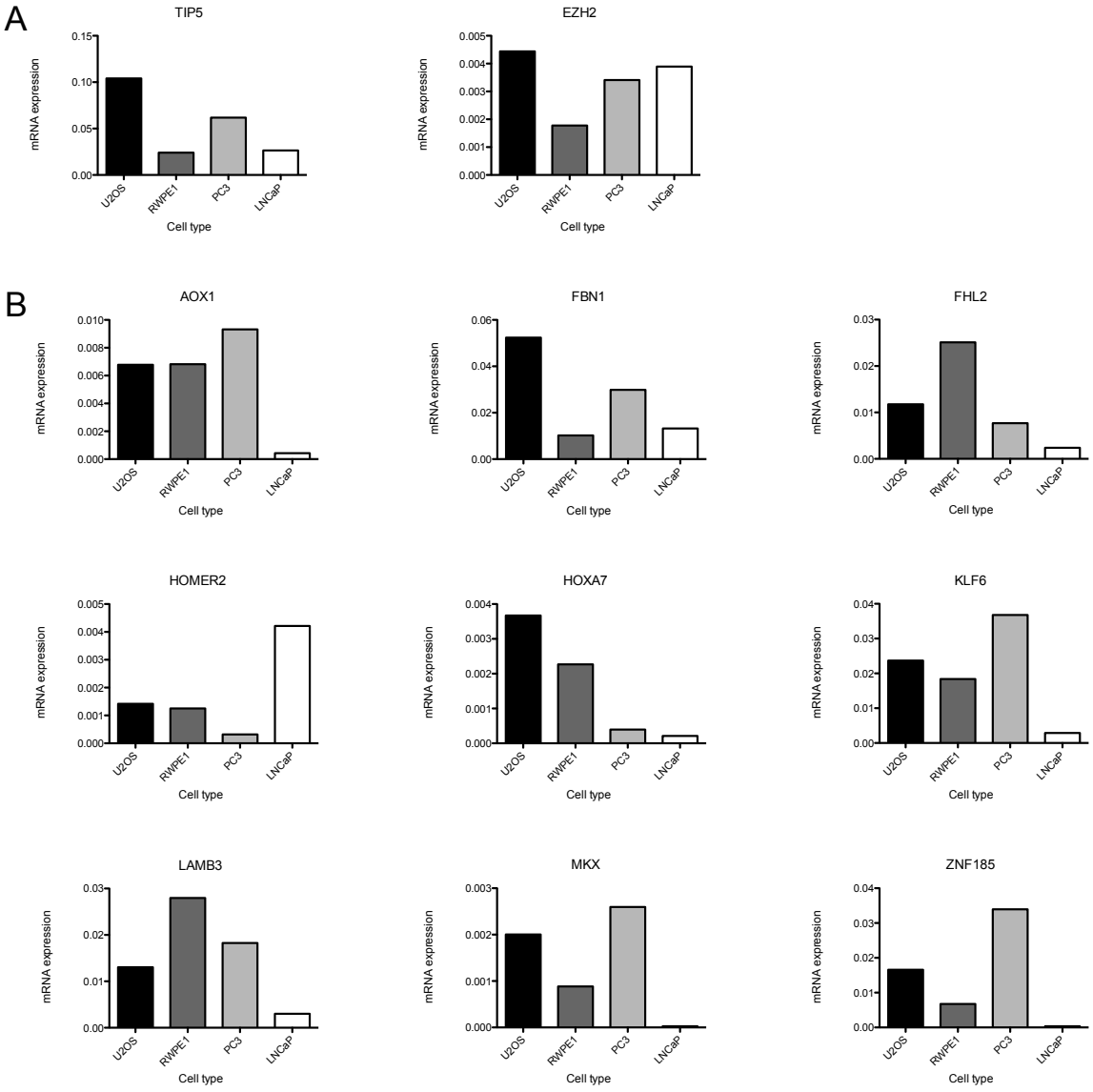

Figure 7 | RTEM genes show different expression levels in different cell types

RNA from RWPE1, PC3 and LNCaP cells was prepared and isolated by Sandra Frommel, PhD student of Dr. Santoro's laboratory.

A | RT-qPCR. TIP5 and EZH2 mRNA levels measured in U2OS, RWPE, PC3 and LNCaP wildtype cells. mRNA levels were normalized against 28S rRNA. **B |** RT-qPCR. AOX1, FBN1, FHL2, HOMER2, HOXA7, KLF6, LAMB3, MKX and ZNF185 mRNA levels measured in U2OS, RWPE, PC3 and LNCaP wildtype cells. mRNA levels were normalized against 28S rRNA.

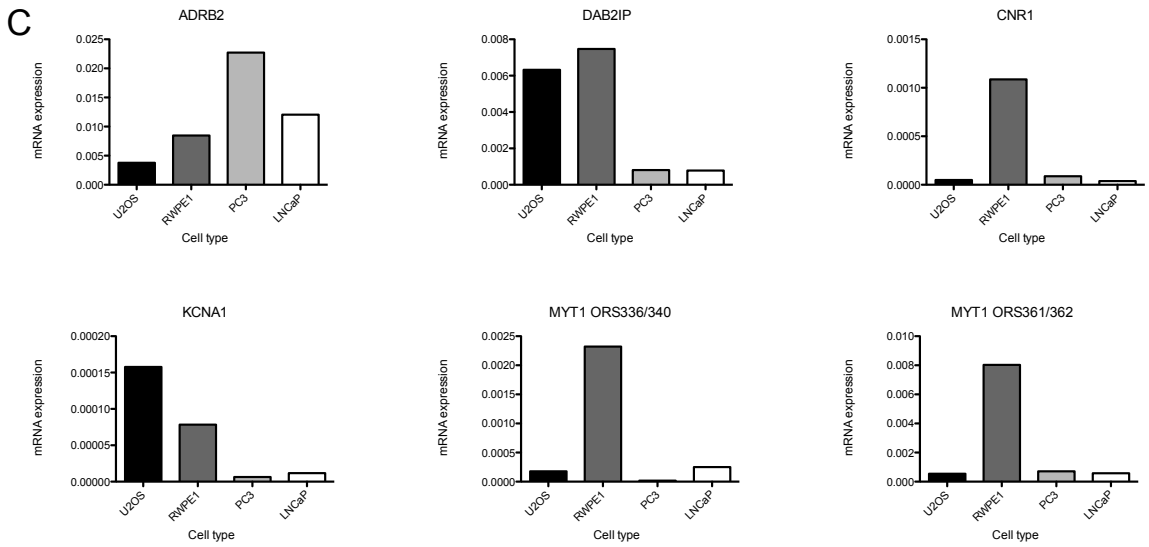

Figure 7 | EZH2-target genes show different expression levels in different cell types
C | RT-qPCR. ADRB2, DAB2IP, CNR1, KCNA1 and MYT1 (two different primer pairs) mRNA levels measured in U2OS, RWPE, PC3 and LNCaP wildtype cells. mRNA levels were normalized against 28S rRNA.

5.5 Analysis of known EZH2-target genes' expression levels in prostate and osteosarcoma cancer cell lines

The role of EZH2 in cancer has been well analyzed in the recent years [63-65, 195, 196]. The oncogenic function of EZH2 was suggested to be mainly mediated through its gene silencing activity and several EZH2-target genes were identified [51]. ADRB2, DAB2IP, CNR1, KCNA1 and MYT1 are well known EZH2-target genes that are implicated in cancer. With the aim to determine whether TIP5 is involved in the EZH2-mediated silencing process of these genes, we initially measured and compared their expression in RWPE1, PC3, LNCaP and U2Os cells.

Adrenoceptor beta 2, surface (ADRB2) gene encodes a beta-2-adrenergic receptor that is a member of guanine-nucleotide-binding protein (G protein)-coupled receptor superfamily [112]. Polymorphisms of the ADRB2 gene were associated with an increased risk of breast and colorectal cancer [197] but not with lung cancer [198]. ADRB2 was identified as a direct target of EZH2 in prostate cancer and found downregulated in metastatic prostate cancer samples with a negative correlation to EZH2 expression [199]. However, in our analysis both PC3 and LNCaP cells showed higher ADRB2 expression when compared to RWPE1 and we could not establish a negative correlation with EZH2 expression (Figure 7 A and C). Only in U2OS cells, ADRB2 showed low expression level (Figure 7 C). Consistent with a previous report showing that ADRB2 was significantly higher in androgen-independent prostate cancer cell lines (LNCaP-C4, LNCaP-C4-2 and DU145) than in androgen-sensitive LNCaP cells [200], we found that ADRB2 levels were higher in PC3 cells than in LNCaP, underscoring the accuracy of our analysis.

Disabled homolog 2 interacting protein (DAB2IP) is a GTPase-activation protein (GAP) that modulates the Ras-mediated signaling and tumor necrosis factor-mediated apoptosis. The expression of this tumor suppressor was reported to be epigenetically suppressed by EZH2 in prostate cancer [196, 201]. DAB2IP was downregulated in human prostate cancer samples [196], in pancreatic cancer tissue samples [202], in hepatcocellular carcinoma tissue samples and cells [203], in human medulloblastoma cells [204], in lung cancer cell lines [205], in gastrointestinal cancer cell lines [206] and in breast cancer cell lines [207] whereas the last three were associated with methylation status. Further, DAB2IP mRNA levels were found lower in six prostate cancer cell lines (MADPC2a, MADPC2b, Du145, LNCaP, TSU-Pr1 and PC3) compared to three normal prostate epithelia cell lines (PrEC, SWNPC2 and PZ-HPV-7) [208]. Consistent with these results, we found the levels of DAB2IP were strongly downregulated in PC3 and LNCaP cells when compared to RWPE1 (Figure 7 C). In contrast, U2OS displayed similar DAB2IP levels than RWPE1 cells.

The gene cannabinoid receptor 1 (brain) (CNR1) encodes one of two cannabinoid receptors that are members of the G protein-coupled receptor family, which inhibit adenylate cyclase activity. The two receptors were found to be involved in the cannabinoid-induced CNS effects experienced by users of marijuana [112]. CNR1 was identified as a target gene of PRC2 complex of which EZH2 is a component [209]. Several studies reported anti-tumor effects of CNR1 signaling such as Δ^9-tetrahydrocannabinol (THC) inhibited proliferation in several human breast cancer cell lines due to blockade of the G_2-M transition [210] or the growth of melanoma cell but not normal melanocytes was inhibited by activation of cannabinoid receptors with cannabinoids [211]. In hepatocellular carcinoma, high expression of CNR1 was significantly associated with improved prognosis [212]. CNR1 expression was lower in human breast tumors than in noncancerous breast tissue [210] but upregulated in mantle cell lymphomas [213, 214]. As shown in Figure 7 C, CNR1 mRNA levels were significantly downregulated in prostate cancer cells PC3, LNCaP and osteosarcoma cells U2OS compared to prostate epithelial cells RWPE1.

Potassium voltage-gated channel, shaker-related subfamily, member 1 (KCNA1) encodes a voltage-gated delayed potassium channel that is phylogenetically related to the Drosophila Shaker channel. It mediates the voltage-dependent potassium ion permeability of excitable membranes [112]. KCNA1 was shown to be a target gene of PRC2 and to be bound by EZH2, which is a component of the PRC2 complex in U2OS and SW480 cells [209]. KCNA1 was less expressed in human cancerous breast than in normal breast tissue [215] and low levels of KCNA1 in breast cancer were associated with an increased risk of metastasis and of dying [216]. As shown in Figure 7 C, expression of KCNA1 was strongly downregulated in PC3 and LNCaP cells while U2OS cells displayed elevated expression levels.

The protein encoded by myelin transcription factor 1 (MYT1) gene is a member of a family of neural specific, zinc finger-containing DNA-binding proteins that binds to the promoter regions of proteolipid proteins of the central nervous system [112]. MYT1 was shown to be a target gene of

PRC2 and of EZH2 in U2OS and SW480 cells [209]. Consistent with these results, MYT1 expression was significantly downregulated in PC3, LNCaP and U2OS cells (Figure 7 C).

Taken together, the results of this analysis revealed that expression of known EZH2-target genes is also significantly downregulated in prostate cancer cells. Understanding whether EZH2 and/or TIP5 are implicated in the transcriptional repression of these genes in U2OS (and PC3) cells is an aim of this study.

5.6 TIP5 knockdown affects expression levels of RTEM genes in U2OS and PC3 cells

To validate the results of the microarray, we measured and compared transcript levels of the selected RTEM genes by RT-qPCR in PC3 cells depleted of TIP5 or EZH2. All analyzed RTEM genes were higher expressed upon knockdown of TIP5 and EZH2 when compared to control cells (siRNA-CTRL, Figure 8 A and B).

To determine whether the regulation of RTEM genes by TIP5 and EZH2 is cancer specific, we extended our analysis to U2OS and RWPE1 cells and measured transcription of RTEM genes upon TIP5 or EZH2 knockdown (Figure 8 A and B). Remarkably, transcription of RTEM genes was not affected in RWPE1 cells by depletion of TIP5 or EZH2 (except FHL2), indicating that TIP5 and EZH2 regulation is specific to prostate cancer cells. Importantly, 6 out of the 9 analyzed RTEM genes were also upregulated in U2OS cells upon TIP5 or EZH2 depletion, suggesting that the role of TIP5 and EZH2 to regulate RTEM genes' transcription is not limited to prostate cancer, but is also true in osteosarcoma cells. Future studies will address whether TIP5 is implicated in other cancer types.

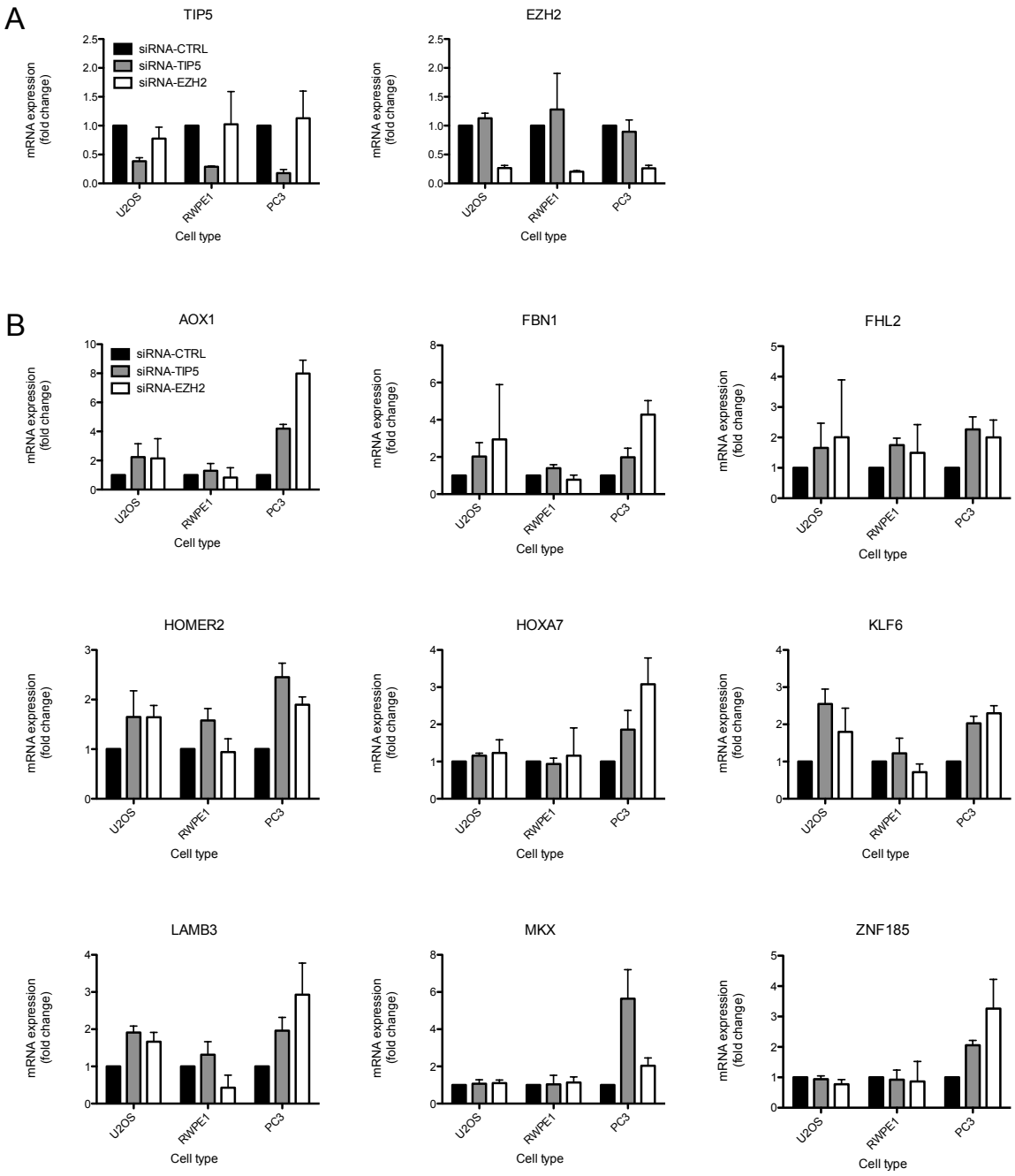

Figure 8 | Expression analysis of RTEM genes upon siRNA-mediated TIP5 and EZH2 knockdown in U2OS, RWPE1 and PC3 cells

The experiments with RWPE1 and PC3 cells were performed by Sandra Frommel, PhD student of Dr. Santoro's laboratory. Error bars indicate SD of two (RWPE1) or three (U2OS and PC3) independent experiments.

A | RT-qPCR. TIP5 and EZH2 mRNA levels in U2OS, RWPE1 and PC3 cells transfected with siRNA-CTRL, -TIP5 and -EZH2. Values of TIP5 and EZH2 mRNA levels were first normalized to L28 or GAPDH mRNA levels and then to levels of siRNA-CTRL transfected cells. **B |** RT-qPCR. AOX1, FBN1, FHL2, HOMER2, HOXA7, KLF6, LAMB3, MKX and ZNF185 mRNA levels in U2OS, RWPE1 and PC3 cells transfected with siRNA-CTRL, -TIP5 and -EZH2. Values of RTEM genes mRNA levels were first normalized to L28 or GAPDH mRNA levels and then to levels of siRNA-CTRL transfected cells.

5.7 TIP5 knockdown affects 45S pre-rRNA levels in U2OS cells

The results described so far indicated that TIP5 is implicated in the transcriptional regulation of RTEM genes. Due to the exclusive nucleolar localization of TIP5 in mouse cells, the first gene described to be regulated by TIP5 was the ribosomal RNA (rRNA) gene [81]. In NIH/3T3 and HEK293T cells the knockdown of TIP5 leads to a decrease in the number of silent rRNA genes and thereby to enhanced rRNA transcription [96]. To determine whether TIP5 maintains its role in repressing rRNA transcription in U2OS cells, we measured 45S pre-rRNA levels by RT-qPCR upon knockdown of TIP5 or EZH2. As shown in Figure 9 A, depletion of TIP5 caused a ~1.9 fold increase in rRNA synthesis when compared to control cells (siRNA-CTRL). Of note is that EZH2 knockdown did not significantly affect rRNA transcription, indicating that TIP5-mediated silencing of rRNA genes is independent of EZH2. We conclude that in U2OS cells TIP5-mediated regulation of rRNA genes is independent of EZH2.

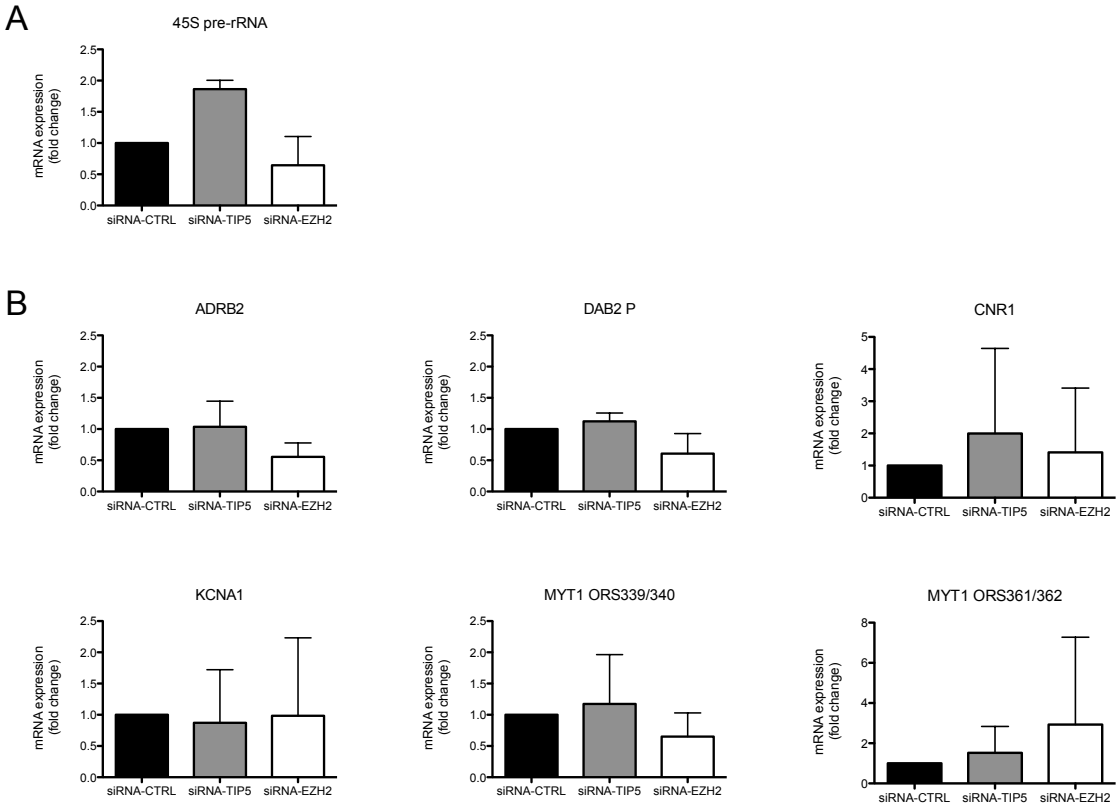

Figure 9 | Expression analysis of 45S pre-rRNA, ADRB2, DAB2IP, CNR1, KCNA1 and MYT1 upon siRNA-mediated TIP5 and EZH2 knockdown in U2OS cells

Error bars indicate SD of three independent experiments.

A | RT-qPCR. 45S pre-rRNA levels in U2OS cells transfected with siRNA-CTRL, -TIP5 and -EZH2. Values of 45S pre-rRNA levels were first normalized to L28 mRNA levels and then to levels of siRNA-CTRL transfected cells.

B | RT-qPCR. ADRB2, DAB2IP, CNR1, KCNA1 and MYT1 mRNA levels in U2OS cells transfected with siRNA-CTRL, -TIP5 and -EZH2. Values of EZH2-target genes mRNA levels were first normalized to L28 mRNA levels and then to levels of siRNA-CTRL transfected cells.

5.8 Analysis of EZH2-target genes in U2OS cells depleted of TIP5 and EZH2

Given the known role of EZH2 in repressing transcription of ADRB2 and DAB2IP in prostate cancer cells and of CNR1, KCNA1 and MYT1 in U2OS cells (see 5.5), we asked whether TIP5 might be implicated in the transcriptional repression of these genes. To test this, we measured expression levels in U2OS cells depleted of TIP5 and EZH2 by siRNA. Surprisingly, and in contrast to a previous published report [71], knockdown of EZH2 did not affect the levels of CNR1, KCNA1 and MYT1 in U2OS cells. We repeated this analysis several times but we have never been able to obtain upregulation of these genes upon EZH2 depletion, despite the good knockdown efficiency and validation of the primers used to measure transcript levels. An important point for the interpretation of these results is that we have not been able to obtain sequence information of the primers used in Vire *et al.*, 2006. Indeed, CNR1, KCNA1 and MYT1 have several transcript variants and there is the possibility that our primers measured other isoforms of MYT1 than the one described in Vire *et al.*, 2006. We conclude that the analyzed transcript variants of CNR1, KCNA1 and MYT1 are not transcriptionally regulated by EZH2 in U2OS cells. As expected, knockdown of TIP5 did not significantly affect transcript levels (Figure 9 B).
Transcription of ADRB2 and DAB2IP was also not affected by TIP5 and EZH2 in U2OS (Figure 9 B), suggesting that these genes, known to be regulated by EZH2 in prostate cancer PC3 and DU145 cells [199, 201], are not regulated by EZH2 in U2OS osteosarcoma cell line. In my master thesis we reported a 1.4 fold increase in ADRB2 expression upon short-time (three days) EZH2 knockdown in PC3 cells while upregulation upon TIP5 knockdown could only be detected after long-time depletion (several weeks). Thus, we cannot exclude the possibility that upregulation of ADRB2 in U2OS cells might require longer exposure to EZH2 or TIP5 depletion to efficiently erase stable epigenetic marks such as DNA methylation required for transcription activation. Indeed, our DNA methylation array analysis in PC3 cells determined that 4 days of TIP5 or EZH2 knockdown were not sufficient to modify DNA methylation profile (data not shown).

Taken together, the results indicated that depletion of EZH2 and TIP5 does not affect transcript levels of genes previously described by others to be regulated by EZH2 under our experimental conditions (primer choice and time of knockdown).

5.9 TIP5 binds to EZH2-target genes in U2OS cells

The analysis described above showed that 6 out of 9 selected RTEM genes (identified in PC3 cells) are transcriptionally regulated by TIP5 and EZH2 in U2OS cells, indicating that TIP5 and EZH2 regulate RTEM genes' transcription not only in prostate cancer cells but also in osteosarcoma cells. In contrast, we were unable to detect upregulation upon 4 days TIP5 or EZH2 knockdown of genes previously described to be EZH-targets in U2OS and prostate cancer cells. To get better insights into EZH2- and TIP5-regulation, we performed chromatin immunoprecipitation (ChIP) analyses to measure the association of TIP5 or EZH2 with the promoter regions of the candidate genes in U2OS cells. My previous results reported in my master thesis showed TIP5 enrichment at ADRB2 gene promoter in

HEK293T and PC3 cells and binding to DAB2IP and MYT1 promoter in PC3 cells. Further experiments (performed by Sandra Frommel, data not shown) revealed that TIP5 and EZH2 associated with the promoter regions of all analysed RTEM genes in PC3 cells, supporting a direct role of TIP5 and EZH2 in the regulation of RTEM genes. As shown in Figure 10 A, anti-TIP5 ChIP assay in U2OS cells revealed the association of TIP5 with the rDNA promoter region but not with the rDNA coding region located at +4 kb from the TSS, a result consistent with previous data that underscores the specificity of this assay [81]. GAPDH and IL6 promoter, genes that are not related to TIP5 and EZH2, were used as additional controls to assess the specificity of the ChIP assay. In contrast to the transcription data presented in Figure 9 B, we found that TIP5 specifically associated with the promoter regions of ADRB2, DAB2IP, CNR1, KCNA1 and MYT1 (Figure 10 A). Binding of EZH2 to these promoters was also enriched when compared to control genes GAPDH and IL6 (Figure 10 B). These results suggest that ADRB2, DAB2IP, CNR1, KCNA1 and MYT1 are indeed EZH2- and TIP5-target genes in U2OS cells. The failure to detect transcriptional upregulation of theses genes upon TIP5 or EZH2 knockdown in U2OS cells (Figure 9 B) might have depended on our experimental condition (such as short time of knockdown) that is not sufficient to erase key epigenetic marks for transcriptional repression (*i.e.* DNA methylation). Alternatively, we cannot exclude the possibility of other factors that are still active in repressing transcription and do not depend on TIP5 or EZH2.

5.10 Association of TIP5 and EZH2 with RTEM genes in U2OS cells

Next, we wanted to determine whether RTEM genes in U2OS cells are directly regulated by TIP5 and EZH2 by measuring the association of TIP5 and EZH2. Studies performed by Sandra Frommel already determined that TIP5 and EZH2 associate with RTEM genes in PC3 cells (data not shown). Three of the selected RTEM genes could not be included in this analysis due to the lack of primers able to efficiently amplify the corresponding promoter regions (FBN1, HOMER2 and MKX). As shown in Figure 10 A, TIP5 binding was enriched at AOX1, HOXB8, KLF6 and LAMB3 while at the other genes the levels were similar to control GAPDH and IL6 promoters. Binding of EZH2 was enriched only at HOXB8, while all the other RTEM genes did not display any evident association with EZH2. Lack of TIP5 and EZH2 binding at HOXA7 and ZNF185 is consistent with our analysis showing the transcription of both genes does not depend on TIP5 and EZH2 in U2OS cells (Figure 8 B). The absence of TIP5 and EZH2 binding to RTEM genes whose transcription depends on TIP5 or EZH2 (Figure 8 B), suggest that the regulation might occur in an indirect way (*i.e.* downregulation or upregulation of an transcriptional activator or repressor of RTEM genes). Thus, although the majority of RTEM genes are regulated by TIP5 and EZH2 in both U2OS and PC3 cells, the mechanisms underlying these processes might considerably be different.

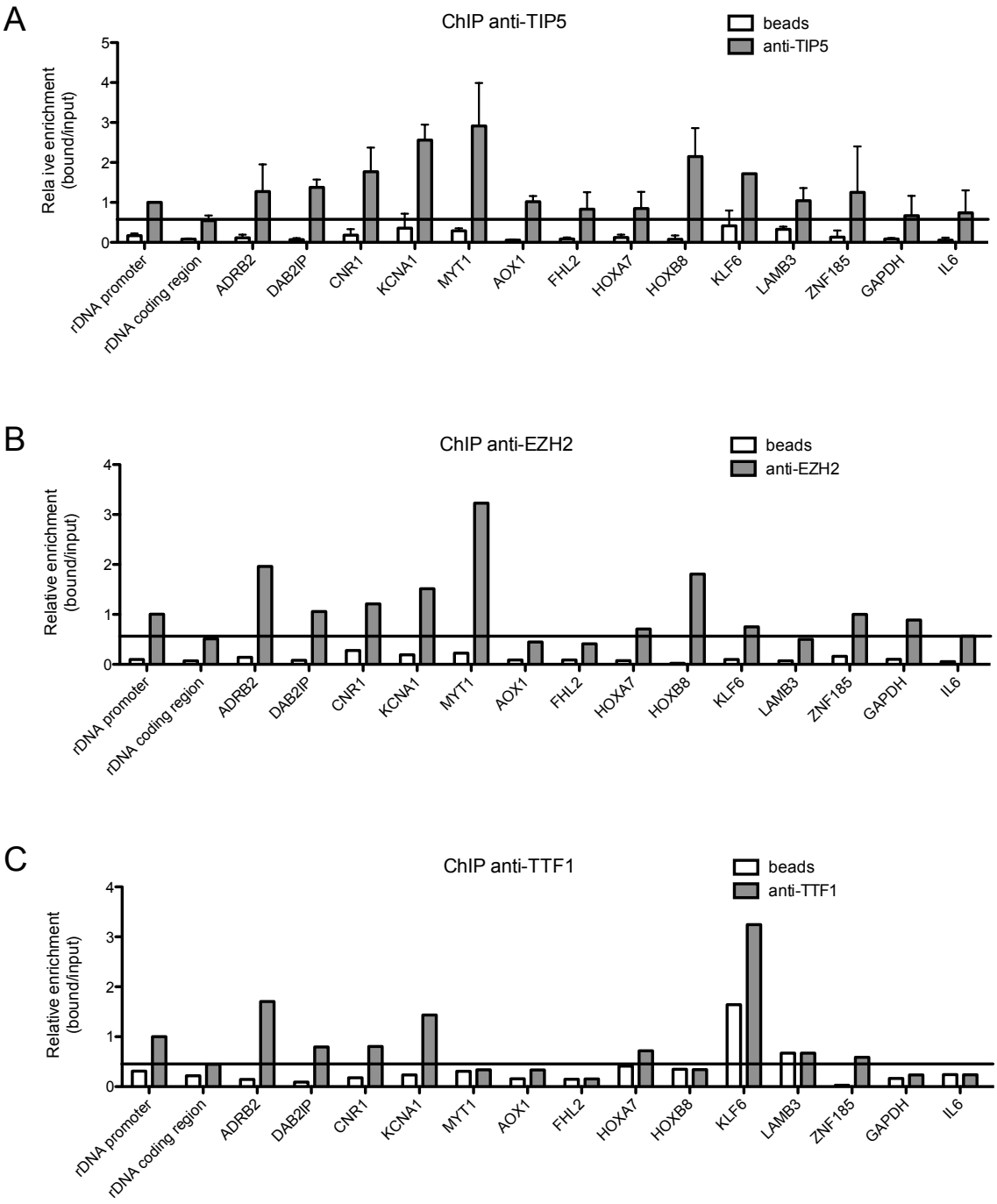

Figure 10 | TIP5-, EZH2-, and TTF1-target genes in U2OS cells

A | ChIP assay showing association of TIP5 with the indicated genes. Values are calculated bound/input and then normalized to rDNA promoter binding. Error bars indicate SD of two independent experiments. **B |** ChIP assay showing association of EZH2 with the indicated genes. Values are calculated bound/input and then normalized to rDNA promoter binding. **C |** ChIP assay showing association of TTF1 with the indicated genes. Values are calculated bound/input and then normalized to rDNA promoter binding.

5.11 Association of TTF1 with EZH2-target genes and RTEM genes in U2OS cells

How is TIP5 recruited to EZH2-target genes (ADRB2, DAB2IP, CNR1, KCNA1 and MYT1) and RTEM genes (AOX1, HOXB8, KLF6 and LAMB3) in U2OS cells?

TIP5 was identified with a two-hybrid screen with the transcription terminator factor 1 (TTF1) as bait [85]. TTF1 binds to terminator (T) elements, sequences that are located at the 5'- and 3'-rDNA sequences and is implicated in several rRNA regulatory processes such as transcript termination, replication fork arrest and transcription [217-219]. The binding of TTF1 to the T_0 element at the rDNA promoter led to propose a role of TTF1 in the recruitment of TIP5 to rDNA [84, 220]. To determine whether TIP5 uses similar recruitment mechanisms as described for rRNA genes, we measured the association of TTF1 with selected genes by ChIP analysis. As shown in Figure 10 C, anti-TTF1 ChIP assay in U2OS cells revealed the association of TTF1 with the rDNA promoter region but not with the rDNA coding region located at +4 kb from the TSS, underscoring the specificity of this assay. Also in this analysis, GAPDH and IL6 promoter – genes that are not related to TTF1 – were used as additional controls to assess the specificity of the ChIP assay. All the EZH2-target genes in U2OS except MYT1 showed enrichment for TTF1 association. Of the RTEM genes, only KLF6 displayed an association with TTF1.

Taken together, the results suggest that TTF1-mediated recruitment of TIP5 to rDNA might be a mechanism used also for other genes than rRNA genes. As TTF1 binds to DNA in a sequence dependent manner, future studies will aim to find the common DNA elements on the regulatory sequences of RTEM and EZH2-/TIP5-target genes.

5.12 Association of TIP5 and EZH2 in PC3 cells

Previous experiments of our laboratory showed an interaction of TIP5 and EZH2 when analyzed in HEK293T cells overexpressing tagged TIP5 and EZH2 (data not shown). To determine whether endogenous EZH2 associates with TIP5 in PC3 cells, we expressed HA-Flag-TIP5 and HA-Flag-TIP5-700 (representing the first 700 amino acids of N-terminal TIP5) and performed co-immunoprecipitation (Co-IP).

Since PC3 cells are hard-to-transfect cells, we transduced the PC3 cells with retroviruses expressing HA-Flag-TIP5. Although the transducing efficiency was elevated (*ca.* 90% according to GFP expression of the control cells), HA-Flag-TIP5 expression levels were very low and we were not able to detect any signal from western blots of nuclear extracts and anti-Flag immune-precipitates. Since previous experiments determined that PC3 cells are not efficiently transfected using calcium phosphate and electroporation methods, we tested some commercial transfection kits. We found that X-tremeGENE HP DNA transfection kit from Roche had the best transfection efficiency in PC3 and the expression of TIP5 could be detected on western blot of nuclear extracts (Input sample of Figure 11). As expected, expression and IP of HA-TIP5-700 were more efficient than with full length TIP5 and we were able to detect co-immunoprecipitation of known TIP5-interacting proteins such as SNF2H and PARP1 [85, 221] but not EZH2 (Figure 11). Unfortunately, HA-Flag-TIP5 full-length expression was still low and, although it could be immune-precipitated, we detected the association

of the very strong interacting protein SNF2H that is part of NoRC complex, but not of PARP1. Similarly, we were not able to identify EZH2 as TIP5-associated protein (Figure 11). Thus, these results cannot be considered conclusive in determining whether TIP5 associates with EZH2 but provides important technical information for the identification of TIP5-interacting proteins in PC3 cells that is currently under study in the laboratory of Dr. Santoro.

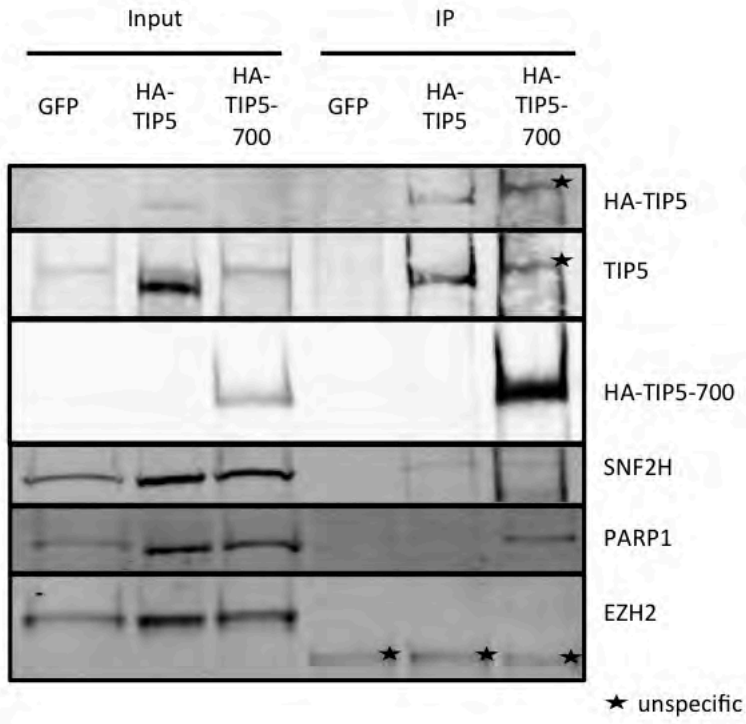

Figure 11 | No association of TIP5 and EZH2 detectable in PC3 cells
Western blots showing FLAG-immunoprecipitation from PC3 cells expressing HA-FLAG-TIP5 or HA-FLAG-TIP5-700. PC3 cells were transfected with GFP-C1, HA-FLAG-TIP5 (RS58F) or HA-FLAG-TIP5-700 (RS322) using the X-tremeGENE HP DNA transfection reagent from Roche.

6 Discussion

Cancer evolution at all stages is driven by an alliance of genetic alterations and epigenetic abnormalities. Epigenetic alterations such as CpG hypermethylation of promoters and histone modifications are common phenomena observed in almost all human tumors and contribute to cancer pathogenesis [222, 223]. Altered expression and/or mutation of epigenetic regulators that have roles as 'writers', 'readers' or 'editors' of DNA methylation, histone modifications and/or functions in chromatin remodeling are common features of tumor cells and have the potential to deregulate genes critical to cancer [224-226]. These alterations may be used to further stratify tumors into subtypes of different histopathological groups or clinical outcomes as exemplified by cancer-specific methylation patterns in selected gene promoter sequences [225, 227-229].
Prostate cancer is the most common non-cutaneous malignancy in men. Despite intensive research, the prediction of clinical behavior remains challenging using the currently available histopathological and biochemical (prostate-specific antigen, PSA) markers, thus novel molecular-based approaches will likely improve prognostic accuracy in the disease. In addition, rationally designed therapies directed at molecular targets beyond the androgen receptor pathway have yet to show clinical impact. Since prostate cancer is characterized by a low frequency of mutations [230], aberrant gene activity contributing to prostate cancer is likely based on alterations in gene expression levels, which can be driven by copy number alterations and/or translocations (such as PTEN, TP53 loss and ERG fusions) or by alterations in transcriptional or post-transcriptional regulation.

The results of my master and doctoral theses started to define an important role of TIP5 in prostate cancer. TIP5 is overexpressed in metastatic prostate tumors and coordinates with EZH2 epigenetic silencing at genes that are frequently repressed in metastatic and aggressive prostate cancer. Further work performed by Sandra Frommel, PhD student in the laboratory of Dr. Santoro, and in collaboration with the laboratories of Prof. C. Plass (DKFZ, Heidelberg), Prof. R. Eils (DKFZ, Heidelberg) and Prof. G. Sauter (University of Hamburg) defined that 1) TIP5 is necessary for proliferation, viability, migration and invasion of prostate cancer cells and that 2) TIP5 level is an independent prognostic marker of recurrence, especially in low/intermediate risk cases as assessed by Gleason score. Intermediate risk cases are a patient sub-cohort where most uncertainty exists to balance between active surveillance or immediate definite therapy in order to avoid overtreatment. Thus, screening of TIP5 levels in biopsies may be a valuable biomarker to distinguish prostate cancer that possesses the potential for disease progression, aiding in therapy decision making this important patient subgroup. The results of this work were recently published online ahead of print in Nature Genetics ("BAZ2A (TIP5) is involved in epigenetic alterations in prostate cancer and its overexpression predicts disease recurrence" Lei Gu, Sandra C. Frommel, Christopher C. Oakes, Ronald Simon, Katharina Grupp, Cristina Y. Gerig, Dominik Bär, Mark D. Robinson, Constance Baer, Melanie Weiss, Zuguang Gu, Ruprecht Kuner, Holger Sültmann, Maurizio Provenzano, ICGC Project on Early Onset Prostate Cancer, Marie-Laure Yaspo, Benedikt Brors, Jan Korbel, Thorsten Schlomm, Guido Sauter, Roland Eils, Christoph Plass and Raffaella Santoro; doi:10.1038/ng.3165).

The results presented here also might have important therapeutic implications. Lethality in prostate cancer is linked to the evolution of a metastatic phenotype. PSA recurrence following radical prostatectomy reveals that tumor cells have gained the ability to invade the surrounding local tissues and/or metastasize prior to surgery. We showed a key role for TIP5 in the regulation of genes related to metastatic features (this work) and in the growth and invasiveness of metastatic prostate cancer cells. Our results suggest that high TIP5 levels in the primary tumor indicate a higher probability of metastasis, linking molecular findings with recurrence in clinical samples. TIP5 may be involved in endowing cells with these abilities and could represent a promising therapeutic target for metastatic prostate cancer. An increasing number of epigenetic regulatory genes, including members of the class bromodomain-containing proteins, are currently found to be dysregulated across many cancer types [231]. These genes represent novel targets of a new generation of potential cancer therapeutics. In line with this, the fact that TIP5 contains a bromodomain previously shown to be important for its silencing function at the rDNA locus [232], might open the possibility to develop compounds to inactivate TIP5 function in cancer.

The identification of genes regulated by TIP5 and EZH2 described in this work underscores a tight link between TIP5 and EZH2. Not only we determined that in PC3 cells about one third of genes regulated by TIP5 are also targets of EZH2 and *vice versa* but also that TIP5- and EZH2-regulated genes are implicated in common biological processes. We discovered two distinct processes. Genes downregulated by TIP5 or EZH2 are involved in immune-response process while upregulated genes belong to developmental functions. Although these genes downregulated upon TIP5 and EZH2 knockdown are likely not direct targets it is to note that this pathways have been previously implicated in prostate cancer. For example, STAT1, a gene downregulated upon TIP5 knockdown, has been recently identified as a proto-oncogene product in a variety of cancers, including metastatic prostate cancer [233]. The Deltex (DTX)-3-like E3 ubiquitin ligase (DTX3L) also known as B-lymphoma and BAL-associated protein (BBAP) was originally identified as a binding parter of PARP9 [234, 235]. Both DTX3L and PARP9 are downregulated upon TIP5 knockdown in PC3 cells (this work). DTX3L is overexpressed in subtypes of high-risk chemotherapy-resistant aggressive HR-DLBCL with an active host inflammatory response and tightly associated with intrinsic IFNγ signaling and constitutive activity of STAT1 [235, 236]. Finally, STAT1, DTX3L and PARP9 have been recently described to mediate proliferation and survival of metastatic prostate cancer cells [237]. Future studies will aim to define how TIP5 and EZH2 contribute to these pathways.

The fact that genes upregulated upon TIP5 and EZH2 knockdown are implicated in developmental process suggest an important link with stem cell features. Recently developed system biology approaches have revealed highly interconnected networks in which multiple regulatory factors act in combination. Interestingly, stem cells and cancer cells share some properties, notably self-renewal and a block in differentiation. Of note is that the expression signatures that are specific to embryonic stem cells (ESCs) are also found in many human cancers and in mouse cancer models, suggesting that these shared features might inform new approaches for cancer therapy. Interestingly, analysis of TIP5 in mouse ESCs revealed a regulation similar to that found in PC3 cells. Knockdown of TIP5 slowed

down proliferation of ESCs and upregulated transcription of genes implicated in development, particularly Hox genes as found in PC3 cells.
This work also explored the possibility that TIP5 is implicated in epigenetic regulation in other cancer than prostate such as osteosarcoma. In U2Os cells 6 out of 9 analyzed RTEM genes showed enhanced transcription following knockdown of TIP5 and EZH2 indicating that the role of TIP5 and EZH2 to regulate RTEM genes' transcription is not limited to prostate cancer, but is also true in osteosarcoma cells. The ChIP analyzes in U2OS cells revealed binding of TIP5 and EZH2 only at a few primes of RTEM genes (Figure 8 A and B) although transcription analyzes determined a transcriptional state mediated by TIP5 or EZH2. The absence of TIP5 and EZH2 binding to RTEM gene promoters whose transcription depends on TIP5 or EZH2 suggests that the regulation in U2OS cells might occur in an indirect way, for instance through downregulation of a transcriptional activator or upregulation of a transcriptional repressor of RTEM genes.

An important question of this study was to define how TIP5 is recruited to RTEM genes. The first genes described to be regulated by TIP5 was the ribosomal RNA gene [81]. TTF1 is the "docking" protein that binds to rDNA promoter in a sequence specific manner and associates with TIP5. We found that *ca.* 50% of the analyzed TIP5-target genes in U2OS associate with TTF1 suggesting that TIP5 recruitment might share similar mechanisms to that one found for rRNA genes. ChIPseq analyzes of TIP5 and TTF1 in PC3 cells (currently performed in Santoro's lab) will unravel important insights on the mechanisms for TIP5 binding and regulation in PC3 cells.

7 Abbreviations

acetyl-CoA	Acetyl coenzyme A
ADP	Adenosine diphosphate
ADRB2	Adrenoceptor beta-2, surface
ALL	Acute lymphoblastic leukemia
AO	Aldehyde oxidase
AOX1	Aldehyde oxidase 1
ATEM	Activated by TIP5 and EZH2 in metastasis
ATP	Adenosine triphosphate
BBAP	B-lymphoma- and BAL-associated protein
BMI-1	B lymphoma Mo-MLV insertion region 1 homolog
bp	Base pair(s)
CBX	Chromobox homolog
cDNA	Complementary DNA
ChIP	Chromatin immunoprecipitation
ChIPseq	Chromatin immunoprecipitation sequencing
cm	Centimeter
CNR1	Cannaboid receptor 1 (brain)
CNS	Central nervous system
CoIP	Co-immunoprecipitation
CpG	Cytosine-phosphate-Guanine
Ct	Cycle threshold
CTRL	Control
DAB2IP	Disabled homolog 2-interacting protein
DAVID	Database for Annotation, Visualization and Integrated Discovery
DNA	Deoxyribonucleic acid
DNAse	Deoxyribonuclease
DNMT	DNA methyltransferase
dNTP	Deoxynucleotide triphosphates
DOT1L	DOT1-like protein
DTX	Deltex
DTX3L	Deltex-3-like E3 ubiquitin ligase
EDTA	Ethylenediaminetetraacetic acid
EED	Embryonic ectoderm development
ERG	V-ets avian erythroblastosis virus E26 oncogene homolog
ESCs	Embryonic stem cells
EtOH	Ethanol
ETV	E-twenty six translocation variant
EZH2	Enhancer of zeste homolog 2

FAS	Tumor necrosis factor receptor superfamily member 6
FBN1	Fibrillin 1
FHL2	Four and a half LIM domains 2
g	Earth's gravitational acceleration
GAP	GTPase-activation protein
GAPDH	Glyceraldehyde-3-phosphate dehydrogenase
GDS	GEO data set
GEO	Gene expression omnibus
GFP	Green fluorescent protein
GO	Gene ontology
h	Hour
HA	Haemagglutinin
HAT	Histone acetyltransferase
HDAC	Histone deacetylase
HMT	Histone methyltransferase
HOMER2	Homer homolog 2 (Drosophila)
HOXA7	Homeobox A7
HOXB8	Homeobox B8
HP1	Heterochromatin protein 1
IGS	Intergenic spacer sequence
IL6	Interleukin 6
IP	Immunoprecipitation
K	Lysine
KCNA1	Potassium voltage-gated channel, shaker-related subfamily, member 1
KLF	Krüppel-like factor 6
K-ras	Kirsten rat sarcoma viral oncogene homolog
kb	Kilobases
kDa	Kilodalton
L28	Ribosomal protein L28
LAMB3	Laminin, beta 3
M	Molar
MBD	Methyl-CpG-binding domain
me	Methylation
mg	Milligram
min	Minute
miRNA	Micro RNA
MKX	Mohawk homeobox
ml	Milliliter
MLL	Myeloid-lymphoid leukaemia
mM	Millimolar

mRNA	Messenger RNA
MuLV	Murine leukemia virus
MYC	V-Myc avian myelocytomatosis viral oncogene homolog
MYO18B	Myosin XVIIIB
MYT1	Myelin transcription factor 1
ng	Nanogram
nl	Nanoliter
nm	Nanometer
NOR	Nucleolar organizing region
NoRC	Nucleolar remodeling complex
nts	Nontranscribed spacer
OD	Optical density
PARP	Poly(ADP-ribose) polymerase
PARP1	Poly(ADP-ribose) polymerase 1
PARP9	Poly(ADP-ribose) polymerase family, member 9
PB	Polybrene
PBS	Phosphate buffered saline
PCa	Prostate cancer
PcG	Polycomb group
PCGF	Polycomb group ring finger
PHC	Polyhomeotic-like
PI	Protease inhibitor
PLAGL1	Pleiomorphic adenoma gene-like 1
PKr	Prostatakrebs
Pol I	RNA polymerase I
PRC1	Polycomb repressive complex 1
PRC2	Polycomb repessive complex 2
pRNA	Promoter RNA
PSA	Prostate-specific antigen
PTEN	Phosphatase and tensin homolog
qPCR	Quantitative polymerase chain reaction
RAS	Rat sarcoma protein
RbAp46/48	Retinoblastoma-binding protein 46/48
rDNA	Ribosomal DNA
RESEs	Ras epigenetic silencing effectors
RING1	Really interesting new gene 1
RNA	Ribonucleic acid
rpm	Rounds per minute
RTEM	Repressed by TIP5 and EZH2 in metastasis
rRNA	Ribosomal RNA

RT	Reverse transcriptase
RT-qPCR	Reverse transcription quantitative polymerase chain reaction
s	Second
S-phase	Synthesis phase
SAM	S-Adenosyl methionine
SCML	Sex comb on midleg-like
SD	Standard deviation
SDS-PAGE	Sodium dodecyl sulfate polyacrylamide gel electrophoresis
SFRP1	Secreted frizzled-related protein 1
siRNA	Small interfering RNA
SL1	Selectivity factor 1
SMARCA5	SWI/SNF related, matrix associated, actin dependent regulator of chromatin, subfamily a, member 5
SMYD1	SET and MYND domain-containing protein 1
SNF2H	Sucrose non-fermenting protein 2 homolog
STAT1	Signal transducer and activator of transcription 1
SUZ12	Suppressor of zeste 12 protein homolog
T	Terminator
THAP2	THAP domain containing, apoptosis associated protein 2
THC	Tetrahydrocannabinol
TIF-IA	Transcription initiation factor IA
TIP5	Transcription termination factor I-interacting protein 5
TP53	Tumor protein 53
TSS	Transcription start site
TTF1	Transcription termination factor, RNA polymerase I
UBF	Upstream binding factor
V	Volt
Y	Tyorsine
ZNF185	Zinc finger protein 185 (LIM domain)
°C	Degree Celsius
µg	Microgram
µl	Microliter

8 References

1. Richmond, T.J. and C.A. Davey, *The structure of DNA in the nucleosome core.* Nature, 2003. 423(6936): p. 145-50.
2. Luger, K., et al., *Crystal structure of the nucleosome core particle at 2.8 A resolution.* Nature, 1997. 389(6648): p. 251-60.
3. Wolffe, A.P., *Histone H1.* The international journal of biochemistry & cell biology, 1997. 29(12): p. 1463-6.
4. Robinson, P.J., et al., *EM measurements define the dimensions of the "30-nm" chromatin fiber: evidence for a compact, interdigitated structure.* Proceedings of the National Academy of Sciences of the United States of America, 2006. 103(17): p. 6506-11.
5. Rouleau, M., R.A. Aubin, and G.G. Poirier, *Poly(ADP-ribosyl)ated chromatin domains: access granted.* Journal of cell science, 2004. 117(Pt 6): p. 815-25.
6. Heitz, E., *Das Heterochromatin der Moose*, in *Jb Wiss Bot*1928. p. 762-818.
7. Dimitri, P., et al., *The paradox of functional heterochromatin.* BioEssays : news and reviews in molecular, cellular and developmental biology, 2005. 27(1): p. 29-41.
8. Straub, T., *Heterochromatin dynamics.* PLoS biology, 2003. 1(1): p. E14.
9. Dillon, N. and R. Festenstein, *Unravelling heterochromatin: competition between positive and negative factors regulates accessibility.* Trends in genetics : TIG, 2002. 18(5): p. 252-8.
10. Stambrook, P.J. and R.A. Flickinger, *Changes i chromosomal DNA replication tterns in developing frog embryos.* The Journal of experimental zoology, 1970. 174(1): p. 101-13.
11. Wallace, J.A. and T.L. Orr-Weaver, *Replication of heterochromatin: insights into mechanisms of epigenetic inheritance.* Chromosoma, 2005. 114(6): p. 389-402.
12. Huidobro, C., A.F. Fernandez, and M.F. Fraga, *The role of genetics in the establishment and maintenance of the epigenome.* Cellular and molecular life sciences : CMLS, 2013. 70(9): p. 1543-73.
13. Jeltsch, A., *Molecular enzymology of mammalian DNA methyltransferases.* Current topics in microbiology and immunology, 2006. 301: p. 203-25.
14. Pradhan, S., et al., *Recombinant human DNA (cytosine-5) methyltransferase. I. Expression, purification, and comparison of de novo and maintenance methylation.* The Journal of biological chemistry, 1999. 274(46): p. 33002-10.
15. Okano, M., et al., *DNA methyltransferases Dnmt3a and Dnmt3b are essential for de novo methylation and mammalian development.* Cell, 1999. 99(3): p. 247-57.
16. Clark, S.J., J. Harrison, and P.L. Molloy, *Sp1 binding is inhibited by (m)Cp(m)CpG methylation.* Gene, 1997. 195(1): p. 67-71.
17. Li, E., T.H. Bestor, and R. Jaenisch, *Targeted mutation of the DNA methyltransferase gene results in embryonic lethality.* Cell, 1992. 69(6): p. 915-26.
18. Bird, A., *DNA methylation patterns and epigenetic memory.* Genes & development, 2002. 16(1): p. 6-21.
19. Bernstein, B.E., A. Meissner, and E.S. Lander, *The mammalian epigenome.* Cell, 2007. 128(4): p. 669-81.
20. Berger, S.L., *The complex language of chromatin regulation during transcription.* Nature, 2007. 447(7143): p. 407-12.
21. Kouzarides, T., *Chromatin modifications and their function.* Cell, 2007. 128(4): p. 693-705.
22. Gardner, K.E., C.D. Allis, and B.D. Strahl, *Operating on chromatin, a colorful language where context matters.* Journal of molecular biology, 2011. 409(1): p. 36-46.
23. Jenuwein, T. and C.D. Allis, *Translating the histone code.* Science, 2001. 293(5532): p. 1074-80.

24. Yang, X.J., *Lysine acetylation and the bromodomain: a new partnership for signaling.* BioEssays : news and reviews in molecular, cellular and developmental biology, 2004. 26(10): p. 1076-87.
25. Bannister, A.J. and T. Kouzarides, *Regulation of chromatin by histone modifications.* Cell research, 2011. 21(3): p. 381-95.
26. Bannister, A.J., et al., *Selective recognition of methylated lysine 9 on histone H3 by the HP1 chromo domain.* Nature, 2001. 410(6824): p. 120-4.
27. Lachner, M., et al., *Methylation of histone H3 lysine 9 creates a binding site for HP1 proteins.* Nature, 2001. 410(6824): p. 116-20.
28. Hassa, P.O., et al., *Nuclear ADP-ribosylation reactions in mammalian cells: where are we today and where are we going?* Microbiology and molecular biology reviews : MMBR, 2006. 70(3): p. 789-829.
29. Messner, S. and M.O. Hottiger, *Histone ADP-ribosylation in DNA repair, replication and transcription.* Trends in cell biology, 2011. 21(9): p. 534-42.
30. Hanahan, D. and R.A. Weinberg, *Hallmarks of cancer: the next generation.* Cell, 2011. 144(5): p. 646-74.
31. Baylin, S.B. and J.E. Ohm, *Epigenetic gene silencing in cancer - a mechanism for early oncogenic pathway addiction?* Nature reviews. Cancer, 2006. 6(2): p. 107-16.
32. Chi, P., C.D. Allis, and G.G. Wang, *Covalent histone modifications--miswritten, misinterpreted and mis-erased in human cancers.* Nature reviews. Cancer, 2010. 10(7): p. 457-69.
33. Fuks, F., *DNA methylation and histone modifications: teaming up to silence genes.* Current opinion in genetics & development, 2005. 15(5): p. 490-5.
34. Santoro, R. and F. De Lucia, *Many players, one goal: how chromatin states are inherited during cell division.* Biochemistry and cell biology = Biochimie et biologie cellulaire, 2005. 83(3): p. 332-43.
35. Howard, G., et al., *Activation and transposition of endogenous retroviral elements in hypomethylation induced tumors in mice.* Oncogene, 2008. 27(3): p. 404-8.
36. Noushmehr, H., et al., *Identification of a CpG Island Methylator Phenotype that Defines a Distinct Subgroup of Glioma.* Cancer cell, 2010. 17(5): p. 510-522.
37. Portela, A. and M. Esteller, *Epigenetic modifications and human disease.* Nature Biotechnology, 2010. 28(10): p. 1057-1068.
38. Bergman, Y. and H. Cedar, *DNA methylation dynamics in health and disease.* Nature structural & molecular biology, 2013. 20(3): p. 274-81.
39. De Carvalho, D.D., et al., *DNA methylation screening identifies driver epigenetic events of cancer cell survival.* Cancer cell, 2012. 21(5): p. 655-67.
40. Neff, T. and S.A. Armstrong, *Recent progress toward epigenetic therapies: the example of mixed lineage leukemia.* Blood, 2013. 121(24): p. 4847-53.
41. Juergens, R.A., et al., *Combination Epigenetic Therapy Has Efficacy in Patients with Refractory Advanced Non-Small Cell Lung Cancer.* Cancer Discovery, 2011. 1(7): p. 598-607.
42. Fraga, M.F., et al., *Loss of acetylation at Lys16 and trimethylation at Lys20 of histone H4 is a common hallmark of human cancer.* Nature genetics, 2005. 37(4): p. 391-400.
43. Halkidou, K., et al., *Upregulation and nuclear recruitment of HDAC1 in hormone refractory prostate cancer.* The Prostate, 2004. 59(2): p. 177-89.
44. Song, J., et al., *Increased expression of histone deacetylase 2 is found in human gastric cancer.* APMIS : acta pathologica, microbiologica, et immunologica Scandinavica, 2005. 113(4): p. 264-8.
45. Sharma, S., T.K. Kelly, and P.A. Jones, *Epigenetics in cancer.* Carcinogenesis, 2010. 31(1): p. 27-36.

46. Krivtsov, A.V. and S.A. Armstrong, *MLL translocations, histone modifications and leukaemia stem-cell development.* Nature reviews. Cancer, 2007. 7(11): p. 823-33.
47. McGarvey, K.M., et al., *Silenced tumor suppressor genes reactivated by DNA demethylation do not return to a fully euchromatic chromatin state.* Cancer research, 2006. 66(7): p. 3541-9.
48. Lanzuolo, C. and V. Orlando, *Memories from the polycomb group proteins.* Annual review of genetics, 2012. 46: p. 561-89.
49. Levine, S.S., et al., *The core of the polycomb repressive complex is compositionally and functionally conserved in flies and humans.* Molecular and cellular biology, 2002. 22(17): p. 6070-8.
50. Valk-Lingbeek, M.E., S.W. Bruggeman, and M. van Lohuizen, *Stem cells and cancer; the polycomb connection.* Cell, 2004. 118(4): p. 409-18.
51. Sauvageau, M. and G. Sauvageau, *Polycomb group proteins: multi-faceted regulators of somatic stem cells and cancer.* Cell stem cell, 2010. 7(3): p. 299-313.
52. Cao, R. and Y. Zhang, *SUZ12 is required for both the histone methyltransferase activity and the silencing function of the EED-EZH2 complex.* Molecular cell, 2004. 15(1): p. 57-67.
53. Czermin, B., et al., *Drosophila enhancer of Zeste/ESC complexes have a histone H3 methyltransferase activity that marks chromosomal Polycomb sites.* Cell, 2002. 111(2): p. 185-96.
54. Kuzmichev, A., et al., *Histone methyltransferase activity associated with a human multiprotein complex containing the Enhancer of Zeste protein.* Genes & development, 2002. 16(22): p. 2893-905.
55. Muller, J., et al., *Histone methyltransferase activity of a Drosophila Polycomb group repressor complex.* Cell, 2002. 111(2): p. 197-208.
56. Lachner, M. and T. Jenuwein, *The many faces of histone lysine methylation.* Current opinion in cell biology, 2002. 14(3): p. 286-98.
57. Boyer, L.A., et al., *Polycomb complexes repress developmental regulators in murine embryonic stem cells.* Nature, 2006. 441(7091): p. 349-53.
58. Lee, T.I., et al., *Control of developmental regulators by Polycomb in human embryonic stem cells.* Cell, 2006. 125(2): p. 301-13.
59. Schwartz, Y.B., et al., *Genome-wide analysis of Polycomb targets in Drosophila melanogaster.* Nature genetics, 2006. 38(6): p. 700-5.
60. Squazzo, S.L., et al., *Suz12 binds to silenced regions of the genome in a cell-type-specific manner.* Genome research, 2006. 16(7): p. 890-900.
61. Leung, C., et al., *Bmi1 is essential for cerebellar development and is overexpressed in human medulloblastomas.* Nature, 2004. 428(6980): p. 337-41.
62. Richly, H., L. Aloia, and L. Di Croce, *Roles of the Polycomb group proteins in stem cells and cancer.* Cell death & disease, 2011. 2: p. e204.
63. Bachmann, I.M., et al., *EZH2 expression is associated with high proliferation rate and aggressive tumor subgroups in cutaneous melanoma and cancers of the endometrium, prostate, and breast.* Journal of clinical oncology : official journal of the American Society of Clinical Oncology, 2006. 24(2): p. 268-73.
64. Kleer, C.G., et al., *EZH2 is a marker of aggressive breast cancer and promotes neoplastic transformation of breast epithelial cells.* Proceedings of the National Academy of Sciences of the United States of America, 2003. 100(20): p. 11606-11.
65. Varambally, S., et al., *The polycomb group protein EZH2 is involved in progression of prostate cancer.* Nature, 2002. 419(6907): p. 624-9.
66. Weikert, S., et al., *Expression levels of the EZH2 polycomb transcriptional repressor correlate with aggressiveness and invasive potential of bladder carcinomas.* International journal of molecular medicine, 2005. 16(2): p. 349-53.

67. Morin, R.D., et al., *Somatic mutations altering EZH2 (Tyr641) in follicular and diffuse large B-cell lymphomas of germinal-center origin.* Nature genetics, 2010. 42(2): p. 181-5.
68. Yap, D.B., et al., *Somatic mutations at EZH2 Y641 act dominantly through a mechanism of selectively altered PRC2 catalytic activity, to increase H3K27 trimethylation.* Blood, 2011. 117(8): p. 2451-9.
69. Bracken, A.P., et al., *Genome-wide mapping of Polycomb target genes unravels their roles in cell fate transitions.* Genes & development, 2006. 20(9): p. 1123-36.
70. Schlesinger, Y., et al., *Polycomb-mediated methylation on Lys27 of histone H3 pre-marks genes for de novo methylation in cancer.* Nature genetics, 2007. 39(2): p. 232-6.
71. Vire, E., et al., *The Polycomb group protein EZH2 directly controls DNA methylation.* Nature, 2006. 439(7078): p. 871-4.
72. McGarvey, K.M., et al., *DNA methylation and complete transcriptional silencing of cancer genes persist after depletion of EZH2.* Cancer research, 2007. 67(11): p. 5097-102.
73. Henderson, A.S., D. Warburton, and K.C. Atwood, *Location of ribosomal DNA in the human chromosome complement.* Proceedings of the National Academy of Sciences of the United States of America, 1972. 69(11): p. 3394-8.
74. Gonzalez, I.L. and J.E. Sylvester, *Complete sequence of the 43-kb human ribosomal DNA repeat: analysis of the intergenic spacer.* Genomics, 1995. 27(2): p. 320-8.
75. Grozdanov, P., O. Georgiev, and L. Karagyozov, *Complete sequence of the 45-kb mouse ribosomal DNA repeat: analysis of the intergenic spacer.* Genomics, 2003. 82(6): p. 637-43.
76. McStay, B. and I. Grummt, *The epigenetics of rRNA genes: from molecular to chromosome biology.* Annual review of cell and developmental biology, 2008. 24: p. 131-57.
77. White, R.J., *RNA polymerases I and III, growth control and cancer.* Nature reviews. Molecular cell biology, 2005. 6(1): p. 69-78.
78. Moss, T., et al., *A housekeeper with power of attorney: the rRNA genes in ribosome biogenesis.* Cellular and molecular life sciences : CMLS, 2007. 64(1): p. 29-49.
79. Conconi, A., et al., *Two different chromatin structures coexist in ribosomal RNA genes throughout the cell cycle.* Cell, 1989. 57(5): p. 753-61.
80. Santoro, R. and I. Grummt, *Molecular mechanisms mediating methylation-dependent silencing of ribosomal gene transcription.* Molecular cell, 2001. 8(3): p. 719-25.
81. Santoro, R., J. Li, and I. Grummt, *The nucleolar remodeling complex NoRC mediates heterochromatin formation and silencing of ribosomal gene transcription.* Nature genetics, 2002. 32(3): p. 393-6.
82. Li, J., et al., *The chromatin remodeling complex NoRC controls replication timing of rRNA genes.* The EMBO journal, 2005. 24(1): p. 120-7.
83. Roussel, P., et al., *The rDNA transcription machinery is assembled during mitosis in active NORs and absent in inactive NORs.* The Journal of cell biology, 1996. 133(2): p. 235-46.
84. Santoro, R. and I. Grummt, *Epigenetic mechanism of rRNA gene silencing: temporal order of NoRC-mediated histone modification, chromatin remodeling, and DNA methylation.* Molecular and cellular biology, 2005. 25(7): p. 2539-46.
85. Strohner, R., et al., *NoRC--a novel member of mammalian ISWI-containing chromatin remodeling machines.* The EMBO journal, 2001. 20(17): p. 4892-900.
86. Zhou, Y., R. Santoro, and I. Grummt, *The chromatin remodeling complex NoRC targets HDAC1 to the ribosomal gene promoter and represses RNA polymerase I transcription.* The EMBO journal, 2002. 21(17): p. 4632-40.
87. Guetg, C., et al., *The NoRC complex mediates the heterochromatin formation and stability of silent rRNA genes and centromeric repeats.* The EMBO journal, 2010. 29(13): p. 2135-46.

88. Mayer, C., et al., *Intergenic transcripts regulate the epigenetic state of rRNA genes.* Molecular cell, 2006. 22(3): p. 351-61.
89. Montanaro, L., D. Trere, and M. Derenzini, *Nucleolus, ribosomes, and cancer.* Am J Pathol, 2008. 173(2): p. 301-310.
90. Ghoshal, K., et al., *Role of human ribosomal RNA (rRNA) promoter methylation and of methyl-CpG-binding protein MBD2 in the suppression of rRNA gene expression.* The Journal of biological chemistry, 2004. 279(8): p. 6783-93.
91. Powell, M.A., et al., *Ribosomal DNA methylation in patients with endometrial carcinoma: an independent prognostic marker.* Cancer, 2002. 94(11): p. 2941-52.
92. Qu, G.Z., et al., *Frequent hypomethylation in Wilms tumors of pericentromeric DNA in chromosomes 1 and 16.* Cancer genetics and cytogenetics, 1999. 109(1): p. 34-9.
93. Shiraishi, M., et al., *Tight interaction between densely methylated DNA fragments and the methyl-CpG binding domain of the rat MeCP2 protein attached to a solid support.* Biological chemistry, 1999. 380(9): p. 1127-31.
94. Chan, M.W., et al., *Hypermethylation of 18S and 28S ribosomal DNAs predicts progression-free survival in patients with ovarian cancer.* Clinical cancer research : an official journal of the American Association for Cancer Research, 2005. 11(20): p. 7376-83.
95. Zhou, X.C., et al., *Epigenetic considerations for endometrial cancer prevention, diagnosis and treatment.* Gynecologic oncology, 2007. 107(1): p. 143-53.
96. Santoro, R., P. Lienemann, and M. Fussenegger, *Epigenetic engineering of ribosomal RNA genes enhances protein production.* PloS one, 2009. 4(8): p. e6653.
97. Gazin, C., et al., *An elaborate pathway required for Ras-mediated epigenetic silencing.* Nature, 2007. 449(7165): p. 1073-7.
98. Panagopoulos, I., et al., *Fusion of ETV6 with an intronic sequence of the BAZ2A gene in a paediatric pre-B acute lymphoblastic leukaemia with a cryptic chromosome 12 rearrangement.* British journal of haematology, 2006. 133(3): p. 270-5.
99. Li, G., et al., *An integrative multi-platform analysis for discovering biomarkers of osteosarcoma.* BMC cancer, 2009. 9: p. 150.
100. Sheu, J.J., et al., *The roles of human sucrose nonfermenting protein 2 homologue in the tumor-promoting functions of Rsf-1.* Cancer research, 2008. 68(11): p. 4050-7.
101. Leite, K.R., et al., *Change in expression of miR-let7c, miR-100, and miR-218 from high grade localized prostate cancer to metastasis.* Urologic oncology, 2011. 29(3): p. 265-9.
102. Huang, D.W., B.T. Sherman, and R.A. Lempicki, *Systematic and integrative analysis of large gene lists using DAVID bioinformatics resources.* Nature Protocols, 2009. 4(1): p. 44-57.
103. Visvader, J.E. and G.J. Lindeman, *Cancer stem cells in solid tumours: accumulating evidence and unresolved questions.* Nature reviews. Cancer, 2008. 8(10): p. 755-68.
104. Kinsella, T.J., et al., *An in vivo comparison of oral 5-iodo-2'-deoxyuridine and 5-iodo-2-pyrimidinone-2'-deoxyribose toxicity, pharmacokinetics, and DNA incorporation in athymic mouse tissues and the human colon cancer xenograft, HCT-116.* Cancer research, 1994. 54(10): p. 2695-700.
105. Sigruener, A., et al., *Human aldehyde oxidase 1 interacts with ATP-binding cassette transporter-1 and modulates its activity in hepatocytes.* Hormone and metabolic research = Hormon- und Stoffwechselforschung = Hormones et metabolisme, 2007. 39(11): p. 781-9.
106. Crnogorac-Jurcevic, T., et al., *Proteomic analysis of chronic pancreatitis and pancreatic adenocarcinoma.* Gastroenterology, 2005. 129(5): p. 1454-63.
107. Oster, B., et al., *Identification and validation of highly frequent CpG island hypermethylation in colorectal adenomas and carcinomas.* International journal of cancer. Journal international du cancer, 2011. 129(12): p. 2855-66.

108. Yagi, K., et al., *Three DNA methylation epigenotypes in human colorectal cancer.* Clinical cancer research : an official journal of the American Association for Cancer Research, 2010. 16(1): p. 21-33.
109. Haldrup, C., et al., *DNA Methylation Signatures for Prediction of Biochemical Recurrence After Radical Prostatectomy of Clinically Localized Prostate Cancer.* Journal of clinical oncology : official journal of the American Society of Clinical Oncology, 2013.
110. Kim, J.H., et al., *Deep sequencing reveals distinct patterns of DNA methylation in prostate cancer.* Genome research, 2011. 21(7): p. 1028-41.
111. Kim, J.W., et al., *Identification of New Differentially Methylated Genes That Have Potential Functional Consequences in Prostate Cancer.* PloS one, 2012. 7(10).
112. *GeneCards - Human Genes*. [Web Page] 1996-2014; Available from: **http://www.genecards.org**
113. Edlund, K., et al., *CD99 is a novel prognostic stromal marker in non-small cell lung cancer.* International Journal of Cancer, 2012. 131(10): p. 2264-2273.
114. Chen, W., et al., *Targets of genome copy number reduction in primary breast cancers identified by integrative genomics.* Genes Chromosomes & Cancer, 2007. 46(3): p. 288-301.
115. Lind, G.E., et al., *Identification of an epigenetic biomarker panel with high sensitivity and specificity for colorectal cancer and adenomas.* Molecular cancer, 2011. 10: p. 85.
116. Wang, Y., et al., *"Promoter array" studies identify cohorts of genes directly regulated by methylation, copy number change, or transcription factor binding in human cancer cells.* Annals of the New York Academy of Sciences, 2005. 1058: p. 162-85.
117. Wang, Y.P., et al., *Survey of differentially methylated promoters in prostate cancer cell lines.* Neoplasia, 2005. 7(8): p. 748-760.
118. Kleiber, K., K. Strebhardt, and B.T. Martin, *The biological relevance of FHL2 in tumour cells and its role as a putative cancer target.* Anticancer Research, 2007. 27(1A): p. 55-61.
119. Brun, J., et al., *FHL2 silencing reduces Wnt signaling and osteosarcoma tumorigenesis in vitro and in vivo.* PloS one, 2013. 8(1): p. e55034.
120. Martin, B.T., et al., *FHL2 regulates cell cycle-dependent and doxorubicin-induced p21Cip1/Waf1 expression in breast cancer cells.* Cell cycle, 2007. 6(14): p. 1779-88.
121. Li, M., et al., *The four-and-a-half-LIM protein 2 (FHL2) is overexpressed in gliomas and associated with oncogenic activities.* Glia, 2008. 56(12): p. 1328-1338.
122. Pasalic, Z., et al., *FHL2 interacts with CALM and is highly expressed in acute erythroid leukemia.* Blood Cancer Journal, 2011. 1.
123. Gabriel, B., et al., *Focal adhesion kinase interacts with the transcriptional coactivator FHL2 and both are overexpressed in epithelial ovarian cancer.* Anticancer Research, 2004. 24(2B): p. 921-927.
124. Labalette, C., et al., *Deficiency of the LIM-only protein FHL2 reduces intestinal tumorigenesis in Apc mutant mice.* PloS one, 2010. 5(4): p. e10371.
125. Wang, J., et al., *Suppression of FHL2 expression induces cell differentiation and inhibits gastric and colon carcinogenesis.* Gastroenterology, 2007. 132(3): p. 1066-76.
126. Amann, T., et al., *FHL2 suppresses growth and differentiation of the colon cancer cell line HT-29.* Oncology Reports, 2010. 23(6): p. 1669-1674.
127. Yan, J., et al., *BRCA1 interacts with FHL2 and enhances FHL2 transactivation function.* FEBS letters, 2003. 553(1-2): p. 183-9.
128. Ding, L., et al., *Human four-and-a-half LIM family members suppress tumor cell growth through a TGF-beta-like signaling pathway.* The Journal of clinical investigation, 2009. 119(2): p. 349-61.
129. Genini, M., et al., *Subtractive cloning and characterization of DRAL, a novel LIM-domain protein down-regulated in rhabdomyosarcoma.* DNA and cell biology, 1997. 16(4): p. 433-42.

130. Kinoshita, M., et al., *Differently regulated androgen receptor transcriptional complex in prostate cancer compared with normal prostate.* International Journal of Urology, 2005. 12(4): p. 390-397.
131. Heemers, H.V., et al., *Androgen induction of the androgen receptor coactivator four and a half LIM domain protein-2: evidence for a role for serum response factor in prostate cancer.* Cancer research, 2007. 67(21): p. 10592-9.
132. Mori, Y., et al., *Novel candidate colorectal cancer biomarkers identified by methylation microarray-based scanning.* Endocrine-related cancer, 2011. 18(4): p. 465-78.
133. Ajima, R., et al., *HOMER2 binds MYO18B and enhances its activity to suppress anchorage independent growth.* Biochemical and biophysical research communications, 2007. 356(4): p. 851-6.
134. Di Vinci, A., et al., *Quantitative methylation analysis of HOXA3, 7, 9, and 10 genes in glioma: association with tumor WHO grade and clinical outcome.* Journal of cancer research and clinical oncology, 2012. 138(1): p. 35-47.
135. Chen, K.N., et al., *Expression of 11 HOX genes is deregulated in esophageal squamous cell carcinoma.* Clinical Cancer Research, 2005. 11(3): p. 1044-1049.
136. Novak, P., et al., *Epigenetic inactivation of the HOXA gene cluster in breast cancer.* Cancer research, 2006. 66(22): p. 10664-70.
137. Ayton, P.M. and M.L. Cleary, *Transformation of myeloid progenitors by MLL oncoproteins is dependent on Hoxa7 and Hoxa9.* Genes & development, 2003. 17(18): p. 2298-2307.
138. Drabkin, H.A., et al., *Quantitative HOX expression in chromosomally defined subsets of acute myelogenous leukemia.* Leukemia, 2002. 16(2): p. 186-95.
139. Nakamura, T., et al., *Cooperative activation of Hoxa and Pbx1-related genes in murine myeloid leukaemias.* Nature genetics, 1996. 12(2): p. 149-53.
140. Starkova, J., et al., *HOX Gene Expression in Phenotypic and Genotypic Subgroups and Low HOXA Gene Expression as an Adverse Prognostic Factor in Pediatric ALL.* Pediatric Blood & Cancer, 2010. 55(6): p. 1072-1082.
141. Cheng, W.J., et al., *Lineage infidelity of epithelial ovarian cancers is controlled by HOX genes that specify regional identity in the reproductive tract.* Nature medicine, 2005. 11(5): p. 531-537.
142. Naora, H., et al., *Aberrant expression of homeobox gene HOXA7 is associated with mullerian-like differentiation of epithelial ovarian tumors and the generation of a specific autologous antibody response.* Proceedings of the National Academy of Sciences of the United States of America, 2001. 98(26): p. 15209-14.
143. Ota, T., et al., *HOXA7 in epithelial ovarian cancer: Interrelationships between differentiation and clinical features.* Reproductive Sciences, 2007. 14(6): p. 605-614.
144. Piura, B. and E. Piura, *Autoantibodies to tumor-associated antigens in epithelial ovarian carcinoma.* Journal of oncology, 2009. 2009: p. 581939.
145. Calvo, R., et al., *Altered HOX and WNT7A expression in human lung cancer.* Proceedings of the National Academy of Sciences of the United States of America, 2000. 97(23): p. 12776-81.
146. Rauch, T., et al., *Homeobox gene methylation in lung cancer studied by genome-wide analysis with a microarray-based methylated CpG island recovery assay.* Proceedings of the National Academy of Sciences of the United States of America, 2007. 104(13): p. 5527-32.
147. Cillo, C., et al., *The HOX gene network in hepatocellular carcinoma.* International journal of cancer. Journal international du cancer, 2011. 129(11): p. 2577-87.
148. Liborio, T.N., et al., *In situ hybridization detection of homeobox genes reveals distinct expression patterns in oral squamous cell carcinomas.* Histopathology, 2011. 58(2): p. 225-233.
149. Vider, B.Z., et al., *Human colorectal carcinogenesis is associated with deregulation of homeobox gene expression.* Biochemical and biophysical research communications, 1997. 232(3): p. 742-748.

150. Vider, B.Z., et al., *Deregulated expression of homeobox-containing genes, HOXB6, B8, C8, C9, and Cdx-1, in human colon cancer cell lines.* Biochemical and biophysical research communications, 2000. 272(2): p. 513-8.
151. Lu, X., et al., *Establishment of a predictive genetic model for estimating chemotherapy sensitivity of colorectal cancer with synchronous liver metastasis.* Cancer biotherapy & radiopharmaceuticals, 2013. 28(7): p. 552-8.
152. Davidson, B., et al., *Gene expression signatures differentiate ovarian/peritoneal serous carcinoma from breast carcinoma in effusions.* Journal of cellular and molecular medicine, 2011. 15(3): p. 535-44.
153. Stavnes, H.T., et al., *HOXB8 expression in ovarian serous carcinoma effusions is associated with shorter survival.* Gynecologic oncology, 2013. 129(2): p. 358-363.
154. Blatt, C., et al., *DNA rearrangement of a homeobox gene in myeloid leukaemic cells.* The EMBO journal, 1988. 7(13): p. 4283-90.
155. Blatt, C., J. Lotem, and L. Sachs, *Inhibition of Specific Pathways of Myeloid Cell-Differentiation by an Activated Hox-2.4 Homeobox Gene.* Cell Growth & Differentiation, 1992. 3(10): p. 671-676.
156. Fujino, T., et al., *Inhibition of myeloid differentiation by Hoxa9, Hoxb8, and Meis homeobox genes.* Experimental hematology, 2001. 29(7): p. 856-63.
157. Knoepfler, P.S., et al., *HoxB8 requires its Pbx-interaction motif to block differentiation of primary myeloid progenitors and of most cell line models of myeloid differentiation.* Oncogene, 2001. 20(39): p. 5440-5448.
158. Perkins, A., et al., *Homeobox Gene-Expression Plus Autocrine Growth-Factor Production Elicits Myeloid-Leukemia.* Proceedings of the National Academy of Sciences of the United States of America, 1990. 87(21): p. 8398-8402.
159. Benzeno, S., et al., *Cyclin-dependent kinase inhibition by the KLF6 tumor suppressor protein through interaction with cyclin D1.* Cancer research, 2004. 64(11): p. 3885-3891.
160. Kimmelman, A.C., et al., *Suppression of glioblastoma tumorigenicity by the Kruppel-like transcription factor KLF6.* Oncogene, 2004. 23(29): p. 5077-83.
161. Kremer-Tal, S., et al., *Downregulation of KLF6 is an early event in hepatocarcinogenesis, and stimulates proliferation while reducing differentiation.* Journal of Hepatology, 2007. 46(4): p. 645-654.
162. Miyaki, M., et al., *Difference in the role of loss of heterozygosity at 10p15 (KLF6 locus) in colorectal carcinogenesis between sporadic and familial adenomatous polyposis and hereditary nonpolyposis colorectal cancer patients.* Oncology, 2006. 71(1-2): p. 131-135.
163. Narla, G., et al., *KLF6, a candidate tumor suppressor gene mutated in prostate cancer.* Science, 2001. 294(5551): p. 2563-6.
164. Slavin, D.A., et al., *A new role for the Kruppel-like transcription factor KLF6 as an inhibitor of c-Jun proto-oncoprotein function.* Oncogene, 2004. 23(50): p. 8196-8205.
165. Tahara, E., et al., *Activation of protein kinase C by phorbol 12-myristate 13-acetate suppresses the growth of lung cancer cells through KLF6 induction.* Cancer Biology & Therapy, 2009. 8(9): p. 801-807.
166. Jeng, Y.M. and H.C. Hsu, *KLF6, a putative tumor suppressor gene, is mutated in astrocytic gliomas.* International Journal of Cancer, 2003. 105(5): p. 625-629.
167. Cho, Y.G., et al., *Genetic alterations of the KLF6 gene in colorectal cancers.* APMIS : acta pathologica, microbiologica, et immunologica Scandinavica, 2006. 114(6): p. 458-64.
168. Reeves, H.L., et al., *Kruppel-Like factor 6 (KLF6) is a tumor-suppressor gene frequently inactivated in colorectal cancer.* Gastroenterology, 2004. 126(4): p. 1090-1103.

169. Ito, G., et al., *Kruppel-Like factor 6 is frequently down-regulated and induces apoptosis in non-small cell lung cancer cells.* Cancer research, 2004. 64(11): p. 3838-3843.
170. Wikman, H., et al., *Identification of differentially expressed genes in pulmonary adenocarcinoma by using cDNA array.* Oncogene, 2002. 21(37): p. 5804-5813.
171. Peng, D., et al., *Alterations in Barrett's-related adenocarcinomas: a proteomic approach.* International journal of cancer. Journal international du cancer, 2008. 122(6): p. 1303-10.
172. Yamashita, K., et al., *Pharmacologic unmasking of epigenetically silenced tumor suppressor genes in esophageal squamous cell carcinoma.* Cancer cell, 2002. 2(6): p. 485-95.
173. Kremer-Tal, S., et al., *Frequent inactivation of the tumor suppressor Kruppel-like factor 6 (KLF6) in hepatocellular carcinoma.* Hepatology, 2004. 40(5): p. 1047-1052.
174. Pan, X.C., et al., *Inactivation of the tumor suppressor Kruppel-like factor 6 (KLF6) by mutation or decreased expression in hepatocellular carcinomas.* Journal of Zhejiang University. Science. B, 2006. 7(10): p. 830-6.
175. Cho, Y.G., et al., *Genetic alterations of the KLF6 gene in gastric cancer.* Oncogene, 2005. 24(28): p. 4588-90.
176. DiFeo, A., G. Narla, and J.A. Martignetti, *Emerging Roles of Kruppel-Like Factor 6 and Kruppel-Like Factor 6 Splice Variant 1 in Ovarian Cancer Progression and Treatment.* Mount Sinai Journal of Medicine, 2009. 76(6): p. 557-566.
177. Chen, C., et al., *Deletion, mutation, and loss of expression of KLF6 in human prostate cancer.* The American journal of pathology, 2003. 162(4): p. 1349-54.
178. Cheng, X.F., et al., *Growth inhibitory effect of Kruppel-like factor 6 on human prostatic carcinoma and renal carcinoma cell lines.* The Tohoku journal of experimental medicine, 2008. 216(1): p. 35-45.
179. Fang, W., et al., *Transcriptional patterns, biomarkers and pathways characterizing nasopharyngeal carcinoma of Southern China.* Journal of translational medicine, 2008. 6: p. 32.
180. Oka, T., et al., *Overexpression of beta3/gamma2 chains of laminin-5 and MMP7 in biliary cancer.* World journal of gastroenterology : WJG, 2009. 15(31): p. 3865-73.
181. Kita, Y., et al., *Clinical significance of LAMB3 and COL7A1 mRNA in esophageal squamous cell carcinoma.* European journal of surgical oncology : the journal of the European Society of Surgical Oncology and the British Association of Surgical Oncology, 2009. 35(1): p. 52-8.
182. Sathyanarayana, U.G., et al., *Epigenetic inactivation of laminin-5-encoding genes in lung cancers.* Clinical cancer research : an official journal of the American Association for Cancer Research, 2003. 9(7): p. 2665-72.
183. Sathyanarayana, U.G., et al., *Molecular detection of noninvasive and invasive bladder tumor tissues and exfoliated cells by aberrant promoter methylation of laminin-5 encoding genes.* Cancer research, 2004. 64(4): p. 1425-30.
184. Zhang, H.Y., et al., *Association of DNA methylation and epigenetic inactivation of RASSF1A and beta-catenin with metastasis in small bowel carcinoid tumors.* Endocrine, 2006. 30(3): p. 299-306.
185. Sathyanarayana, U.G., et al., *Aberrant promoter methylation of laminin-5-encoding genes in prostate cancers and its relationship to clinicopathological features.* Clinical cancer research : an official journal of the American Association for Cancer Research, 2003. 9(17): p. 6395-400.
186. Calaluce, R., et al., *Laminin-5 beta 3A expression in LNCaP human prostate carcinoma cells increases cell migration and tumorigenicity.* Neoplasia, 2004. 6(5): p. 468-479.
187. Reis, S.T., et al., *The role of micro RNAs let7c, 100 and 218 expression and their target RAS, C-MYC, BUB1, RB, SMARCA5, LAMB3 and Ki-67 in prostate cancer.* Clinics, 2013. 68(5): p. 652-657.
188. Wu, X.X., et al., *Identification of genes with higher expression in human uterine leiomyomas than in the corresponding myometrium.* Molecular Human Reproduction, 2002. 8(3): p. 246-254.

189. Medina, P.P., et al., *Transcriptional targets of the chromatin-remodelling factor SMARCA4/BRG1 in lung cancer cells.* Human molecular genetics, 2005. 14(7): p. 973-82.
190. Gonzalez, H.E., et al., *Identification of 9 genes differentially expressed in head and neck squamous cell carcinoma.* Archives of otolaryngology--head & neck surgery, 2003. 129(7): p. 754-9.
191. Vanaja, D.K., et al., *Transcriptional silencing of zinc finger protein 185 identified by expression profiling is associated with prostate cancer progression.* Cancer research, 2003. 63(14): p. 3877-3882.
192. Zhang, J.S., A. Gong, and C.Y. Young, *ZNF185, an actin-cytoskeleton-associated growth inhibitory LIM protein in prostate cancer.* Oncogene, 2007. 26(1): p. 111-22.
193. Sasaki, H., et al., *The knock-down of overexpressed EZH2 and BMI-1 does not prevent osteosarcoma growth.* Oncology Reports, 2010. 23(3): p. 677-684.
194. Chen, K., et al., *Expression and significance of Kruppel-like factor 6 gene in osteosarcoma.* International orthopaedics, 2012. 36(10): p. 2107-11.
195. Alford, S.H., et al., *Increased risk for distant metastasis in patients with familial early-stage breast cancer and high EZH2 expression.* Breast Cancer Research and Treatment, 2012. 132(2): p. 429-437.
196. Min, J., et al., *An oncogene-tumor suppressor cascade drives metastatic prostate cancer by coordinately activating Ras and nuclear factor-kappaB.* Nature medicine, 2010. 16(3): p. 286-94.
197. Takezaki, T., et al., *Association of polymorphisms in the beta-2 and beta-3 adrenoceptor genes with risk of colorectal cancer in Japanese.* International journal of clinical oncology, 2001. 6(3): p. 117-22.
198. Wang, H., et al., *Beta-2 adrenergic receptor gene (ADRB2) polymorphism and risk for lung adenocarcinoma: a case-control study in a Chinese population.* Cancer letters, 2006. 240(2): p. 297-305.
199. Yu, J., et al., *Integrative genomics analysis reveals silencing of beta-adrenergic signaling by polycomb in prostate cancer.* Cancer cell, 2007. 12(5): p. 419-31.
200. Ramberg, H., et al., *Hormonal regulation of beta(2)-adrenergic receptor level in prostate cancer.* The Prostate, 2008. 68(10): p. 1133-1142.
201. Chen, H., S.W. Tu, and J.T. Hsieh, *Down-regulation of human DAB2IP gene expression mediated by polycomb Ezh2 complex and histone deacetylase in prostate cancer.* The Journal of biological chemistry, 2005. 280(23): p. 22437-44.
202. Duan, Y.F., et al., *Decreased expression of DAB2IP in pancreatic cancer with wild-type KRAS.* Hepatobiliary & pancreatic diseases international : HBPD INT, 2013. 12(2): p. 204-9.
203. Zhang, X., et al., *Low expression of DAB2IP contributes to malignant development and poor prognosis in hepatocellular carcinoma.* Journal of gastroenterology and hepatology, 2012. 27(6): p. 1117-25.
204. Smits, M., et al., *EZH2-Regulated DAB2IP Is a Medulloblastoma Tumor Suppressor and a Positive Marker for Survival.* Clinical Cancer Research, 2012. 18(15): p. 4048-4058.
205. Yano, M., et al., *Aberrant promoter methylation of human DAB2 interactive protein (hDAB2IP) gene in lung cancers.* International journal of cancer. Journal international du cancer, 2005. 113(1): p. 59-66.
206. Dote, H., et al., *Aberrant promoter methylation in human DAB2 interactive protein (hDAB2IP) gene in gastrointestinal tumour.* British journal of cancer, 2005. 92(6): p. 1117-25.
207. Dote, H., et al., *Aberrant promoter methylation in human DAB2 interactive protein (hDAB2IP) gene in breast cancer.* Clinical cancer research : an official journal of the American Association for Cancer Research, 2004. 10(6): p. 2082-9.
208. Chen, H., et al., *Differential regulation of the human gene DAB2IP in normal and malignant prostatic epithelia: cloning and characterization.* Genomics, 2002. 79(4): p. 573-81.

209. Kirmizis, A., et al., *Silencing of human polycomb target genes is associated with methylation of histone H3 Lys 27.* Genes & development, 2004. 18(13): p. 1592-605.
210. Caffarel, M.M., et al., *Delta(9)-tetrahydrocannabinol inhibits cell cycle progression in human breast cancer cells through Cdc2 regulation.* Cancer research, 2006. 66(13): p. 6615-6621.
211. Blazquez, C., et al., *Cannabinoid receptors as novel targets for the treatment of melanoma.* Faseb Journal, 2006. 20(14): p. 2633-+.
212. Xu, X., et al., *Overexpression of cannabinoid receptors CB1 and CB2 correlates with improved prognosis of patients with hepatocellular carcinoma.* Cancer genetics and cytogenetics, 2006. 171(1): p. 31-8.
213. Ek, S., et al., *Mantle cell lymphomas express a distinct genetic signature affecting lymphocyte trafficking and growth regulation as compared with subpopulations of normal human B cells.* Cancer research, 2002. 62(15): p. 4398-4405.
214. Islam, T.C., et al., *High level of cannabinoid receptor 1, absence of regulator of G protein signalling 13 and differential expression of Cyclin D1 in mantle cell lymphoma.* Leukemia, 2003. 17(9): p. 1880-90.
215. Brevet, M., et al., *Expression of K+ channels in normal and cancerous human breast.* Histology and histopathology, 2008. 23(8): p. 965-72.
216. Lallet-Daher, H., et al., *Potassium Channel KCNA1 Modulates Oncogene-Induced Senescence and Transformation.* Cancer research, 2013. 73(16): p. 5253-65.
217. Evers, R. and I. Grummt, *Molecular coevolution of mammalian ribosomal gene terminator sequences and the transcription termination factor TTF-I.* Proceedings of the National Academy of Sciences of the United States of America, 1995. 92(13): p. 5827-31.
218. Gerber, J.K., et al., *Termination of mammalian rDNA replication: polar arrest of replication fork movement by transcription termination factor TTF-I.* Cell, 1997. 90(3): p. 559-67.
219. Langst, G., et al., *RNA polymerase I transcription on nucleosomal templates: the transcription termination factor TTF-I induces chromatin remodeling and relieves transcriptional repression.* The EMBO journal, 1997. 16(4): p. 760-8.
220. Nemeth, A., et al., *The chromatin remodeling complex NoRC and TTF-I cooperate in the regulation of the mammalian rRNA genes in vivo.* Nucleic acids research, 2004. 32(14): p. 4091-9.
221. Guetg, C., et al., *Inheritance of silent rDNA chromatin is mediated by PARP1 via non-coding RNA.* Molecular cell, 2012. In print.
222. Ledford, H., *Epigenetics: Marked for success.* Nature, 2012. 483(7391): p. 637-9.
223. Sandoval, J. and M. Esteller, *Cancer epigenomics: beyond genomics.* Current opinion in genetics & development, 2012. 22(1): p. 50-5.
224. Plass, C., et al., *Mutations in regulators of the epigenome and their connections to global chromatin patterns in cancer.* Nature reviews. Genetics, 2013. 14(11): p. 765-80.
225. Sturm, D., et al., *Hotspot Mutations in H3F3A and IDH1 Define Distinct Epigenetic and Biological Subgroups of Glioblastoma.* Cancer Cell, 2012. 22(4): p. 425-437.
226. Turcan, S., et al., *IDH1 mutation is sufficient to establish the glioma hypermethylator phenotype.* Nature, 2012. 483(7390): p. 479-83.
227. Brena, R.M., et al., *Aberrant DNA methylation of OLIG1, a novel prognostic factor in non-small cell lung cancer.* PLoS medicine, 2007. 4(3): p. e108.
228. Figueroa, M.E., et al., *Leukemic IDH1 and IDH2 mutations result in a hypermethylation phenotype, disrupt TET2 function, and impair hematopoietic differentiation.* Cancer Cell, 2010. 18(6): p. 553-67.
229. Toyota, M., et al., *CpG island methylator phenotype in colorectal cancer.* Proceedings of the National Academy of Sciences of the United States of America, 1999. 96(15): p. 8681-6.
230. Grasso, C.S., et al., *The mutational landscape of lethal castration-resistant prostate cancer.* Nature, 2012. 487(7406): p. 239-43.

231. Dawson, M.A., T. Kouzarides, and B.J. Huntly, *Targeting epigenetic readers in cancer.* The New England journal of medicine, 2012. 367(7): p. 647-57.
232. Zhou, Y. and I. Grummt, *The PHD finger/bromodomain of NoRC interacts with acetylated histone H4K16 and is sufficient for rDNA silencing.* Curr Biol, 2005. 15(15): p. 1434-8.
233. Patterson, S.G., et al., *Novel role of Stat1 in the development of docetaxel resistance in prostate tumor cells.* Oncogene, 2006. 25(45): p. 6113-22.
234. Takeyama, K., et al., *The BAL-binding protein BBAP and related Deltex family members exhibit ubiquitin-protein isopeptide ligase activity.* The Journal of biological chemistry, 2003. 278(24): p. 21930-7.
235. Juszczynski, P., et al., *BAL1 and BBAP are regulated by a gamma interferon-responsive bidirectional promoter and are overexpressed in diffuse large B-cell lymphomas with a prominent inflammatory infiltrate.* Molecular and cellular biology, 2006. 26(14): p. 5348-59.
236. Camicia, R., et al., *BAL1/ARTD9 represses the anti-proliferative and pro-apoptotic IFNgamma-STAT1-IRF1-p53 axis in diffuse large B-cell lymphoma.* Journal of cell science, 2013. 126(Pt 9): p. 1969-80.
237. Bachmann, S.B., et al., *DTX3L and ARTD9 inhibit IRF1 expression and mediate in cooperation with ARTD8 survival and proliferation of metastatic prostate cancer cells.* Molecular cancer, 2014. 13: p. 125.

Acknowledgements

First of all, I thank my supervisor PD Dr. Raffaella Santoro for her support in the laboratory, her scientific input, the correction of my texts and the great canoe trip. Thanks for your patience!

In addition, I thank Prof. Dr. med. vet. Hanspeter Nägeli for being my co-supervisor, reading and rating my thesis.

Furthermore, I thank the former director of the institute Prof. Dr. Ulrich Hübscher and the present director of the institute Prof. Dr. Michael Hottiger for the opportunity to work on my doctoral thesis at their institute.

Thanks to my lab mates Sandra, Sergio, Natasa, Eva and Dominik for the help in the lab and the pleasant time during breaks.

Many thanks to my family – especially to Pat and Mellow!

Last but not least, thanks to all the members of IVBMB for the nice atmosphere and the willingness to help.

Curriculum vitae

Personal:

Name	Cristina Yasoma Gerig
Date of birth	February 6th, 1985
Place of birth	Basel, Switzerland
Nationality	Swiss
Hometown	Basel BS and Wassen UR

Education:

02/2013 – 12/2014	Doctoral thesis at Institute of Veterinary Biochemistry and Molecular Biology at the Vetsuisse Faculty at University of Zurich, Zurich Switzerland
11/2012 – 01/2013	Final exams "Eidgenössische Prüfung" at the Vetsuisse Faculty at University of Zurich, Zurich, Switzerland Degree: vet. med.
09/2010 – 09/2012	Master program veterinary medicine at the Vetsuisse Faculty at Universitiy of Zurich, Zurich, Switzerland Degree: Master of Veterinary Medicine
09/2007 – 08/2010	Bachelor program veterinary medicine at the Vetsuisse Faculty at University of Zurich, Zurich, Switzerland Degree: Bachelor of Veterinary Medicine
09/2006 – 06/2007	Biology studies at ETH Zurich, Zurich, Switzerland
09/2005 – 06/2006	Computer science studies at ETH Zurich, Zurich, Switzerland
08/1999 – 06/2004	High School at Gymnasium Kirschgarten, Basel, Switzerland Focus biology and chemistry Degree: Matura
08/1996 – 06/1999	Middle School at Orientierungsschule Gellert, Basel, Switzerland
08/1992 – 06/1996	Primary School at Primarschule Sevogel, Basel, Switzerland

Work:

10/2013 – 09/2014	Tierärztliches Überweisungszentrum (TÜZ): Intern (full time), Tenniken, Switzerland
08/2011 – 10/2013	Tierspital Zürich: keeper assistant (part time), Zurich, Switzerland
10/2008 – 01/2013	TÜZ: assistant for stationary patients care and emergency medical service (several weekends), Tenniken, Switzerland